Dopamine in the prefrontal cortex and its relevance for working memory

Graduate School for Cellular and Biomedical Sciences
University of Bern
PhD Thesis

Submitted by

Kay Thurley

from Germany

Thesis advisor

Prof. Dr. Hans-Rudolf Lüscher
Department of Physiology
Medical Faculty of the University of Bern

Bern, 2008

Accepted by the Faculty of Medicine, the Faculty of Science and the Vetsuisse Faculty of the University of Bern at the request of the Graduate School for Cellular and Biomedical Sciences

Bern, Dean of the Faculty of Medicine
Prof. Dr. Peter Eggli

Bern, Dean of the Faculty of Science
Prof. Dr. Urs Feller

Bern, Dean of the Vetsuisse Faculty Bern
Prof. Dr. Andreas Zurbriggen

An das Publikum

Summary

The prefrontal cortex plays a primary role in working memory, the mental ability to transiently store and manipulate information to guide decision making and forthcoming actions. Stored information can, for example, be the representation of a sensory stimulus or a memory item retrieved from long-term memory, or a combination of both. Such memory items are integrated with information about motivational and intentional states to generate decisions and actions.

Dopaminergic projections from the midbrain are known to play an important role in the modulation of prefrontal cortical activity. Dopamine affects prefrontal function in cognitive processes including working memory. However, several contradictory experimental findings and functional proposals have been reported on the role of dopamine modulation; in part because the neuronal substrate of working memory is difficult to measure.

In order to investigate the biophysical mechanisms of working memory in the prefrontal cortex, the present PhD thesis combines *in vitro* electrophysiological experiments at the cellular level with computational modeling. I performed whole-cell patch-clamp recordings at the somata of layer V pyramidal neurons in acute slices of the rat prefrontal cortex and investigated the influence of dopamine on these cells. The results were used to perform computer simulations of neural networks that are biologically motivated. On a basic level, the direct link could be established between cellular properties *in vitro* and network behavior *in silico*, spanning the range from slice electrophysiology to computational modeling of cognitive functions.

Experiments focused on the properties of single neurons, which we presume to be relevant for working memory. These properties are collectively described by the neuronal input-output function, which allows conclusions about the putative behavior of the neuron in a neural network. In response to electrical stimulation,

e.g., by current injection, a neuron typically fires a train of action potentials. Determining the rate of action potential discharge in response to different levels of stimulation, gives its input-output response function. Injecting noisy stimuli, one can mimic inputs from other (presynaptic) neurons like they would occur *in vivo* and the neuronal input-output function can be studied *in vitro* close to what one would expect *in vivo*. Using noisy currents, we investigated the effects of the neuromodulator dopamine on the input-output response function of layer V pyramidal neurons in prefrontal cortex. In the experiments, dopamine increased the gain of the input-output function. This gain-increase could be attributed to a reduction of conductances, which are related to the slow after-hyperpolarization that follows increased action potential discharge. The dopaminergic modulation of these response properties was mainly mediated by dopamine D1 receptors.

Based on the experimental results, we performed computer simulations in order to understand how the effect of dopamine onto single neuron activity translates into the behavior of the recurrently connected neural network in the prefrontal cortex. Input-output functions offer a direct way to enable conclusions about the putative behavior of the neuron in a neural network. We fitted integrate-and-fire model neurons to the experimentally recorded input-output functions and formed a network composed of these model neurons. The gain increase induced by dopamine facilitated and stabilized persistent activity that was sustained by synaptic reverberation in the model network. *In vivo* working memory is supposed to be represented by such persistent neural activity. Neurons showing persistent activity are not only found in the prefrontal cortex but here they are especially abundant. The simulation results thus suggest that dopamine may support working memory abilities via gain modulation. The present work therefore links *in vitro* experiments on dopaminergic modulation of the properties of single prefrontal neurons, to the stabilization of persistent activity in attractor neural networks, and its possible role for enhancing the signal-to-noise ratio in working memory tasks.

Contents

Preface

How to communicate between different disciplines of neuroscience like neurophysiology and computational neuroscience? An issue often encountered is that experimental neurophysiologists do not understand the mathematical approaches used in computational neuroscience to model experimental data, i.e., mathematical formalizations that are inherited from physics and the physical understanding of natural phenomena. The reverse way – grasping experimental approaches and results as a theoretical neuroscientist – seems often less intricate, although as often it is taken as too less intricate. In the present thesis I tried to communicate between neurophysiological experiments in vitro and computational modeling that aims at explaining higher cognitive functions. My approach hopefully not only connects both disciplines but also fosters mutual understanding.

Part I gives an extended overview of the field, spanning the range from electrophysiology and related pharmacology to the biophysical plausible modeling of human cognitive functions. I start with a general introduction of the cerebral cortex and the prefrontal cortex, mentioning briefly the most important terms before focusing on specific prefrontal features that are more relevant for the present study in the subsequent chapters, namely dopamine modulation in Chapter 2 and working memory in Chapter 3. I seek to explain the computational approaches intuitively in Part I, skipping mathematical formalizations on purpose. I included a brief summary at the end of each chapter in Part I, to point out the connection between the particular chapter and my own contribution, which I present later in Part II.

The publication in Part II covers the actual scientific work. In the study, we investigated the dopaminergic modulation of the features of single prefrontal pyramidal neurons that are supposed to be relevant for the interaction in neural

networks, serving cognitive functions.

In Part III I provide a brief general discussion, meant rather as concluding remarks than a repetition of the specific discussion found in the publication.

* * *

The following thesis was done in the Group of Prof. Dr. Hans-Rudolf Lüscher at the Department of Physiology, University of Bern, Switzerland between January 2006 and September 2008.

All analyses and simulations were performed on standard Personal Computers. Original programs were written in IGOR Pro (WaveMetrics, Inc., Portland, OR, USA) or MATLAB (The MathWorks, Inc., Natick, MA, USA).

The thesis was written in LaTeX and complied with pdfLaTeX, using two great open source tools that make LaTeX even more convenient and fun, and are highly recommended: LEd LaTeX Editor and JabRef for managing BibTex reference libraries.

Part I

Introduction

CHAPTER 1

Cerebral, neo- and prefrontal cortex

The cerebral cortex is the most differentiated part of the mammalian brain. In its most evolved form, the cerebral cortex is only found in humans and therefore often regarded as the biological foundation of the segregation of humans from animals. It takes a key role in sensory processing, movement, learning and memory, attention, thought, and language. The prefrontal cortex is at the developmental "apex" of the cerebral cortex, subserving "higher order" cognitive functions. The present chapter gives an introduction to the cerebral and specifically the prefrontal cortex.

1.1 The cerebral cortex

The cerebral cortex is divided into two hemispheres, whose surfaces are folded in many mammals into grooves called *sulci* alternating with ridges called *gyri*. The human cerebral cortex contains five lobes: laterally one sees the frontal, parietal, temporal, and occipital lobes; on the medial surface a fifth lobe can be distinguished, the limbic lobe (Fig. 1.1A). The parietal, temporal, and occipital lobes house primary somatosensory, auditory, and visual cortices, respectively. The limbic lobe is part of the limbic system, whose parts play roles in emotion, behavior and memory; the frontal lobe contains the primary motor area. However,

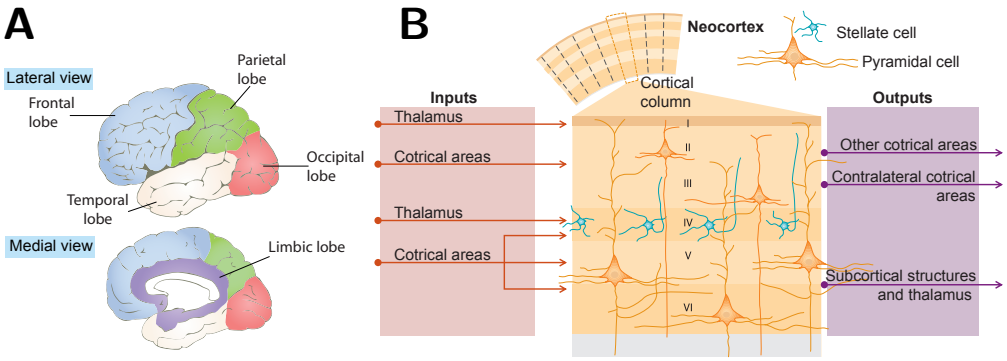

Figure 1.1: THE CEREBRAL CORTEX. (A) The five lobes of the human cerebral cortex. (B) The cellular organization of the six layered (I-VI) neocortex, including major inputs and outputs. For simplicity only the main excitatory neurons are depicted. Adapted from Klinke et al. (2005).

the most salient anatomical feature is the large size of cortical areas in between the primary cortices. These areas are secondary areas involved in the analysis of sensory information, the association of different sensory modalities and their integration with memory. Most of the frontal lobe comprises the prefrontal cortex. The prefrontal cortex constitutes the highest level in the "cortical hierarchy" integrating information of all sensory modalities with internal goals (desires, intentions) and is devoted to the representation and execution of "complex" actions (Fuster, 2001).

Histology of the cerebral cortex. Different nerve cells or *neurons* populate all of the cerebral cortex. The neurons form intricate networks in which they communicate with each other by means of electrical signals, the *action potentials* or "spikes", i.e., fast and fairly uniform deflections of the membrane potential, which are transmitted via contacts to other neurons called *synapses*. On relatively coarse inspection one observes that the cell bodies of cortical neurons are arranged in horizontal layers. The phylogenetically older paleo- (olfactory system) and archicortices (hippocampus) comprise three layers, whereas the neocortex is subdivided into six layers (I-VI); see Fig. 1.1 and, e.g., Trepel, 2004; FitzGerald et al., 2007.

Pyramidal neurons are the principal cell type in the cerebral cortex, named after their pyramidally shaped soma. In the neocortex, pyramidal neurons are mainly found in layers II/III and V/VI. They extend their *apical dendrite* to upper layers and *basal dendrites* radially within the same layer as the soma. The dendrites show a lot of small protrusions from their surface, the *dendritic spines*, that are the major sites for excitatory synaptic input. Pyramidal neurons via their axons send efferent output to structures out of the cortex or to other cortical

areas. In addition, recurrent branches of the axons project to neighboring cells. All pyramidal cells are excitatory and usually use glutamate as neurotransmitter. Postsynaptically, glutamate acts on two classes of receptors, N-methyl-D-aspartic acid (NMDA) and non-NMDA. The latter are mainly α-amino-3-hydroxy-5-methyl-4-isoxazolepropionic acid (AMPA) receptors.

A variety of interneurons populates the cerebral cortex and interacts with pyramidal cells. Fast-spiking interneurons preferentially innervate the soma and the axonal initial segment of pyramidal cells to control the firing of action potentials. The other types of interneurons primarily regulate dendritic excitability and the efficacy of excitatory inputs. The majority of the interneurons use the inhibitory neurotransmitter γ-aminobutyric acid (GABA).

A third class of cells, the spiny stellate cells, are preferentially found in layer IV of primary sensory areas. These cells route input from thalamic nuclei that themselves transmit sensory information from the periphery.

The six-layered structure is found in all neocortical areas, except for some parts of the frontal lobe comprising motor and prefrontal areas. Compared with the six-layered or granular cortex, here layers II and IV are weakly formed (dysgranular) or missing (agranular).

Vertically the neocortex is organized into groups of cells that reach across all layers and are horizontally and vertically linked by synapses. These groups have been termed *cortical columns* and are thought of as the basic functional neocortical units. They can be further subdivided into microcolumns, a narrow chain of neurons sharing vertical connections. The columnar organization was discovered in the somatosensory cortex, subsequent research, however, indicated that cortical columns are a general feature of the neocortex (reviewed in Mountcastle, 1997).

1.2 The prefrontal cortex

It has already been mentioned that the prefrontal cortex (PFC) is involved in higher order cognitive functions. For that it integrates sensory with memorized information to form internal goals (desires, expectations) and to coordinate behavior. According to Joaquin Fuster, the PFC closes the sensory-motor cycle that links the organism with its environment, integrating representations of perception with action (Fuster, 2001). In humans, the PFC is implicated in personality expression and social behavior.

1.2.1 Anatomy

The prefrontal cortex is the part of the frontal lobe that lies rostral to the precentral motor cortex. It has attained maximum relative growth in the human brain, where it constitutes nearly one-third of the neocortex (Fuster, 2001).

The PFC can be subdivided into three major areas: orbital, medial, and (dorso)lateral (Fig. 1.2A). The different subregions are interconnected with each other, allowing information to be distributed. Figure 1.2B gives a schematic overview of the different connections within and out of the PFC (Miller & Cohen, 2001; Tzschentke, 2001).

Information enters the PFC from sensory cortical areas and subcortical structures. The different PFC regions are connected with secondary sensory or association cortices of all modalities, but not with primary sensory cortices. Often inputs from different sensory modalities converge in most PFC areas rather than being separated. Some inputs even come from cortical regions that already process different sensory modalities.

Outputs are send from the PFC to the different parts of the motor system, being central to the prefrontal control over behavior. There are no direct connections between prefrontal and primary motor cortex. However, the dorsolateral PFC projects to premotor areas such as the (pre-)supplementary motor area which, in turn, are connected to primary motor cortex and the spinal cord. There are also connections with the cerebellum. Important are the dense interconnections between PFC and basal ganglia. The basal ganglia also receive inputs from many other cortical areas, its major output is routed via the mediodorsal nucleus of the thalamus to the frontal cortex.

The orbital and medial PFC areas are closely associated with medial temporal limbic structures and are functionally involved in emotional behavior. The connections include direct and indirect – via the medial dorsal thalamus – linkages with the hippocampus and associated neocortex, the amygdala, and the hypothalamus. The connections with the hippocampus are related to long-term memory and the connections with amygdala and hypothalamus are critical for the processing of internal states, such as motivation.

Prefrontal histology and morphology. The prefrontal cortex of primates including humans contains agranular, i.e., a layer IV is lacking, dysgranular, and granular areas (Öngür & Price, 2000). The posterior orbital and medial areas consist of five-layered agranular cortex, while the central orbital areas are dysgranular. The rostral orbital and medial areas, and dorso-lateral PFC are granular. In contrast, the rat prefrontal cortex is composed exclusively of agranular cortex, making it difficult to establish homologies to areas like the dorsolateral prefrontal cortex in primates (see, e.g., Uylings et al., 2003).

In several mammalian species, PFC areas have been reported to show some specialized histological and morphological features, which divide them from other cortical areas. Prefrontal pyramidal neurons are extensively connected horizontally and receive reciprocal inhibition (Rao et al., 1999; Constantinidis et al., 2002). The dendritic trees of PFC pyramidal cells are more branched and con-

tain more spines than in primary and secondary cortical areas (Yang et al., 1996; Elston, 2003). Similar morphological findings in ferret PFC were reported to correlate with physiological features like synaptic facilitation and a lack of firing rate adaptation (Wang et al., 2006). Peculiar synaptic facilitation was also reported in rat PFC before (Hempel et al., 2000). Highly branched and spinous pyramidal neurons are supposed to provide an anatomical basis that supports persistent network activity (Elston, 2003; Wang et al., 2006). Persistent activity is thought to be the neural correlate of working memory as discussed in depth in Chapter 3.

1.2.2 Function

In general, achieving a certain goal in daily life demands an extended sequence of actions being executed, certain subordinate decisions being made and distractions being resisted. "The ability to orchestrate thoughts and actions in accordance with internal goals" (Miller & Cohen, 2001), is often presumed as the main function of the PFC and denoted with the term executive function. Executive function refers to the ability to differentiate among conflicting thoughts, working toward a defined goal (goal-directed behavior), suppressing maladaptive responses and predicting outcomes. These abilities link the PFC to subordinate functions like working memory, i.e., the temporary storage and manipulation of information, and decision making. Since working memory is most relevant for the present study, it will be discussed in detail in Chapter 3.

Miller & Cohen (2001) proposed based on anatomical, psychological, and neurophysiological considerations a distinction between ventral and (dorso-)lateral subregions. Ventral regions (orbital and medial) support the maintenance of sensory information and integrate it with emotional and motivational information, due to its direct connections with the limbic system. Whereas, dorsolateral regions are responsible for the manipulation of such information, supporting the temporal organization of behavior. According to Miller & Cohen (2001) the PFC provides top-down signals to other brain areas, i.e., signals that are send from "hierarchically" higher back to lower areas. If demanded by the task, such top-down signals bias the competition between different bottom-up signals, favoring those which normally would not lead to action, against stronger alternative stimuli that cause routine behaviors. Top-down signals therefore relate to attention (Rolls et al., 2008). This bridges to the notion emphasized by Fuster (2001), that routine, or automatic behaviors do not engage the PFC and may be entirely organized in subcortical structures like basal ganglia, cerebellum, and lateral thalamus. In automatic sequences, one act leads to the next; no contingencies need to be mediated across time. Behavioral sequences with contingencies across time, or with ambiguities and uncertainties in sensory stimuli or motor actions, do engage the PFC.

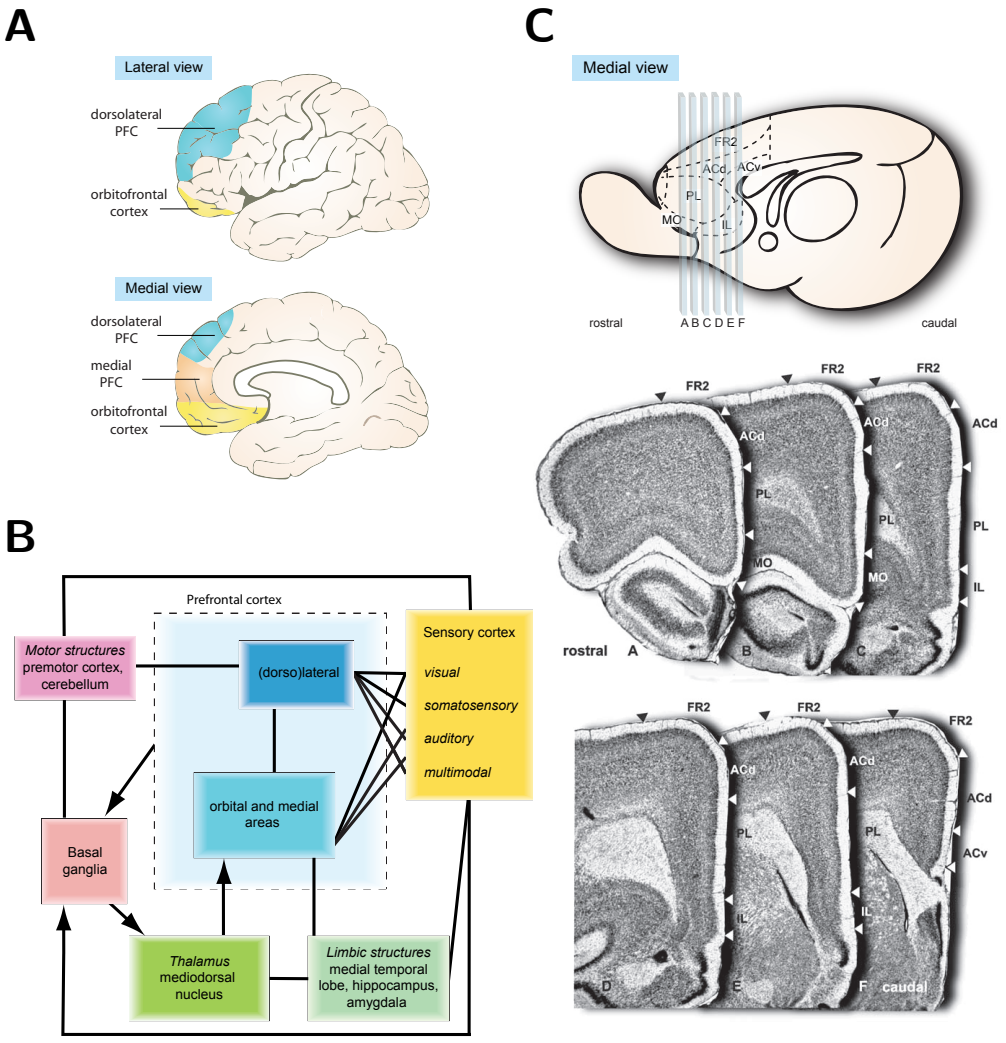

Figure 1.2: The prefrontal cortex in humans and rats. (A) Location of the major PFC areas in the human brain. Adapted from Sanfey (2007). (B) The principal connections of the PFC with subcortical and other cortical areas. Arrows indicate one directional projections. Adapted from Miller & Cohen (2001). (C) Slices of the rat brain containing the medial PFC. The upper part depicts the approximate position of the slices below. Abbreviations: ACd, dorsal anterior cingulate area; ACv, ventral anterior cingulate area; FR2, frontal cortex area 2; IL, infralimbic area; MO, medial orbital area; PL, prelimbic area. Upper part adapted from Krettek & Price (1977) and lower part from Heidbreder & Groenewegen (2003).

1.2.3 Specific characteristics of the rat prefrontal cortex

In general, rats have a smaller cortex than primates. Moreover, rat cortical areas are less differentiated. These anatomical differences led to a lot of discussions about whether or not particular cortical areas in the rat brain are comparable with cortical areas in primates. Naturally, also the question came up whether or not rats possess a prefrontal cortex like primates. The rat PFC is also divided into lateral, medial, and orbital regions. It is, however, the rat medial PFC (mPFC) that is supposed to be analogous to the primate PFC (Uylings et al., 2003). That is why most experimental work on prefrontal function in rats has been devoted to the mPFC.

There exists a main subdivision of the rat mPFC into a dorsal component, including frontal cortex area 2, the dorsal anterior cingulate area, and the dorsal part of the prelimbic area; and a ventral component that encompasses the ventral prelimbic, infralimbic and medial orbital areas (Fig. 1.2C and Öngür & Price, 2000; Heidbreder & Groenewegen, 2003). Comparable with the entire primate PFC (Fig. 1.2B), the dorsal mPFC has connections with sensorimotor and association neocortical areas; the ventral mPFC rather lacks such connections. Instead, the ventral areas have extensive connections with the amygdala and limbic cortices and "limbic" subcortical structures such as the hypothalamus. The rat mPFC serves functions, being implicated in attentional processes, working memory, and behavioral flexibility.

1.2.4 Neuromodulatory inputs to the prefrontal cortex

Prefrontal function is affected by innervation from all brain areas that produce typical neuromodulators (see, e.g., Bear et al., 2007). Dopamine has most relevance for the present work and is therefore described with more detail. Dopamine and its modulatory influence on the PFC will be the topic of the upcoming chapter. Here I give an overview of the main dopaminergic brain systems and pathways, extending the description somewhat beyond the PFC. First of all, however, the other three main modulatory agents are briefly introduced.

Serotonin. The serotonergic innervation of the cerebral cortex originates mainly from the raphe nuclei. Serotonin facilitates motor functions and is related to the control of the sleep-wake cycle. It has, e.g., been reported to enhance the gain of the input-output response of prefrontal pyramidal neurons *in vitro* (see Sec. 3.4 and Zhang & Arsenault, 2005) and might be relevant for working memory (see Chapter 3 and Williams et al., 2002).

Noradrenaline. The PFC shares reciprocal innervation with the locus coeruleus from where it receives noradrenergic innervation. Noradrenaline can decrease

basal neuronal activity and increase extracellular levels of dopamine in the PFC (Heidbreder & Groenewegen, 2003).

Acetylcholine. Cholinergic diffuse modulatory systems arise from the basal forebrain complex and different brain stem nuclei. The basal nucleus of Meynert provides most of the cholinergic innervation to the neocortex. Acetylcholine heightens arousal in the PFC, which is required for processing of both sensorimotor information and spatial working memory. Muscarinic antagonists impair spatial working memory (Heidbreder & Groenewegen, 2003).

Dopamine The cell bodies of most dopamine (DA) producing cells are located in a small group of mesencephalic neurons in the substantia nigra pars compacta and the ventral tegmental area (VTA); Fig. 1.3 and Seamans & Yang, 2004; Bear et al., 2007. In total there are about 10,000 DA neurons in rats and 200,000 in rhesus monkeys and humans on each side of the brain. The dopaminergic cells send their axons to 1000 times more postsynaptic neurons in the forebrain and basal ganglia. This huge divergence is borne by the abundant ramification of DA axons. Such an axon has about 500,000 varicosities from which dopamine is released (Schultz, 2002, 2007b; Lapish et al., 2007).

Dopamine projections are subdivided into three major pathways (Fig. 1.3 and, e.g., Tzschentke, 2001): (1) DA neurons project from the substantia nigra pars compacta to the basal ganglia (nigrostriatal pathway); (2) the mesolimbic pathway arises from the VTA and projects to the ventral striatum including nucleus accumbens; (3) the mesocortical pathway also arises in the VTA but from a separate neuronal population and sends projections to the neocortex.

The basal ganglia, in particular the striatum, receive by far the densest dopaminergic input. Within the neocortex, motor cortical and prefrontal (especially orbitofrontal and anterior cingulate) areas are most densely innervated. However, dopaminergic input to primary sensory areas is virtually lacking. The mesocortical dopamine innervation has a laminar distribution: In rat prefrontal cortex, the deep layers V-VI receive strongest DA input while in primates superficial layers I-III are at least as densely innervated (Tzschentke, 2001).

Classically synapses in the central nervous system (CNS) are subdivided into symmetric and asymmetric synapses. Symmetric synapses (or Gray's type II) are characterized by darkened pre- and postsynaptic sides and found for inhibitory synapses. Asymmetric synapses (or Gray's type I) show only a darkened postsynaptic side and are found with excitatory synapses (Bear et al., 2007). About 80% of the dopaminergic synapses are symmetric, the rest is asymmetric. Since DA synapses show both characteristics, DA is neither a classical excitatory nor inhibitory transmitter. Dopamine is released from synapses that contact somatic and dendritic sites. Dopamine neurons synapse to the shafts of dendritic spines

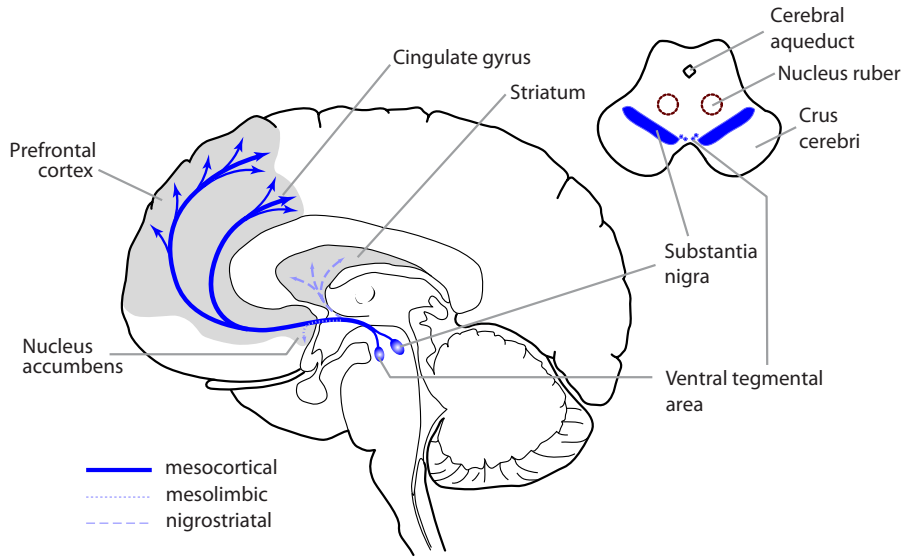

Figure 1.3: DOPAMINERGIC PATHWAYS. The picture shows projections from the substancia nigra to the dorsal striatum (nigrostriatal), from the VTA to the nucleus accumbens (mesolimbic), and from the ventral tegmental area (VTA) to the prefrontal cortex (mesocortical). In the upper right corner the dopaminergic nuclei on both sides of the brain are shown in a slice of the midbrain. As landmarks are given the paired crura cerebri and nuclei ruber as well as the cerebral aqueduct. Adapted from Trepel (2004); Hyman et al. (2006).

whose heads are innervated by glutamatergic terminals and contain DA receptors. This arrangement has been termed *synaptic triad* (Goldman-Rakic et al., 2000; Yao et al., 2008). More important, however, is the fact that DA synapses are not found in immediate proximity to DA receptors. To about 50%, DA is distributed via axonal varicosities that constitute unspecific release sites. From these DA has to diffuse in the tissue over longer distances to reach its receptor sites; one speaks of *volume transmission* (Seamans & Yang, 2004; Lapish et al., 2007).

It is worth mentioning that projections from the VTA are not only dopaminergic but may also use other neurotransmitters. In particular, only about 30% of the VTA-prefrontal projections are dopaminergic. The non-dopaminergic part of VTA projections to the PFC is on the one hand inhibitory, using GABA as its neurotransmitter; on the other hand, DA neurons exert excitatory input to PFC via glutamate that is co-released with DA (Seamans & Yang, 2004; Lavin et al., 2005; Lapish et al., 2007). Note furthermore that the PFC sends backprojections to the VTA, which exert both excitatory and inhibitory influences onto mesencephalic DA neurons (Gao et al., 2007).

1.3 Chapter summary

The present chapter introduced the PFC and its outstanding role in higher order cognitive functions, including working memory. Prefrontal areas show some specific histological, morphological and cellular features like extensive horizontal excitatory connections and reciprocal inhibition (Rao et al., 1999; Constantinidis et al., 2002), highly branched dendritic trees with a lot of spines (Elston, 2003) and synaptic facilitation (Hempel et al., 2000; Wang et al., 2006) putatively related to PFC function. In rats the mPFC is the region, which is the most comparable to the primate PFC and therefore received most attention in neuroscience studies. We also devoted our experimental work to the rat mPFC (Thurley et al., 2008b, in Part II).

CHAPTER 2

Dopamine and its relevance for the prefrontal cortex

Dopamine is one of the – if not the – most important catecholamine neurotransmitters in the mammalian brain. Since its discovery by Arvid Carlsson in the 1950s (Carlsson et al., 1958), dopamine has been found in a lot of vertebrate and invertebrate species. Mammalian mesencephalic (midbrain) dopaminergic cells generate dopamine (DA) as an intermediate product in the biosynthesis of the hormone adrenaline from the amino acid tyrosine. Three dopaminergic pathways (nigrostriatal, mesolimbic, mesocortical, see Sec. 1.2.4 for details) project from the mesencephalon to different brain areas, controlling a variety of brain functions involved in the reactivity of the organism to the environment (Tzschentke, 2001; Schultz, 2007b). Experimental studies suggest a role in locomotor activity, food intake, and endocrine regulation. Dopamine is important for the body's own reward system, hence drug usage and drug addiction are related to the dopamine systems (Hyman et al., 2006). It also acts peripherally, e.g., as a modulator of cardiovascular function, hormone secretion, and renal function (Missale et al., 1998). The influence of DA on the prefrontal cortex is related to cognition, emotion, and learning specifically reinforcement learning (reward and punishment). The impact on "higher order cognitive functions" especially working memory are

of particular interest for the present thesis (see Chapter 3).

The dopaminergic brain systems received a lot of research over the past decades, mainly because several pathological conditions have been linked to a dysregulation of dopaminergic transmission, most prominently Parkinson's disease and schizophrenia (see, e.g., Charney & Nestler, 2004). In Parkinson's disease degeneration of the nigrostriatal DA system leads to deficits in movement, cognition, and motivation. Dopamine receptor agonists are effective in alleviating the (movement) deficits in Parkinson's disease. The so-called cognitive symptoms of schizophrenia, i.e., distractability, attention deficits, and impaired working memory, have been linked to altered DA modulation of the prefrontal cortex. Dopamine receptor antagonists are used clinically to block hallucinations and delusions of schizophrenic patients (Charney & Nestler, 2004).

The present chapter describes actions of DA in the brain, focusing on the mesocortical dopamine system and its relevance for the prefrontal cortex (PFC). First, an overview is given of the different DA receptors and DA signaling. Then, I describe the DA modulation of neurophysiological properties *in vitro* and *in vivo* at the example of the PFC. At the end of the chapter, I briefly introduce some theoretical hypotheses on DA function. Computational implications are discussed with relevance to working memory in detail in Chapter 3.

2.1 Dopamine receptors

Dopamine receptors are G protein-coupled receptors, i.e., receptors that mediate their effects via a guanine nucleotide-binding protein (G protein) composed of three subdivisions α, β, γ. The G protein signalizes the binding of a ligand ("first messenger", i.e., external signal) to the receptor and stimulates intracellularly the production of a so-called *second messenger*. The second messenger is part of a cascade of processes that functionally modulate other receptors and ion channels, and/or induce gene expression. Thus, G protein-coupled receptors are metabotropic receptors, i.e., receptors that unlike ionotropic receptors do not form an ion channel pore themselves but modulate cellular properties through signal transduction mechanisms. That is why activation of DA receptors normally does not induce large postsynaptic currents rather slower, more subtle changes are observed. That is why DA can not be viewed as one of the classic, fast ionotropic neurotransmitters like glutamate or γ-aminobutyric acid (GABA). In case of DA the term *neuromodulator* is more suitable (Seamans & Yang, 2004).

Like all G protein-coupled receptor proteins DA receptors comprise seven transmembrane domains. The amino (N) terminal of the protein lies in the extracellular space; the carboxyl (C) terminal is located intracellularly (Fig. 2.1A). Five receptor subtypes exist in the central nervous system (CNS): D1, D2, D3, D4, and D5. The subtypes are grouped into two major classes based on the type

of coupled G protein and the length of the third intracellular loop and of the carboxyl tail (Fig. 2.1A; Missale et al., 1998; Neve et al., 2004) . The D1 family includes D1 and D5 receptors, having a short third intracellular loop and a long carboxyl tail. D1-class receptors couple to a "stimulating" G protein (G_s, G_{olf}, G_q). The D2 family comprises D2, D3, and D4 receptors, having a longer third intracellular loop and a shorter carboxyl tail. These receptors couple to an "inhibiting" G protein ($G_{i/o}$). If not indicated otherwise, I use the terms D1 and D2 receptors to refer to D1 and D2 receptors families, respectively.

In general, D1 and D2 receptors are found in a large number of brain areas, like striatum, nucleus accumbens, limbic system including the PFC, hypothalamus, and thalamus (Missale et al., 1998; Goldman-Rakic et al., 2000; Tzschentke, 2001; Seamans & Yang, 2004). Dopamine D1 receptors are the most widespread and abundant DA receptors in the brain. In the PFC, for instance, D1-class receptors are 20-fold more abundant than receptors of the D2 family. Dopamine receptors are found on PFC pyramidal and non-pyramidal neurons. However, the majority of DA receptors is located on pyramidal neurons. D1 receptors are located primarily on the dendritic spines and shafts of pyramidal neurons in proximity to glutamate receptors. GABAergic interneurons have D1 receptors on their distal dendrites and on their axon terminals. Dopamine D2 receptors are also found on the terminals of afferents from the ventral tegmental area (VTA), maybe constituting release-regulating autoreceptors (Yao et al., 2008).

2.1.1 Dopamine signaling

Dopamine D1 and D2 receptor families differ in their effects onto adenylate cyclase (AC) and the concentration of cyclic adenosine monophosphate (cAMP). D1-like receptors activate AC and hence increase cAMP concentration; D2-like receptors have opposite effects (Fig. 2.1B1-3; Greengard, 2001; Neve et al., 2004; Seamans & Yang, 2004). Here I give a short overview of the principal DA signaling pathways that are active in the prefrontal cortex.

D1-receptors In general, D1 receptors can transfer their signals via two different pathways: Firstly, activation of the G_s and G_{olf} coupled D1 receptor is classically known to stimulate AC and the formation of cAMP. As second messenger, cAMP activates a protein kinase A (PKA)-dependent intracellular signaling cascade, in which PKA alters ion channel activity via two ways (Fig. 2.1B2): either it phosphorylates ion channels directly or the dopamine- and cyclic AMP-regulated phosphoprotein with molecular weight 32 kDa (DARPP-32) becomes activated and inhibits dephosphorylation of ion channels by protein phosphatase 1 (PP-1). Since in the phosphorylated state DARPP-32 is sustained for prolonged time, it is a candidate mechanism by which either delayed or prolonged responses to DA may be mediated. D1 receptor stimulation also induces expression of

transcription factors, which take part in the control of gene transcription and protein synthesis. Some transcription factors depend on the cAMP response element-binding protein (CREB) that is phophorylated by PKA (Fig. 2.1B2). Since CREB has to be primed by Ca^{2+}, it offers a site for integration of DA and N-methyl-D-aspartic acid (NMDA) signals, providing a candidate mechanism for gene expression related to synaptic plasticity.

Secondly, the D1 receptor can be coupled to the protein kinase C (PKC)-pathway through a special protein, calcyon, primed by Ca^{2+} influx (Fig. 2.1B1). Signaling here is mediated by a G_q protein which stimulates as a second messenger diacylglycerol (DAG) formation by phospholipase C (PLC); acDAG in turn activates PKC.

D2-receptors D2 receptors have opposite effects onto the pathways that are stimulated by D1 receptors. Adenylyl cyclase is inhibited by D2 receptors and hence both are opposed PKA and DARPP-32 activation. DARPP-32 can also be inhibited directly via a D2-PKC pathway (Fig. 2.1B3).

2.2 Dopaminergic modulation of prefrontal activity

The existence of dopaminergic terminals within the rat cortex has been first shown by Thierry et al. (1973). Since then a huge number of studies investigated the impact of DA onto prefrontal activity and function, revealing that DA is an important source of extrinsic modulation of the PFC. The most important features are described next.

2.2.1 Dopamine modulation of voltage-gated currents in vitro

Sodium channels. Dopamine lowers the action potential threshold in PFC pyramidal neurons and hence increases spike firing, by enhancing the slowly *inactivating, persistent sodium current*, I_{NaP} (Yang & Seamans, 1996; Gorelova & Yang, 2000, but see Maurice et al., 2001). The DA effect on I_{NaP} is mediated by a D1-PKC pathway (Fig. 2.1B1 and Neve et al., 2004; Seamans & Yang, 2004). Since the coupling between the D1 receptor and the PKC-pathway has to be "primed" by Ca^{2+} influx, preceding action potential firing is necessary. Hence I_{NaP} enhancement might occur with some latency but then acts as a mechanism for long-lasting potentiation of excitability (Chen et al., 2007). D1-mediated amplification of I_{NaP} has also been implied in increasing the amplitude of exitatory postsynaptic potentials (EPSPs) (Rotaru et al., 2007). Dopamine modulation seems to be restricted to slow sodium currents that affect excitability. It has, e.g., no effect on the fast voltage gated sodium current that underlies action potential waveform (Gulledge & Stuart, 2003).

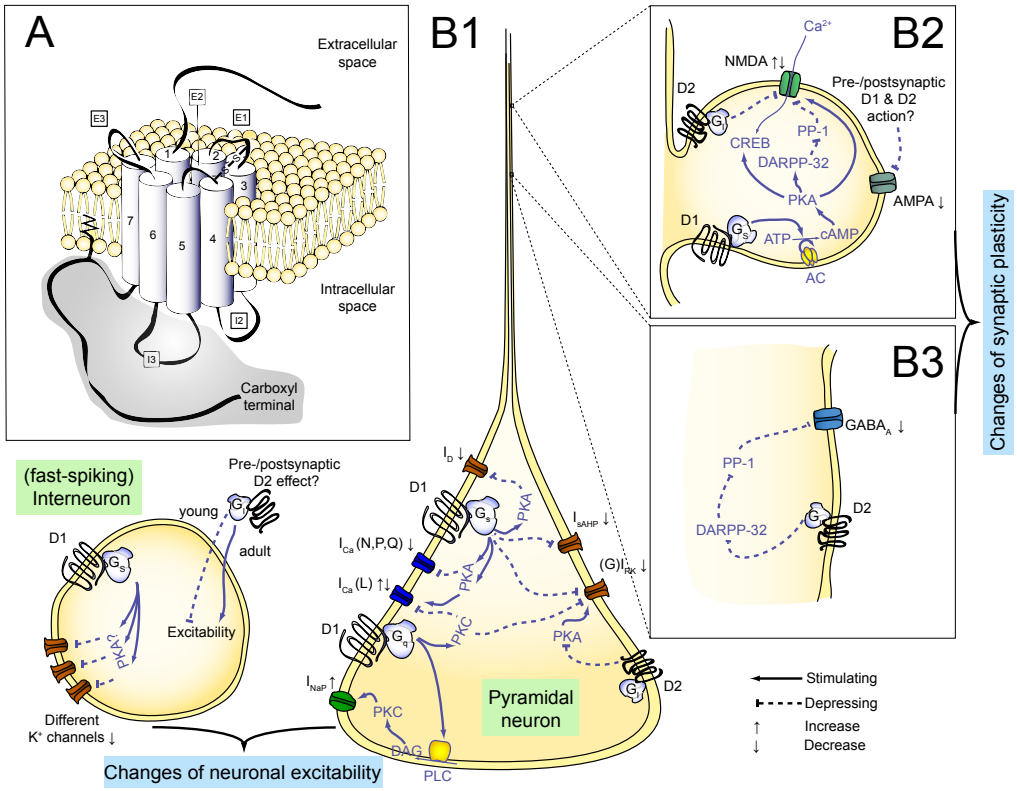

Figure 2.1: DOPAMINE RECEPTOR SIGNALING IN THE PFC. (A) Structure of a D1-like receptor. D2-like receptors are characterized by a shorter carboxyl terminal tail and a bigger 3rd intracellular loop (shaded area). 1-7, transmembrane domains; E1-E3, extracellular loops; I2-I3, intracellular loops. Adapted from Missale et al. (1998). (B1-3) Overview of the different signaling pathways of D1- and D2-like receptors. For clarity not all signaling steps are shown, rather – if known – the involved protein kinase (PKA/PKC) is given aside from a few more detailed examples. See text for details. Adapted from Missale et al. (1998); Neve et al. (2004); Lapish et al. (2007).

Potassium channels. The regulation of the firing threshold by the persistent sodium current is opposed by a *slowly inactivating, outwardly rectifying potassium current* (I_{D} or I_{KS}) in PFC pyramidal neurons. Bath application of D1 receptor agonists blocks I_{D} (Yang & Seamans, 1996; Dong & White, 2003). The suppression of I_{D} is due to D1 triggered phosphorylation of K^+ channels by PKA (Fig. 2.1B1, Neve et al., 2004; Seamans & Yang, 2004). In addition, DA blocks inwardly rectifying potassium channels (IRKCs) via synergistic D1 and D2 actions ($(G)I_{\mathrm{RK}}$, Fig. 2.1B1): (1) cAMP whose formation is stimulated by D1 receptors directly acts on IRKCs and (2) D2 receptors inhibit phosphorylation of IRKCs by PKA (Dong et al., 2004). In addition, G protein-coupled IRKCs, GIRKs, might be inhibited via D1-PKC (Witkowski et al., 2008).

D1 receptors enhance the excitability of fast spiking interneurons by suppressing different potassium currents, i.e., a voltage-independent leak, an inwardly rectifying and a slow K^+ current (Gorelova et al., 2002; Kröner et al., 2007). This D1 receptor mediated depolarization of interneurons can be reversed by subsequent application of a D2 agonist in slices from young rats (Gorelova et al., 2002). In adult animals, however, D2 receptor activation is synergistic with the D1-mediated excitability enhancement and is not restricted to fast-spiking interneurons (Tseng & O'Donnell, 2007). The mechanism that underlies D2 receptor mediated changes in interneurons remains unknown (Fig. 2.1B1).

Slow after-hyperpolarization conductance. We could show that D1 receptor stimulation reduces the slow after-hyperpolarization (AHP) (sAHP) that is triggered by repetitive firing at high rate (I_{sAHP}, Fig. 2.1B1; Thurley et al., 2008b, and Part II). The underlying signaling pathway remains unknown but may involve cAMP and PKA like in hippocampal pyramidal neurons (Pedarzani & Storm, 1995). The slow AHP is thought to reflect Ca^{2+}- and Na^+- dependent K^+ conductances that are involved in spike frequency adaptation and possibly take part in the modulation of neuronal output rates (Sah & Faber, 2002). Direct evidence is lacking that DA modulates Ca^{2+}- and Na^+- dependent K^+ conductances in the PFC (Seamans & Yang, 2004).

Calcium channels. Dopamine differentially affects various *high-voltage-activated calcium channels* (Yang & Seamans, 1996; Young & Yang, 2004). Such channels are present on apical and basal dendrites of cortical pyramidal neurons and can mediate calcium and/or NMDA spikes (Larkum et al., 1999b,a; Schiller et al., 2000; Nevian et al., 2007). D1 receptor stimulation leads to bidirectional modulation of dendritic calcium potentials via different intracellular pathways in PFC pyramidal neurons. L-type Ca^{2+} channels are potentiated transiently via the D1-PKA pathway and then suppressed by the D1-PKC pathway that becomes activated by the increased Ca^{2+} influx (Fig. 2.1B1; Young & Yang, 2004). Fur-

thermore, D1 receptors via PKA suppress N-, P-, and Q-type calcium channels in PFC pyramidal neurons (Fig. 2.1B1; Yang & Seamans, 1996).

2.2.2 Dopamine modulation of synaptic conductances in vitro

AMPA conductance. D1 receptor stimulation has been shown to slightly reduce exitatory postsynaptic currents (EPSCs) or EPSPs, respectively, of α-amino-3-hydroxy-5-methyl-4-isoxazolepropionic acid (AMPA)-receptors (Gao et al., 2001; Seamans et al., 2001a, but see Gonzalez-Islas & Hablitz, 2003). Activation of presynaptic D1 sites might underly the reduced glutamate release (Seamans et al., 2001a). However, the results are somewhat contradictory and are subject to neuron, synapse, and even species specificity (Seamans & Yang, 2004). D2 receptors might also be involved, suppressing presynaptic glutamate release and/or postsynaptic receptors (Fig. 2.1B2).

NMDA conductance. Dopamine exerts bidirectional effects on NMDA receptors in a concentration dependent manner. Low doses ($< 10\mu$M) of DA or D1 agonists potentiate NMDA EPSCs (Seamans et al., 2001a; Tseng & O'Donnell, 2004; Wang & O'Donnell, 2001; Zheng et al., 1999). At higher DA doses ($> 50\mu$M) the NMDA current decreases due to activation of D2 receptors (Seamans et al., 2001a; Zheng et al., 1999) or D4 receptors (Wang et al., 2003), respectively. Combined effects of DA on NMDA currents and glutamate release probability could make DA-modulation of synaptic input trains frequency- and duration-dependent: D1 agonists decrease single EPSPs that occur early in a train or series of EPSPs at low input frequency (mainly AMPA-mediated), yet enhance late depolarization and high-frequency inputs (Seamans et al., 2001a). Another indication is the D1-dependent enhancement of EPSPs at depolarized membrane potential (Rotaru et al., 2007). Thus, DA may favor sustained high frequency as opposed to brief and/or low-frequency inputs (Durstewitz & Seamans, 2002).

One important feature of the D1-NMDA modulation *in vitro* is its delayed onset and prolonged duration. The D1 influence comes to effect with a latency of several minutes after the offset of agonist application and lasts for tens of minutes, even up to hours (Seamans et al., 2001a). Initially, the response is thought to be mediated by delayed PKA mediated activation of DARPP-32, which in turn inhibits the dephosphorylation of NMDA currents by PP-1 (Fig. 2.1B2). The long-lasting response then involves activation of Ca^{2+}-dependent kinases and phosphatases that in turn activate transcription factors like CREB to trigger protein synthesis for structurally changing dendritic spines (Fig. 2.1B2; Seamans & Yang, 2004). In line with this the expression of NMDA receptors on the surface of prefrontal pyramidal neurons was shown to be increased by D1 receptors (Gao & Wolf, 2008). Activation of D2 receptors reduces NMDA currents (Wang et al., 2003; Tseng & O'Donnell, 2004).

$GABA_A$ conductance. Dopamine modulation of GABAergic responses in pyramidal neurons occurs presynaptically, either by increasing the excitability of interneurons via D1 receptors to enhance GABA release, or via D2 receptors to depress GABA release. Various biophysical mechanisms are involved, which realize a biphasic modulation of inhibitory postsynaptic potentials (IPSPs) in PFC pyramidal neurons (Gao et al., 2003; Gao & Goldman-Rakic, 2003; Gonzalez-Islas & Hablitz, 2001; Seamans et al., 2001b). Initially a D2-mediated decrease of the IPSP amplitude occurs, followed by an increase due to D1 receptor activation (Seamans et al., 2001b). In pyramidal neurons the D2 effect on the amplitude of inhibitory postsynaptic currents (IPSCs) is largely postsynaptic. It is mediated by a special pathway that involves downregulation of DARPP-32 and hence disinhibits $GABA_A$ receptor dephosphorylation through PP-1, leading to reduced $GABA_A$ currents (Fig. 2.1B3, Trantham-Davidson et al., 2004). In addition, D4 receptors reduce $GABA_A$ currents through inhibition of PKA (Wang et al., 2002). The effect of DA on IPSPs depends on the specific synapse that evokes the IPSPs. Gao et al. (2003) have shown that DA diminishes synaptic inputs from fast-spiking interneurons that innervate the soma and axon initial segment. However, DA amplifies inhibitory synaptic inputs from non-fast spiking interneurons which make contacts with the dendrites of pyramidal neurons. Underlying this interneuron-subtype specificity might be postsynaptic $GABA_A$ receptors and their different subunit compositions that can be modulated differentially by several types of protein kinases and are potential targets of DA receptors.

Metabotropic neurotransmitter receptors. Dopamine also acts on metabotropic glutamate receptors, involved in long-term plasticity (Seamans & Yang, 2004). Direct dopaminergic influence on $GABA_B$ receptors has not been described. However, since $GABA_B$ activate GIRK channels, $GABA_B$ influences might be reduced by DA or D1 agonists (see Sec. 2.2.1 and Witkowski et al., 2008).

2.2.3 Physiological effects of prefrontal dopamine in vitro

Dopamine via D1 receptors has been shown to enhance the *excitability* of PFC neurons by bath application of DA or a D1 receptor agonist *in vitro* (Yang & Seamans, 1996; Shi et al., 1997; Henze et al., 2000; Lavin & Grace, 2001; Wang & O'Donnell, 2001; Tseng & O'Donnell, 2004) as well as by synaptically evoked DA release from terminals of VTA neurons *in vitro* (Lewis & O'Donnell, 2000; Chen et al., 2007) and *in vivo* (Lavin et al., 2005). Enhanced excitability in these studies typically refers to an increased number of action potentials evoked by injecting a depolarizing current pulse. On the network level, the excitability increase of single neurons results in DA-mediated changes of the spatial and temporal extent of evoked activity (Bandyopadhyay et al., 2005; Bandyopadhyay & Hablitz, 2007).

The dopamine mediated increase of excitability in PFC neurons has been reported to be *biphasic*, comprising "transient" – seconds to minutes – and longer lasting components – tens of minutes (Geijo-Barrientos & Pastore, 1995; Gulledge & Jaffe, 1998). Gulledge & Jaffe (1998, 2001) showed that it is possible to get both a decrease and an increase of evoked firing of PFC neurons by a single brief application of DA. Bath-applied DA initially reduced evoked spike firing via D2 receptors for several minutes and then reversed and stabilized at increased levels, mediated by D1 receptors. Biphasic effects of DA might be due to voltage-gated calcium channels (Sec. 2.2.1) as well as NMDA and $GABA_A$ synaptic transmission (Sec. 2.2.2).

Dopamine acts *bidirectionally*, i.e., it might be facilitatory or suppressive, depending on the membrane potential and/or the DA concentration – as is the case for NMDA-receptor modulation (Sec. 2.2.2). Bidirectional effects are related to the classical notion form working memory experiments *in vivo* that DA effects follow an inverted-U curve (see Sec. 2.2.4 and Goldman-Rakic et al., 2000).

Dopamine also influences *synaptic plasticity* in the PFC. It has even been suggested to enable the induction of long-term potentiation (LTP) by electrical signals that without DA lead to long-term depression (LTD) (Otani et al., 2003; Matsuda et al., 2006).

Furthermore, dopaminergic effects on PFC function are *age-dependent*, i.e., some DA effects change after puberty. For example, the induction of LTP, the D1-NMDA triggered up-state activity as well as the D2 receptor mediated excitability increase of prefrontal interneurons depends on the age of the animal (Gurden et al., 2000; Tseng & O'Donnell, 2005, 2007).

2.2.4 Dopamine modulation of prefrontal activity in vivo

Functional implications for the DA modulation of prefrontal activity *in vivo* have been mostly investigated in relation to working memory performance. In such experiments the subject has to remember a sensory stimulus for a delay of a few seconds and then respond accordingly. Working memory will be the topic of Chapter 3. Optimal working memory performance depends on D1 rather than D2 receptor activation. Depletion of DA within the PFC or antagonists of D1 but not D2 receptors dramatically reduce the performance of monkeys and rats in working memory experiments (Brozoski et al., 1979; Simon et al., 1980; Sawaguchi & Goldman-Rakic, 1991, 1994; Seamans et al., 1998). Furthermore, working memory performance depends on the DA concentration. Effects follow an inverted-U curve, i.e., there is a certain optimal concentration for which one gets maximum working memory performance. Low as well as high levels of DA or D1 receptor agonists produce deficits. These results might be due to sole D1 receptor activation (Goldman-Rakic et al., 2000; Vijayraghavan et al., 2007) or opposite effects of D1 and D2 receptors (Seamans & Yang, 2004). Biphasic and

bidirectional effects of DA *in vitro* correspond to the inverted-U curve *in vivo* (Sec. 2.2.3).

In single cell recordings *in vivo*, DA exerts a predominantly inhibitory effect on PFC pyramidal neurons. Specifically, spontaneous spike firing is suppressed by activation of projections from the VTA. The suppression has been suggested to be mediated by D2 receptors, since it is blocked by antagonizing D2 receptors. It might, however, not be due to simple DA release from VTA terminals; rather, the GABAergic component of VTA signals could play a role as well (Seamans & Yang, 2004).

Dopamine D1 receptors are necessary for the ability to preserve working memory items over delay-periods (Vijayraghavan et al., 2007). The function of D2 receptors, however, seems to be related to changes in working memory activity. Wang et al. (2004) found that in primate PFC, activity is selectively responsive to D2 agents in the response phase at the end of working memory trials. Furthermore, set-shifting is D2 receptor-dependent in rats, i.e., adapting to changes of the rule according to which the subject has to act in behavioral experiments (Floresco et al., 2006). Thus, D2 receptors seem to be important for flexibly changing contents of working memory or adapting to dynamic changes in the demands of the task. For more information about behavioral studies see the review by Floresco & Magyar (2006).

The discharge of VTA neurons and its relevance for PFC dopamine levels. Mesocortical dopamine neurons show two predominant patterns of firing activity termed *tonic* and *phasic*. Tonic activity of DA neurons consists of a regular spike firing pattern of a few Hertz. It maintains basal extracellular levels of DA in the nanomolar range within afferent regions when salient sensory stimuli are absent. During phasic activity, DA neurons increases their firing rates to about 20 Hz, resulting in significant increases of DA levels in target areas (Seamans & Yang, 2004).

Most DA neurons in the substantia nigra and VTA respond to food and liquid rewards, to visual and auditory reward-predicting stimuli, and to novel or unexpected stimuli. The response appears to code for the discrepancy between the reward and its prediction ("prediction error"). An unpredicted reward elicits an activation (positive prediction error), reward omission induces a depression at the time of the predicted reward ("negative error"), and a fully predicted reward elicits no response (Schultz, 2006).

At their terminals in the PFC, mesocortical DA neurons express lower levels of DA re-uptake transporters than DA neurons projecting to the striatum. The re-uptake transporters also have slower kinetics and are not placed close to DA release sites. Furthermore, DA synapses are distant to receptor sites. Thus, DA diffuses over longer distance and is cleared less rapidly from the extracellular

space. A DA "tone" is present in the PFC, extending DA presence and its potential influence considerably in time and space, compared with the striatum.

When DA midbrain neurons become activated phasically at the onset of working memory tasks (Watanabe et al., 1997; Schultz, 1998), their influence outlasts the initiating event and may be sufficient to alter currents in PFC neurons during the entire task period. The long-lasting elevation of DA is mirrored by the persistent action of DA mediated by DARPP-32 and other intracellular signaling mechanisms outlasting a brief drug application *in vitro*. Moreover, negative events increase prefrontal DA levels. All this is in conflict with the fast "prediction error" signal via VTA DA (Seamans & Yang, 2004). However, there is indication of a co-release of DA and glutamate in the mesocortical pathway, with the glutamate being a candidate for transmitting "prediction error" to the PFC and hence leaving DA simply with providing the processing environment via increased excitability (Seamans & Yang, 2004; Lapish et al., 2007).

2.3 Computational role of dopamine modulation in the prefrontal cortex

Dopamine and its modulation of brain functions received considerable attention from theoretical neuroscience, resulting in a multitude of hypotheses on its role.

The indication from *in vivo* experiments that DA signals a reward-prediction error (Schultz, 2002; Montague et al., 2004; Daw et al., 2006; Schultz, 2007a), naturally became appealing for reinforcement learning theories (Montague et al., 2004). Reinforcement learning is concerned with how organisms learn to select actions that maximize reward over time. Reinforcement learning mechanisms have been widely used, for example, in theories of the basal ganglia (see, e.g., Gurney et al., 2004). However, whether the phasic DA signal is in general more suited for maximizing reward or rather supports the discovery of the nature of unpredicted events and the development of new actions has been questioned (Redgrave & Gurney, 2006).

Phasic DA release in the PFC has been implied as a *gating signal* for updating working memory (Braver et al., 1999). In terms of reinforcement learning this corresponds to a positive reward-prediction error signal, i.e., the actual reward or state would be better than expected. However, as we saw above (Sec. 2.2.4), it remains unclear if the slow time course of DA in the PFC is suited for precise signaling of prediction error. The problem might be resolved by glutamate signals from the VTA (Seamans & Yang, 2004). However, other models indicate that the temporal aspects of PFC DA promote rather "locking against" than "gating of" new information to prefrontal networks (Durstewitz et al., 1999, 2000a; Brunel & Wang, 2001; Frank et al., 2001; Dreher & Burnod, 2002; Tanaka, 2002a,b; Gruber et al., 2006; O'Reilly & Frank, 2006).

Other hypotheses focused on the role of DA for increasing the *signal-to-noise ratio*, it was actually the first proposal for a role of DA in the PFC. Servan-Schreiber et al. (1990) elaborated this idea in a connectionist framework. Biophysical models, using attractor neural networks, confirmed and expanded the hypothesis to a reduction of *distractability* of working memory – the "locking against" new information. The biophysical models furthermore explain how the diverse and unrelated features of DA modulation in the PFC, converge on a common function, namely augmenting stability and robustness of working memory representations.

2.4 Chapter summary

The present chapter described dopamine as an neuromodulator that has major impacts on PFC function. Dopamine exerts its neuromodulatory role via a variety of influences on different voltage-gated and synaptic conductances in the PFC. A general notion is that DA increases the excitability of PFC pyramidal neurons and fast-spiking interneurons *in vitro*. Modeling studies suggest that this apparent contradiction might in fact help to increase the signal-to-noise ratio and reduce the distractability of working memory *in vivo*. Since most of the computational modeling on prefrontal function is devoted to working memory or at least borders it, I am going to describe the models in more detail in Chapter 3. It is, nevertheless, hard to directly draw conclusions from *in vitro* data – that, e.g., focuses on a single conductance – on the collective influence of DA, which is relevant for PFC network function *in vivo*. Focusing at the DA modulation of the input-output function of single PFC pyramidal neurons, we tried to circumvent this issue (Thurley et al., 2008b, in Part II).

The bath-application of DA used in *in vitro* studies like ours seems to be appropriate in view of the slow time course of PFC DA representing tonic rather than phasic signaling.

CHAPTER 3

Working memory as a function of the prefrontal cortex

In the literature on working memory, a frequently met example is the process of keeping in mind a newly read phone number until it is dialed and then soon forgotten. Working memory thus denotes the ability to keep events "in mind" for immediate need like guiding future actions (Goldman-Rakic et al., 2000).

In the 1940s, Donald O. Hebb postulated the segregation of short-term memory, i.e., a memory usually active for a few seconds, from long-term memory, i.e., the permanent inscription on the neuronal circuitry due to learning (Hebb, 1949). Such a strict distinction was shown not to be entirely valid by cognitive psychologists in the 1960s and 1970s. They introduced the concept of working memory, which includes short-term memory but puts emphasis on a second component, i.e., the manipulation of information instead of passive maintenance (Baddeley, 1992, 2003). Unlike long-term memory, working memory interfaces the utilization of acquired knowledge with ongoing perception. Therefore information, which is handled in working memory, may be the representation of a sensory stimulus or a memory item retrieved from long-term memory, or a combination of both. Since working memory encompasses the manipulation of information held in short-term memory, it bridges temporal gaps between perception and action allowing the or-

ganism to plan action based on memory. In this way, working memory constitutes what Joaquin M. Fuster calls "working with memory" or "remember for action" (Fuster, 2001).

Since the seminal neurophysiological experiments in the 1970s, working memory has been connected to the prefrontal cortex (Goldman-Rakic, 1995). The corresponding experimental evidence is the topic of the upcoming section. Afterwards, I am going to focus on the mathematical modeling of working memory. The last section of the chapter is devoted to a side topic being, however, relevant for the present thesis, namely *neuronal gain modulation*.

3.1 Neurophysiological experiments on working memory

Working memory in animals has been studied with *delayed response tasks*, in which first a stimulus is presented and then removed during a delay period of several seconds. Following the delay period, the animal must remember the stimulus in order to respond properly. More than thirty years ago, it was found in neurophysiological studies with awake behaving monkeys that cells in the prefrontal cortex (PFC) fire persistently during the delay period of delayed-response tasks, such cells were named memory cells (Fuster & Alexander, 1971; Kubota & Niki, 1971; Fuster, 1973). Persistent delay period activity is often specific to a particular type of information, and might, e.g., encode the presented cue, a forthcoming response, or an expected choice situation or reward. It therefore likely reflects the short-term storage and on-line manipulation of information for generating a forthcoming response (Goldman-Rakic, 1995).

In the classical experiments, visual-spatial information had to be retained and the response was made with a hand-movement – spatial working memory (Fuster & Alexander, 1971; Kubota & Niki, 1971). Meanwhile various other types of delay tasks have been designed. Goldman-Rakic and colleagues frequently used an oculomotor variant, in which monkeys are required to respond with eye-movements to visual stimuli (Fig. 3.1B; Funahashi et al., 1989; Rao et al., 1999; Constantinidis et al., 2002). Other experiments showed persistent activity in lateral PFC that was stimulated by visual-nonspatial, auditory, or tactile stimuli – object working memory (see e.g. Miller et al., 1996; Romo et al., 1999). Often different sensory modalities are combined in the PFC. Many neurons in lateral PFC are selective for both the identity and the location, or the color and the movement of visual stimuli (Rao et al., 1997; Rainer et al., 1998). Some neurons respond context-dependently to the same stimulus (Asaad et al., 2000). Even two temporally separate stimuli of different sensory modality (auditory and visual) can be associated (Fuster et al., 2000).

Not all prefrontal neurons are activated at the same time during working memory tasks, rather the intensity of activity changes throughout the delay

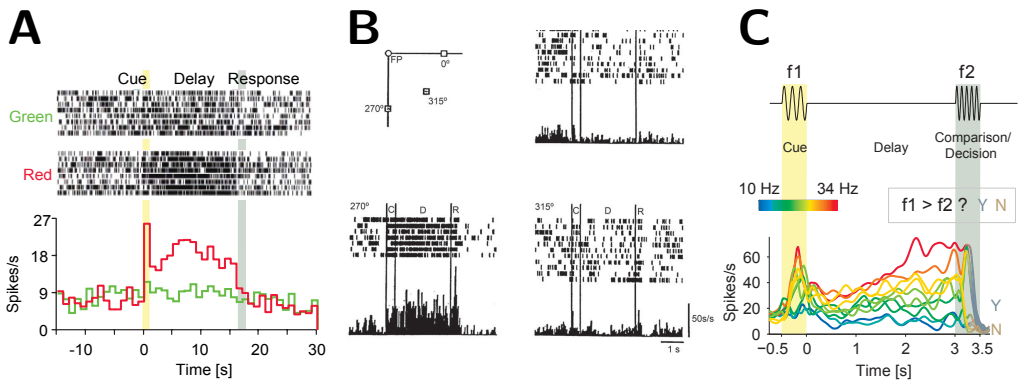

Figure 3.1: TYPES OF WORKING MEMORY. (A) Discrete working memory. A neuron in monkey inferotemporal cortex shows persistent activity when a red but not green colored visual object is presented. First panel and second panel are the response for green and red cue, respectively. Action potentials are given as tick marks. Rows are different trials. *Bottom panel:* Spikes per second averaged over different trials for responses to green and red cues. Adapted from Fuster & Jervey (1981). (B) Spatial working memory. In a delayed oculomotor task a prefrontal neuron is selective to cue presentation at a certain location, here 270°, of the visual field with respect to the fixation point (FP). In each panel, action potentials are given as tick marks, rows are different trials and a histogram is given at the bottom. For convenience data is only given for three angles of cue location. Adapted from Funahashi et al. (1989). (C) Parametric working memory. In flutter discrimination tasks a prefrontal neuron shows delay period activity proportional to the frequency of the presented cue. *Upper panel:* task design. A vibrating stimulus is given that has to be maintained for a delay period. After the delay a second stimulus is delivered and the monkey has to decide, which stimulus had the larger frequency. *Bottom panel:* Time development of the firing frequency of a PFC neuron over the different parts of the task. Adapted from Machens et al. (2005).

(Goldman-Rakic, 1995; Romo & Salinas, 2003; Durstewitz & Seamans, 2006). Some cells prolong their cue-triggered firing into the first part of the delay, but become silent before the response phase. Other neurons do the opposite, they are initially silent but increase their activity towards the end of the delay period. A third class of neurons spans the full interval between stimuli. The firing profiles of prefrontal neurons seem to correspond to the subfunctions of registration, memory, and motor control, respectively.

Different types of working memory are distinguishable (Fig. 3.1):

(A) Discrete working memory. Object or discrete working memory refers to the storage of a single feature of a stimulus object, e.g., the color or the meaning of a word (Fuster & Jervey, 1981).

(B) Spatial working memory. In spatial working memory, the location of a stimulus is stored. However, neurons selective to neighboring locations might also be somewhat activated, therefore the representation is not discrete (Funahashi et al., 1989; Goldman-Rakic, 1995).

(C) Parametric working memory. In parametric working memory the firing rate of neurons varies proportional to the stimulus parameter. An example are flutter discrimination tasks, in which the subject has to distinguish mechanically vibrating stimuli of different frequency (Romo et al., 1999; Romo & Salinas, 2003).

Working memory and other brain areas. Persistent delay period activity is not restricted to prefrontal areas (see, e.g., Fuster & Jervey, 1981; Romo et al., 1999; Fuster, 2001; Romo & Salinas, 2003). Persistent activity is found in both sensory and motor cortices. There is evidence that the PFC interacts with these other areas during working memory. There are neurons in somatosensory area S2, which show activity up to several seconds beyond the end of brief tactile stimulation. Likewise, delay period activity emerges for visual stimuli in inferotemporal cortex and for location in posterior parietal cortex. Some neurons in premotor cortex are active during the entire delay period, but usually premotor neurons increase their activity towards the end of the delay period. The hippocampal formation is also activated along with prefrontal areas during performance of working memory tasks. Neuronal activity in rat hippocampus is associated with certain responses of the animal in delayed response tasks (see Goldman-Rakic, 1995; Castner et al., 2004).

What appears to distinguish the PFC from the other areas is the ability to sustain activity in the face of intervening sensory stimuli (Miller et al., 1996). Sustained activity is easily disrupted by distractors in inferotemporal and posterior parietal cortices but not in the PFC.

Working memory in rats. As we saw above, working memory experiments with animals are usually performed in monkeys, i.e., non-human primates, which offer a close way to assess working memory mechanisms similar to humans. Nevertheless, working memory has also been investigated in rats. Spatial working memory could be tested in rats using radial arm mazes, figure-8 shaped mazes or open fields, where the animal is required to remember visited arms or places, respectively (Baeg et al., 2003; Castner et al., 2004; Euston & McNaughton, 2006). Auditory and sensory stimuli (vibrations) were also used to investigate working memory and delay activity in rats (Cowen & McNaughton, 2007).

Experiments in rats provided some indication that working memory is processed in populations of neurons in their medial PFC (mPFC). However, usually working memory tasks in rats evoke a strong co-activation of the hippocampus,

especially when a number of trials are necessary (Castner et al., 2004). The hippocampus might be recruited for memory consolidation that helps task solving. This of course limits the testability of working memory in rats or at least necessitates the careful design of tasks that indeed recruit working memory and can not be solve differently. Attention is further advised, since large portions of rat mPFC neurons show sensorimotor activity, e.g., related to head position, even during delay periods (Cowen & McNaughton, 2007).

Working memory in humans. Classically, working memory in humans was investigated with neuropsychological tests like the Wisconsin card sort test: A test person is asked to match cards from a deck with a variable number of colored geometric shapes. The cards can be ordered according to different rules, the "active" rule has to be learned by trial and error and is changed thereafter. People with prefrontal lesions have difficulties when the rules of tasks are changed during the experiment, revealing the importance of the PFC in working memory and task-switching. A large part of working memory studies in humans is related to pathological conditions. Deficits in working memory and prefrontal dysfunction have been demonstrated in schizophrenia, in Parkinson's disease, in age-related memory decline, and in many other neuropathological conditions in which impairments of higher cortical processing are expressed (see Miller & Cohen, 2001; Goldman-Rakic et al., 2000; Bear et al., 2007, and references therein).

Studies using positron emission tomography (PET) and functional magnetic resonance imaging (fMRI) revealed numerous prefrontal areas to be involved in working memory. The dorsolateral region, from which multielectrode recordings are made in macaque monkeys, is activated when human subjects carry out spatial working memory tasks. Moreover, regions of the dorsolateral and medial PFC are activated in non-spatial working memory. In agreement with microelectrode recordings in monkeys, neuroimaging studies in humans failed to demonstrate a clear specialization of separate prefrontal areas in spatial and nonspatial working memory. The activation of both PFC and hippocampal formation has also been reported (Miller & Cohen, 2001).

Dopamine in working memory. Using selective dopamine (DA) depletion already Brozoski et al. (1979) in primate and Simon et al. (1980) in rats indicated the importance of mesocortical DA in working memory. Moreover, D1 receptor antagonists reduce working memory performance (Sawaguchi & Goldman-Rakic, 1991, 1994; Seamans et al., 1998). Effects follow an inverted-U curve, i.e., there is a certain optimal concentration for which one gets maximum working memory performance; low as well as high DA levels produce deficits (Goldman-Rakic et al., 2000). For more details see Sec. 2.2.4.

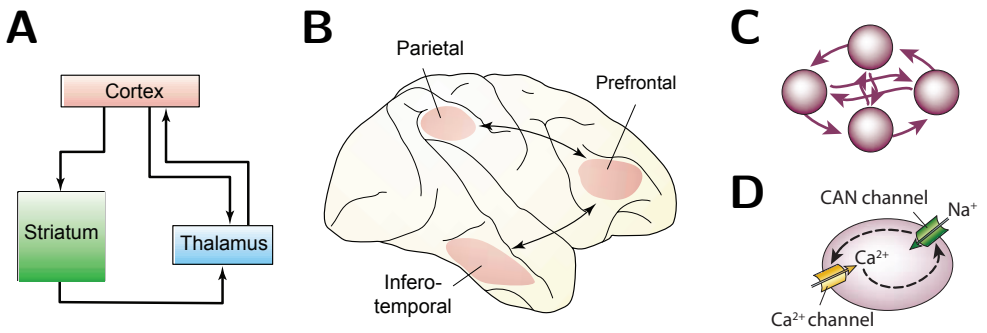

Figure 3.2: TYPES OF NEURAL REVERBERATIONS (A) Reverberations might occur in thalamo-cortical or cortico-striato-thalamic loops (arrows). (B) Activity reverberating between cortical areas might also underly persistent activity. (C) Recursive activity (arrows) might store memory items in a network of recurrently connected neurons (circles). (D) Persistent activity in single neurons might be triggered by Ca^{2+} that enters through voltage-gated channels and activates Ca^{2+}-dependent cation channels (CAN), through which, e.g., Na^{+} ions enter, excite the neuron, and close the feedback-loop. (A, B) adapted from Wang (2001); (C,D) adapted from Connors (2002).

3.2 Reverberatory activity and working memory

The *in vivo* recordings of persistent delay activity brought up the idea that some kind of reverberatory activity is underlying. The concept of reverberations was already contemplated in the 1930s by Lorente De Nó (1938). Donald O. Hebb later postulated a reverberatory mechanism for short-term memory in a local cortical circuit, which he termed *cell assembly* (Hebb, 1949). Since then this idea was investigated experimentally and elaborated by mathematical modeling (Goldman-Rakic, 1995; Wang, 2001; Durstewitz et al., 2000b; Compte, 2006).

Regarding the anatomical substrate of reverberations one can think of different scenarios (Fig 3.2):

(A) Reverberation between cortical and subcortical areas. Persistent activity could arise from reciprocal connections extending over cortical and even subcortical areas. For example, since thalamic neurons show elevated activity during delay periods of working memory tasks (Fuster & Alexander, 1973), thalamo-cortical loops are conceivable. However, it is unclear whether such subcortical mnemonic activity is merely inherited from persistently active PFC areas.

(B) Reverberation between cortical areas. It is also possible that different cortical areas form reciprocal loops to maintain persistent activity – an opinion favored by Fuster (2001). However, working memory experiments with interven-

ing/distracting stimuli showed that the PFC is capable of maintaining persistent activity by itself. Above it was already mentioned that distractors disrupt activity, e.g., in inferotemporal cortex, but not in PFC (Miller et al., 1996).

(C) Reverberation in a local circuit of cortical neurons. Another idea is excitatory synaptic reverberation within a network of recurrently connected cortical neurons (Goldman-Rakic, 1995). The idea goes in line with electrophysiological and anatomical data, possibly supporting reverberatory activity. It assigns a role to the extensive horizontal excitatory connections, the reciprocal inhibition (Rao et al., 1999; Constantinidis et al., 2002), and the particular short-term plasticity in the PFC (Hempel et al., 2000; Wang et al., 2006).

Experiments *in vitro* provided evidence for the ability of the neocortical circuitry to sustain activity through synaptic reverberations. Collective network activity ("up-states") occurs spontaneously in cortical slices (McCormick et al., 2003; Beggs & Plenz, 2003) and slice cultures (Seamans et al., 2003), or can be triggered electrically by distributed extracellular (Shu et al., 2003b) or direct single cell (Lau & Bi, 2005) stimulation. Elevated network activity ("up-states") has been implied as the *in vitro* counterpart for persistent delay activity *in vivo*. Dopamine modulation of single cell properties changes the spatial and temporal extent of similar *in vitro* network activity (Bandyopadhyay et al., 2005; Bandyopadhyay & Hablitz, 2007). Dynamic-clamp experiments provided furthermore insight into the conditions under which single cells are able to sustain activity (Fellous & Sejnowski, 2003). The studies support the relevance of N-methyl-D-aspartic acid (NMDA) receptors as suggested by modeling studies (but see Lau & Bi, 2005, for mainly α-amino-3-hydroxy-5-methyl-4-isoxazolepropionic acid (AMPA)-driven persistent activity). However, since its relation to true sensory stimuli *in vivo* remains unclear, persistent activity *in vitro* characterizes inner network properties rather than stimulus-triggered persistent activity. The activity also is just episodic and not truly persistent. Moreover, during the persistent state neurons fire with low-rate (usually about 1-5 Hz), corresponding to spontaneous activity in awake animals rather than persistent delay activity of several tens of Hertz (Compte, 2006).

(D) Cellular multistability. Feedback excitation is also conceivable on the single cell level in form of cellular bi- or multistability. First suggested from theoretical considerations (Marder et al., 1996; Camperi & Wang, 1998) cellular bistability has been confirmed experimentally meanwhile. Egorov et al. (2002) found that single layer V pyramidal neurons in the entorhinal cortex can self-sustain multiple graded levels of activity, relying on an activity-dependent Ca^{2+}-sensitive cationic current and the activation of cholinergic muscarine receptors. They found a similar phenomenon in amygdala neurons (Egorov et al., 2006). Recently, similar

single cell persistent activity was reported in layer III entorhinal cortex cells depending on metabotropic glutamate receptors (Yoshida et al., 2008). Graded persistent activity has been shown in PFC neurons, being driven by hyperpolarization activated cation currents, I_h (Winograd et al., 2008).

3.3 Computational modeling of working memory

The foundation wiring together all different modeling approaches is the maintenance of selective activity beyond stimulus presentation. Models of working memory can be broadly classified according to how persistent activity is generated. The classes correspond to the types of reverberations we got to know in the last section. However, they are not mutually exclusive. The most prominent mechanism is based on the idea that activity is sustained through strong recurrent excitatory connections in a small group of interconnected cells – a cell assembly (Hebb, 1949). Experimental work and biophysical modeling oriented mainly to this idea and our own modeling takes the same approach (see Part II). Therefore, I am going to focus mainly on this variant in the upcoming section. The other hypotheses I briefly describe are activity circulating in loops, called synfire chains; and models for cellular multistability. Recently, emphasis has been put onto another mechanism, namely the possibility to use synaptic short-term plasticity as a buffer for short-term memory. Finally, the impact of neuromodulation via DA will be described.

3.3.1 Recurrently connected neural networks

Dating back to the 1970s, theoretical modeling centered on the attractor framework to describe different activity states of a network of recurrently connected neurons (see Fig. 3.3A; Wang, 2001, and references therein). The basic principle underlies the Hopfield model for storing memory items in the synaptic weights of a neural network (Hopfield, 1982). In this model, neurons that collectively encode the same pattern are wired together reciprocally by strong excitatory synaptic weights, forming a cell assembly; whereas neurons that participate in different representations are connected by weak synaptic weights. These synaptic connection patterns can be acquired by Hebbian learning that reinforces connections between co-active neurons through long-term potentiation. Working memory – or better its short-term memory aspect – would correspond to the activation of one of the synaptically stored patterns and the retention of that activity. In a seminal study, Amit & Brunel (1997) elaborated the approach, by separating excitatory and inhibitory cell types, and by adding biological plausible descriptions of single cell and synaptic properties. Let us consider the general idea by means of Figure 3.3:

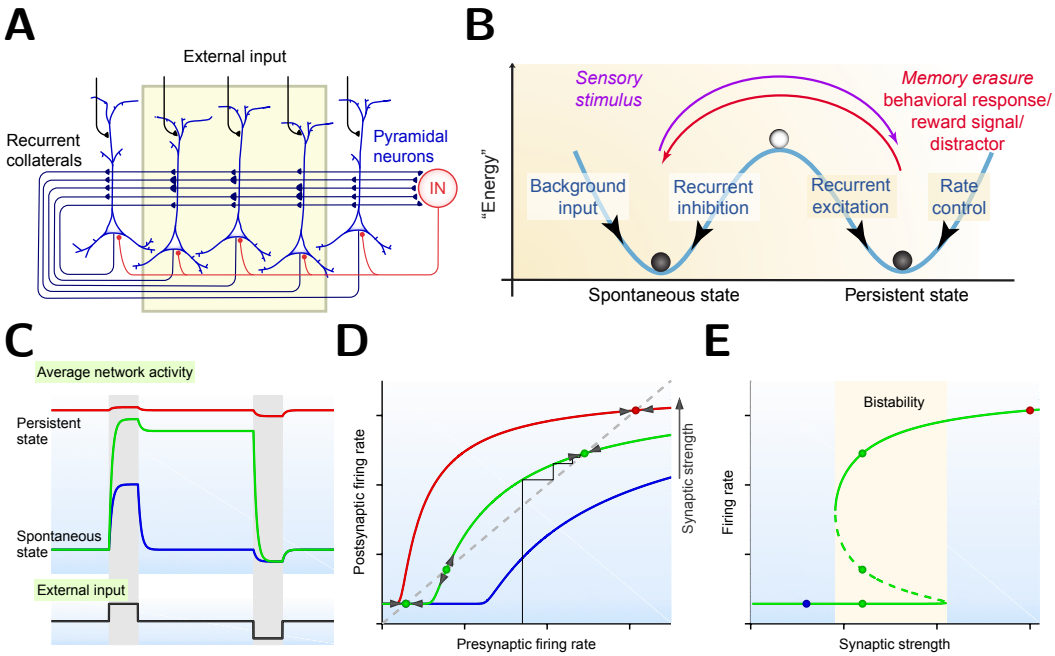

Figure 3.3: PERSISTENT ACTIVITY IN A RECURRENTLY CONNECTED NETWORK (A) Architecture of a model network. Pyramidal neurons are connected by recurrent collaterals via excitatory synapses of different strength (represented by the size of the triangles). A subpopulation that is selective for a certain stimulus is connected by strong synapses (highlighted area). Interneurons (IN) can be included to deliver feedback inhibition. From external excitatory input is delivered when a stimulus is present or inhibitory input is injected to signal a distracting stimulus or the transition into the response phase. (B) Schematic illustration of bistability. One can think of an energy landscape, in which stable states correspond to minima. There are the two stable and one unstable fixed-point. (C) Average response of the model network (upper panel), to external input (lower panel). See main text for details. (D) Mean-field representation. The network input-output relationship is given as a function of the presynaptic input firing rate for 3 different levels of synaptic strength (colors like in (C)). Intersections with the bisection line are fixed-points of the system (colored circles). Arrow heads indicate their stability, i.e., pointing into for stable and away for unstable fixed-points. The thin black line gives the temporal evolution from an exemplary presynaptic firing rate. (E) Number of fixed-points and corresponding firing rates as a function of the synaptic strength. Stable fixed-points are given as solid lines, unstable are dashed. The range of bistability is highlighted. Colored circles correspond to (D). Part (B) is adapted from Wang (2001) and Durstewitz & Seamans (2008).

In its simplest form a recurrently connected network can assume two self-sustained activity states, i.e., activity states into which the network settles after some time without external input. Since these states are assumed time dependently, i.e., the network is attracted towards the particular state, they are called *attractors* – a term borrowed from dynamical systems theory. The coexistence of two attractors is termed *bistability*. In a working memory network two stable states represent, e.g., low spontaneous activity and elevated persistent activity – the state that represents memory storage. The average network behavior is schematized in Fig. 3.3B and plotted in Figure 3.3C (green trace): At rest the whole network shows spontaneous activity at a rate of a few Hertz. This corresponds to *in vivo* observations and is due to background input and recurrent inhibition that dominates excitation and keeps the network in the spontaneous state. A subpopulation of neurons – or cell assembly – that is embedded in a larger neural network is selective for a certain sensory stimulus. Upon stimulus presentation the subpopulation increases its activity, i.e., the neurons start firing with an elevated rate of a few ten Hertz. After stimulus withdrawal, activity is sustained through recurrent excitation between the interconnected cells – the memory trace of the stimulus reverberates in the network. Rate control mechanisms restrict the firing rate to biologically realistic levels. An inhibitory signal (negative input) can break down the elevated activity and force the network back into the spontaneous state. Such an input might either signal a distracting stimulus or that a response took place (feedback from motor areas and/or a reward signal).

The possibility of self-sustained persistent activity coexisting with spontaneous activity depends on the recurrent connections within the neuronal network. The recurrent connections have to transmit synaptic potentials that are strong enough and long-lasting to evoke action potential firing in the postsynaptic cell and hence feed the activity back into the network. Two limits can be found, which curtail the range of bistability, in terms of the strength of the synapses, i.e., the strength of the postsynaptic response (Fig. 3.3E): Below a certain synaptic strength only the spontaneous state exists. Above a second threshold only the high activity state is found, i.e., the whole network always is strongly/persistently active independent of external stimuli – think of an epileptic seizure as an illustration. In between the network can reside in one of the two activity states – it is bistable. Stimuli, however, have to be sufficiently large to drive the network from spontaneous to persistent activity. The same is true for inputs in order to disrupt persistent activity and drive it back to spontaneous levels.

What are sufficiently strong stimuli in the above sense? How do the two self-sustained activity states remain stable, e.g., why does not the low spontaneous network activity drive the network into the persistent state? And for which values of synaptic parameters do spontaneous and persistent states co-exist? These

questions can be addressed using a mean-field approximation to the model network with spiking neurons (Amit & Brunel, 1997). The problem of what are long-lasting stimuli in the above sense, is tackled in the paragraph "Importance of NMDA receptors" thereafter.

Mean-field approximation. The basic assumption in mean-field theory is that a single cell reflects the average behavior of all cells in a homogeneous group of neurons of a network. Therefore one can look at the response dynamics of a single cell exemplary for the whole group. Using the input-output function of a single cell weighted with the synaptic parameters (time constants and amplitude of the postsynaptic potential), one gets the input-output function of the network. Since a single neuron receives input from as well as provides output to the network it is embedded in, self-sustained states are assumed, when the input equals the output. In Figure 3.3D this is described via the pre-/postsynaptic firing rates as input/output parameters. Examples are given for three different synaptic strengths (color coded). Self-sustained states, i.e., fixed-points, of the system are the intersections with the bisection line. The synaptic strength determines the gain, i.e., the steepness, of the input-output function.

For small synaptic strength only one fixed-point exists representing spontaneous activity (blue line and circle in Fig. 3.3D). Correspondingly, the network just shows one state of activity and cannot sustain firing beyond stimulus presentation (blue line in Fig. 3.3C).

For intermediate synaptic strength three fixed-points exist (green line and circles). The low one represents the spontaneous and the high one the persistent state. The third fixed-point in between the two others is unstable and will never be assumed under realistic conditions, i.e., when noise is present. Rather this unstable fixed-point divides the ranges of presynaptic firing rate for which one of the two other states is reached. For presynaptic firing larger than the middle fixed-point the system will drift into the upper fixed-point (black solid line in Fig. 3.3D); for smaller values the lower fixed-point will be reached. To the picture, transient external inputs can be added via the presynaptic firing rate – oversimplifying a bit but providing an intuitive idea, how the state of the network can be changed: A brief positive input leading to a presynaptic firing rate that is larger than the middle fixed-point drives the network from the spontaneous into the persistent state. A brief negative input that reduces presynaptic firing below the middle fixed-point breaks persistent activity down to spontaneous levels. Thus, the necessary input level is given by the distance of the two stable fixed-points from the unstable fixed-point in between both. Another intuitive understanding can be gained, when the stable states are viewed as minima in an energy landscape. The unstable fixed-point then is the energy level that has to be overcome to reach the other stable state (Fig. 3.3B).

When the synaptic strength is very large only the upper fixed-point exists and the network always resides in the high activity state. With that in mind we see that Figure 3.3E simply plots the number of fixed-points and the corresponding firing rate of the network as a function of the synaptic strength.

Importance of NMDA receptors. Beside the synaptic strength, the duration of synaptic activity is a second important factor for persistent activity in a recurrently connected network. Persistent activity is easier to realize and more stable, if the network's recurrent synapses are primarily mediated by slow excitatory synaptic currents (Durstewitz & Seamans, 2006). Slow excitatory inputs smooth out fluctuations that are caused by random presynaptic spiking. The result is a flat profile of the input current. Negative feedback processes, such as inhibition and synaptic depression, determine what means "slow" excitatory. AMPA receptor-mediated synaptic transmission has a time constant of about 5 ms and hence is about three times faster than γ-aminobutyric acid $(\mathrm{GABA})_\mathrm{A}$ inhibitory synaptic currents and 100 times faster than synaptic depression (Tsodyks & Markram, 1997). NMDA receptor-mediated currents have decay times in the order of tens of seconds and are ten times slower than AMPA currents. NMDA receptors were therefore suggested to be crucial for stable working memory (Wang, 1999; Tanaka, 2002a).

Furthermore, a larger relative contribution of AMPA versus NMDA receptor currents leads to more synchronized and less robust delay activity that is vulnerable to noise and interfering input (Wang, 1999; Compte et al., 2000; Brunel & Wang, 2001; Durstewitz et al., 2000a). Fast AMPA excitatory inputs necessitate larger amplitudes, i.e., synaptic strength, to maintain persistent activity. However, at the upper end of the range of synaptic strengths for bistability, the network activity shifts from asynchronous spike discharge into synchronous oscillations (Mongillo & Amit, 2001).

Physiologically plausible spike rates. Another problem for working memory models is to keep activity at physiologically plausible spike rates that are in the range of *in vivo* observations, i.e., between 15 and 40 Hz. Biophysical mechanisms that possibly control the firing rates in such networks include feedback inhibition (Amit & Brunel, 1997), short-term depression (Giudice et al., 2003) and saturation at high firing rates, e.g., by saturation of the input-output function through intrinsic cellular properties (Fusi & Mattia, 1999; Brunel, 2000).

Other forms of attractors

Bump attractors. In spatial working memory experiments like oculomotor tasks, prefrontal neurons show spatial tuning curves, i.e., they respond maximally when

a stimulus is presented at a certain location, the response for other locations decays as a function of the distance to the location of maximal response (Fig. 3.1B; Funahashi et al., 1989; Rao et al., 1999; Constantinidis et al., 2002). Bistability of two discrete attractor states can not account for such experimental results. Continuous attractors have to be introduced.

So-called bump attractors arise, when a network's neurons are interconnected, such that the strength of synaptic connections, a particular neuron shares with another, decays as a function of the distance between their locations of maximal response (Camperi & Wang, 1998; Compte et al., 2000; Gruber et al., 2006). Bump attractors are not entirely stable. In presence of noise the activity drifts in the network over time like a random walk, activating neurons that are not selective for the initial stimulus – that means information gets lost.

True continuous attractors or line attractors In parametric working memory tasks, like flutter discrimination, subjects have to remember the frequency of a vibrating tactile stimulus. The frequency can vary monotonically and PFC neurons respond with monotonically valued delay firing rates (Romo et al., 1999; Romo & Salinas, 2003). Such continuously valued stimuli can be coded in networks which create a *line attractor*, i.e., a continuous number of attractor states that the network can assume. Line attractors have been described in different models (Seung et al., 2000; Koulakov et al., 2002; Miller et al., 2003; Machens et al., 2005, reviewed in Brody et al., 2003). Emergence of line attractors requires fine tuning of network parameters. Moreover, like bump-attractors, line attractors are vulnerable to perturbations. It is under investigation how fine tuning and stability can be realized in a biological plausible way (Koulakov et al., 2002; Machens & Brody, 2008).

Problems of attractor neural networks

The retention of persistent activity, however, simply represents the rather passive short-term memory aspect of working memory and most models do not account for a possible manipulation of memory content; with regard to changes of working memory content see also Sec. 3.3.5. Moreover, dynamical changes of delay-period firing or different types of activity profiles are mostly ignored and just start to be considered in computational models (reviewed in Durstewitz & Seamans, 2006). Another aspect that poses a significant problem for computational models of working memory is the fact that delay-type firing in the models is often very regular despite the inclusion of noise. A single neuron receives strong synaptic drive when the network is firing persistently at high rate. The strong drive pushes the cell constantly above the firing threshold and small fluctuations become less important. However, fine analysis of *in vivo* data showed highly irregular spiking during delay-phases (Compte et al., 2003). Irregular spike firing is hard to achieve,

at least with recurrently connected neural networks (Renart et al., 2007; Roudi & Latham, 2007).

3.3.2 Synfire chains

An alternative way to evoke persistent activity is a *synfire chain*, i.e, a wave of synchronous activity that travels through feedforward-connected subgroups of neurons arranged in a chain (Abeles, 1991; Diesmann et al., 1999). Activity propagates from subpopulation to subpopulation through asymmetric connections, i.e., groups have no direct feedback between successive groups. Closed loops might maintain activity within the chain. The concept of synfire chains is related to reverberations between different cortical and/or subcortical areas (Figs. 3.2A&B and Sec. 3.2).

3.3.3 Cellular multistability

Since recurrent excitation models and synfire chains rely on specific synaptic contacts formed by prior learning to maintain activity, accounting for the ability to generalize novel stimuli immediately poses a significant problem. A possible solution is cellular bistability, in which the single neurons itself and not the interconnected network show two different stable states (Fig. 3.2D). In such a model calcium enters the cell through voltage-gated Ca^{2+} channels during action potential discharge triggered by the working memory stimulus (Camperi & Wang, 1998; Fransén et al., 2006). The increased intracellular calcium activates Ca^{2+}-dependent cationic currents that lead to depolarization and further spiking, closing the positive feedback loop. The hyperpolarization activated potassium current, I_h, has been reported to serve a similar function in PFC neurons (Winograd et al., 2008). It, however, remains open, if cellular bistability indeed takes place *in vivo* and accounts for persistent activity or at least contributes to it.

The nonlinear current-voltage relationship of the NMDA receptor, comprising two zero voltage-crossings, could also provide a basis for bistability. Lisman et al. (1998) showed that the magnesium block of NMDA receptor channels can be removed in stimulus selective neurons, since these are more depolarized than non-selective neurons during stimulus presentation. As a result the selective group of the network shows enhanced synaptic reverberations and persistent activity (Lisman et al., 1998). In fact, this mechanism adds to the necessity of NMDA receptors for persistent activity in recurrently connected networks discussed above (Sec. 3.3.1).

3.3.4 Working memory with a short-term memory buffer

Recently, Mongillo et al. (2008) introduced the possibility of using synaptic facilitation for working memory. Synapses between prefrontal pyramidal neurons

show particular short-term potentiation, i.e., facilitation, lasting several seconds (Hempel et al., 2000; Wang et al., 2006). This feature is of particular interest, since synapses between cortical pyramidal neurons are usually thought to be simply depressing. Hempel et al. (2000) suggested that facilitation might simply enhance the ability of neural networks to sustain persistent activity. Mongillo et al. (2008), however, propose that facilitation could directly be used as a buffer for short-term storage. In the model a subpopulation of neurons in a recurrently connected network is selective for a stimulus and gets facilitated upon stimulus presentation, i.e., the memory is short-term stored in the synapses. A read-out signal would activate the subpopulation and reveal the stored memory item. Since in the model the memory fades away with the time constant of facilitation, no explicit external signal is necessary to remove an item from memory. The mechanism however relies on a specific synaptic matrix formed by prior learning to maintain activity. Why this predefinition is necessary and why synaptic facilitation can not directly be used to associate the cell assemblies remains unclear.

The use of facilitation as a short-term buffer for sensory input, has been used by Thurley et al. (2008a) to explain the occurrence of the theta phase precession phenomenon in the hippocampus.

3.3.5 Neuromodulation in models of working memory

Neuromodulation in the prefrontal cortex usually refers to or at least is related to the dopaminergic input from the mesencephalon. I already mentioned some of the hypotheses on the role of dopamine in the brain in Chapter 2. Here I am going to discuss in more detail the hypothesis of DA modulation of working memory. For the sake of completeness and since it displays the foundation of the theory of dopamine function in the PFC, let us first of all take up the topic of dopamine and the signal-to-noise ratio.

Connectionist models. The first computational models on the function of dopamine proposed that it might increase the signal-to-noise ratio, i.e., the differentiation between background firing and firing due to afferent stimulation. This idea was formulated within a connectionist framework, and focused on information processing (Servan-Schreiber et al., 1990). Connectionist models use networks of interconnected units that are simply described by a neuronal input-output response function. Biophysical detail is left aside. Within this framework, DA effects were simulated as a change in the slope (or gain) of the input-output function of processing units. In presence of DA the signal-to-noise ratio of single neurons would not be improved but the signal-to-noise ratio at the network level. A more biologically justified variant of the model has been elaborated by Ashby & Casale (2003), using a theoretical approach coming from pharmacology.

Biophysical models. More recently, computational studies have focused on biophysically detailed accounts of DA action within the PFC. These models account for the cellular effects of DA (Secs. 2.2.1 and 2.2.2). In general, a model network of recurrently connected excitatory neurons is used similar to Figure 3.3. Subgroups of the pyramidal cell network are selective for different external stimuli, i.e., cells in the same subgroup are wired together by stronger synapses than cells of different subgroups, forming cell assemblies.

In a series of papers Daniel Durstewitz and colleagues addressed the effects of DA on the stability of persistent activity in such a network. They incorporate five experimentally observed effects of DA D1 receptors: an enhancement of the persistent sodium current, a reduction of the slow potassium current, a reduction of high-voltage calcium currents, a suppression of glutamatergic exitatory postsynaptic currents (EPSCs), and an enhancement of GABA inhibitory postsynaptic potentials (IPSPs). The first version (Durstewitz et al., 1999) uses simple leaky integrators and a firing rate output in a two compartment model (dendrite and soma) for the pyramidal neurons. The model was later extended to two (dendrite and soma) and three compartment versions (apical dendrite, basal dendrite, and soma) with a Hodgkin-Huxley-like description of the membrane dynamics (Durstewitz et al., 2000a; Durstewitz & Seamans, 2002). Additionally, it was taken into account that DA acts differentially on NMDA and AMPA currents, by increasing the first and decreasing the latter. The stability of persistent network activity was measured as the strength of a distracting stimulus that was necessary to break down persistent activity. Dopamine made persistent activity more stable, i.e., less susceptible for distractors. The D1-mediated conductance modulations made it more difficult to switch from persistent activity to spontaneous levels. One can think of an increase of the energy barrier between persistent and spontaneous networks states (Fig. 3.3B). The D1-induced increase in NMDA and voltage-dependent currents that push single cells closer to firing threshold boost recurrent excitation within the network, i.e., distracting stimuli can not disturb the cell assembly so easily. Concomitantly increased $GABA_A$ as well as the reduction of AMPA currents, makes it harder for external stimuli to evoke responses in the network and hence to be stored. Increased $GABA_A$ also accounts for the suppressive influence of DA on spontaneous activity as often found *in vivo* (Sec. 2.2.4).

Brunel & Wang (2001) proposed a similar network model, using recurrent synaptic excitation via NMDA receptors and feedback $GABA_A$ to get stable persistent activity, and to keep spontaneous background activity and spread of activity low. The single cells were described by integrate-and-fire neurons. They provided also a mean-field description of their network to investigate its properties quantitatively. With regard to DA modulation they focused on the effects on NMDA and $GABA_A$ synaptic conductances. Similarly to the results of Durste-

witz and colleagues, concomitant increase of NMDA and $GABA_A$ conductances led to a decrease of spontaneous activity and an increase of persistent activity. Brunel & Wang (2001) also tested a hypothesis, according to which NMDA receptors in pyramidal and interneurons are differentially affected by DA. The result was an inverted-U-shaped curve for persistent activity, corresponding to *in vivo* data (Sec. 2.2.4).

The former models mainly considered the maintenance of single memory items. Since working memory has the ability to deal with several items, Shoji Tanaka investigated the capacity for storing multiple items at once (Tanaka, 2002a,b). Out of excitatory and inhibitory integrate-and-fire neurons, he formed a typical network for spatial working memory, in which single units show direction specificity and stimuli are stored as bump attractors (Sec. 3.3.1). Modulatory input via D1 receptors, is modeled similar to the two models above, i.e., NMDA conductance is increased, AMPA conductance is decreased, persistent Na^+ current is increased, and slow K^+ current is decreased. The simulations show that the NMDA/AMPA ratio determines three different operational network states: (1) for low ratio a previously loaded item is replaced upon presentation of new one; (2) at intermediate levels, a new memory item is added; and (3) for high ratio new memory items are rejected from storage. In addition, Tanaka found that increasing the level of what he calls cross-inhibition, i.e., lateral inhibition between units coding for different directions, erases all stored working memory items.

Collectively the above models suggest that, although D1 receptors at first glance appear to regulate a number of diverse and unrelated neuronal features, all converge on a common function, namely augmenting stability and robustness of working memory representations. These models also point to the concept of a DA-induced increase of the signal-to-noise ratio in the connectionist model by Servan-Schreiber et al. (1990). An increased signal-to-noise ratio, here, means the differentiation between activity associated with active memory states and spontaneous activity. The model we implemented (Thurley et al., 2008b, and Part II) complements both the biophysical and the connectionist approaches, since a DA-induced change in the gain of the single neuron input/output function as in connectionist models directly translates into more stable persistent activity as in biophysical models.

Since the state of attractor neural networks is determined solely by the inputs, proper updating is problematic, i.e., stability against distractors implies also that overwriting stored information with new stimuli is hard. Attractor models therefore need to impose a special mechanism to flexibly switch between updating information with incoming stimuli or rejecting them. Durstewitz and colleagues (Durstewitz et al., 1999, 2000a; Durstewitz & Seamans, 2002) and Brunel & Wang (2001) use signals of the motor responses to break down persistent activity

and reset PFC. Tanaka more directly tackled this problem, proposing changes in the NMDA/AMPA ratio as a solution (Tanaka, 2002a,b). Another variant is opened up by the fact that D2 receptors often tend to act opposite to D1 receptors. In addition, *in vitro* D2 actions are more rapid and transient compared with D1 influences. So it is feasible that upon phasic DA release transiently and relatively locally D2 receptor actions open the gate for updating working memory activity and then D1 receptors take over to stabilize the updated network again (Durstewitz & Seamans, 2008). Other possibilities are discussed next.

Gating hypothesis. Several studies proposed that DA release may "gate" access to the PFC by modulating the influence of its afferent connections. By amplifying external input via phasic DA, Braver et al. (1999) use DA as a gate that facilitates read-in to working memory. However, since DA projections to the PFC are diffuse and the dynamics of DA in the PFC is relatively slow, the phasic DA release might not be appropriate to enable rapid updating of working memory content (see 2.2.4).

Dreher & Burnod (2002) proposed a network model with simple firing rate neurons in which DA increases the threshold for incoming stimuli. Tonic DA sets the baseline level of the threshold and therefore the general responsiveness to stimulation. Phasic DA increases the threshold transiently, making the network less susceptible to distractors.

Some computational models proposed that the basal ganglia may serve as a gate for information entering the PFC. Recently, *in vivo* experiments supported this hypothesis (McNab & Klingberg, 2008). In some models, DA was simply incorporated as a training signal (Frank et al., 2001; O'Reilly & Frank, 2006). Gruber et al. (2006), however, included the short-term modulatory effects of DA in the basal ganglia. They used a model of spatial working memory, which was implemented in the standard way resulting in bump attractors to store memory items (Sec. 3.3.1). They further included the basal ganglia as gating the access to PFC working memory. Dopamine effects were modeled as a gain increase in PFC pyramidal neurons and as a shift to cellular bistability in basal ganglia medium spiny neurons. Sole DA modulation of the PFC reduced the distractability by external input. Concomitant DA modulation of the basal ganglia reduced the effect of internal noise in the model by Gruber et al. (2006), stabilizing the bump attractor. As second effect, the bistability of basal ganglia neurons further reduces the influence of external inputs and hence the distractability, i.e., "the basal ganglia lock the gate to working memory". Dopamine as a way to curtail rather than to directly gate access to working memory, in the sense of the Dreher & Burnod (2002) and Gruber et al. (2006) is similar to what is proposed by the biophysical/attractor models above.

O'Donnell (2003) proposed that up-state activity triggered by D1-NMDA

interactions might as well take over gating mechanisms, when one divides phasic from tonic DA signals. In accord with that idea is the proposal by Seamans & Yang (2004) that ventral tegmental area (VTA) neuron firing could signal errors in reward predictions via glutamate release and exitatory postsynaptic potential (EPSP) generation in PFC.

3.4 Neuronal gain modulation

Our brain needs to adjust the relationship between variable input and output that is limited to range of amplitudes. Think, for example, of the adjustments our visual system performs between daylight and dark nights. Such adjustments are termed *gain modulation*. At the neuronal level, gain modulation is not a simple enhancement or suppression of neuronal responses by excitation or inhibition, which would shift the neuronal input-output function of a neuron in an additive fashion. Gain modulation is a change in the slope of the input-output function, corresponding to a multiplicative or divisive scaling. Gain modulation is a widespread phenomenon in the cortex and in subcortical structures. Cellular responses in the parietal cortex to sensory stimuli are gain modulated by eye and head position. Gain modulation has further been implicated in eye and reaching movements, attention, navigation, and object recognition (reviewed in Salinas & Thier, 2000; Salinas & Sejnowski, 2001).

3.4.1 Mechanisms for neuronal gain modulation

How does neuronal gain modulation arise biophysically? Different mechanisms have been reported:

Background noise. Chance et al. (2002) showed in a seminal study how synaptic background noise can change neuronal gain. Changing the net conductance of the neuron alone (i.e., a shunt), simply shifts the input-output curve, because of simultaneous decreases in membrane input resistance and time constant. However, noisy background synaptic current composed of balanced excitatory and inhibitory inputs so that no change in the total conductance occurred, decreases the neuronal gain by a constant scaling factor. The larger the noise, the more gain-decrease. Other groups later confirmed that the composition of background synaptic activity of excitatory and inhibitory can modulate the input-output properties of single neurons (Fellous et al., 2003; Rauch et al., 2003; Shu et al., 2003a).

Higgs et al. (2006) and Arsiero et al. (2007) showed that noisy inputs can increase the gain of the input-output function. In these studies, the gain increases monotonically with the fluctuation amplitude of the input current. We got similar

results, which were, however, not altered by dopamine (Thurley et al., 2008b, and Part II).

Shunting inhibition. Chance et al. (2002) reported tonic (shunting) inhibition not to affect the gain during tonic excitation. However, shunting inhibition can reduce the gain of input-output relationships when realistic synaptic waveforms are used as inputs rather than tonic inhibition (Mitchell & Silver, 2003).

Dendritic input. In cortical layer V pyramidal neurons, input to the apical dendrite results in gain changes of the neuronal input-output function (Larkum et al., 2004). Sodium action potentials that back-propagate into the apical dendrites of layer V pyramidal cells can activate dendritic calcium conductances (Larkum et al., 1999a), which in interaction with dendritic depolarization leads to a gain-increase of the input-output function.

Neuromodulators. Gain modulation is also possible with neuromodulatory substances. Nor-adrenaline and serotonin have been reported to increase the gain of cortical pyramidal neurons (Zhang & Arsenault, 2005; Higgs et al., 2006). Indications for DA inducing gain modulation in PFC layer V pyramidal neurons were found by Lavin & Grace (2001). Using square pulses of few hundred milliseconds, they found a gain-increase after DA administration. We confirmed these findings and proved that a DA mediated gain increase is not counteracted by noisy inputs (Thurley et al., 2008b, and Part II).

Slow after-hyperpolarization. Conductances contributing to slow adapting processes and the slow after-hyperpolarization (AHP) (sAHP) are classically known to underly the increase of the neuronal gain (Viana et al., 1993). In their experiments, Higgs et al. (2006) directly suggested that the reduction of the sAHP by noise occludes slow firing rate adaptation in the order of several seconds and leads to a gain increase. Neuromodulators, that were reported to evoke gain-increase, generally also decrease the (slow) AHP. Gain-increase by serotonin is accompanied by a AHP reduction AHP (Zhang & Arsenault, 2005; Higgs et al., 2006). Similarly, we found dopamine to reduce the (slow) AHP (Thurley et al., 2008b, and Part II).

3.5 Chapter summary

Working memory, i.e., the ability to keep events “in mind” for immediate need like guiding future actions, is one of the best investigated functions of the PFC. Most experimental work has been performed in primates, finding persistently active neurons that are supposed to be involved in the storage of working memory

items. Like in our study, rats mainly have been used for *in vitro* experiments on cellular properties of the PFC and its modulation by neuromodulators like DA.

Excitatory synaptic reverberation within the network of recurrently connected cortical neurons is currently the most widely accepted hypothesis for the mechanism of persistent activity underlying working memory. Most computational modeling was addressed therefore to attractor neural networks. Dopamine has been suggested from such models to stabilize persistent activity and increase the signal-to-noise ratio. We also stayed in the attractor framework in our modeling approach. The modeling focuses on the DA modulation of experimentally measured input-output functions (Thurley et al., 2008b, in Part II).

Part II

Publication

CHAPTER 4

Dopaminergic modulation of the pyramidal cell response function and implications for working memory

Cognitive functions like working memory need to be investigated in behaving animals. However, the acute brain slice *in vitro* is the currently best established way for studying single neuron properties and its potential relevance in the living animal. Brain slices allow the detailed investigation of single neuron properties in an environment wherein the experimenter can control most influences. We attempted to mediate between the brain slice and behavioral phenomena relating single cell recordings *in vitro* to network phenomena *in vivo*. All methods, experimental and computational, were standard techniques of the particular field. We simply tried to exploit each approach and demonstrated how they could be used for interaction.

Here, I outline the aims, the results and the design of the study. Details are given in the attached paper, which was published under the following reference:

Thurley K, Senn W, Lüscher HR (2008) Dopamine increases the gain of the input-output response of rat prefrontal pyramidal neurons. J Neurophysiol 99: 2985–2997.

4.1 Aims of the study

As discussed in the Introduction (Part I), a lot is known about the dopamine (DA) impact onto different voltage-gated and synaptic conductances (Chapter 2). How the particular features integrate into the function of the whole cell has only been assembled in theoretical studies (Sec. 3.3.5). We sought at investigating the DA modulation of the response properties of individual prefrontal cortex (PFC) pyramidal neurons, which are relevant for understanding persistent network activity. These features can best be characterized by means of the input-output response function, i.e., the $f-I$ curve, giving the rate of action potential discharge as a function of the amplitude of the injected current. This approach treats the cell more or less as a black box, producing some output for certain input. Focusing on the DA influence of the $f-I$ curve, we tried to answer the following questions:

- Does DA simply shift the $f-I$ curve or is its gain (steepness) also changed?
- Are the effects D1 or D2 receptor mediated, or both?
- If both, what are the differential contributions of the receptor subclasses?
- Are the DA effects concentration-dependent? Do they follow an inverted U-curve?
- Do the DA effects depend on application time?

We furthermore wanted to understand how the experimental single cell data translate into network behavior underlying working memory and did neurocomputational modeling to answer the following specific questions:

- Do the DA effects on single cells translate in a significant way into network behavior?
- If yes, what do are the implications for persistent activity and working memory?

4.2 Results

Bath application of DA increased the excitability of the pyramidal cells by shifting the $f-I$ curve to lower input currents and increasing its gain. The DA induced effects were mediated by D1 receptor activation. Testing for different DA concentrations (25-100 μM), we found both to increase with the DA level the shift and the gain-increase of the $f-I$ curve. The DA modulation was stable for 25 min after the begin of application. D1 receptor activation also reduced the slow after-hyperpolarization (AHP) following action potential discharge at high rate. Since this was shown to directly correlate with gain-increase in somatosensory

cortex pyramidal cells (Higgs et al., 2006), we propose the slow AHP decrease to underly gain-increase by DA.

Incorporating our findings into a model neural network, we could show that the experimentally observed DA mediated gain-increase of the single cell input-output function facilitates and stabilizes persistent activity. A mean-field description of the network confirmed the simulation results and revealed how facilitation and stabilization arise:

- *Facilitation:* DA shifts the strength of the recurrent excitatory connections that is necessary for bistability to smaller values.
- *Stabilization:* DA enlarges the basin of attraction for the persistent activity state, i.e., it deepens the valley of the corresponding attractor in the energy landscape of the states of the neural network (see Fig. 3.3 for illustration).

Dopamine, moreover, increases the range of synaptic strength wherein bistability can be found, making the representation more robust against changes in synaptic strength. See also Sec. 4.5.2 in the Appendix for some extension of the mean-field approach presented in the paper.

4.3 Experimental approach

Electrophysiology. The experiments were done in acute brain slices containing the mPFC and taken from young adult rats (about p30, i.e., 30 days of postnatal age). Recordings were made from the soma of layer V pyramidal neurons located in the dorsal anterior cingulate and prelimbic parts of the mPFC (see Figs. 4.1A and 1.2C). The whole-cell patch-clamp method was used for recording (Fig. 4.1B). Recordings were performed in current-clamp mode, i.e., using current stimuli and recording at the same time the membrane voltage. The patch-clamp technique in all its variants has been extensively described in a lot of publications and textbooks (e.g., Numberger & Draguhn, 1996; Walz et al., 2002).

In vivo-like stimulation current. In the intact brain neocortical neurons are connected to a huge number of other neurons. Resting activity in such a network is characterized by spontaneous spiking of individual cells at random times and low rate. In a single cell one presynaptic spike evokes only an input of small amplitude compared to the firing threshold. The large number of small random inputs, however, results in a randomly fluctuating membrane potential. A slice preparation, in which a cell is almost completely torn out of its natural network, lacks ongoing spontaneous activity, therefore single cells have a smooth membrane potential. In order to overcome this essential difference between *in vivo* and *in vitro* conditions, we used a noisy stimulation protocol that we assume to resemble synaptic input *in vivo*. For a large number of excitatory and inhibitory

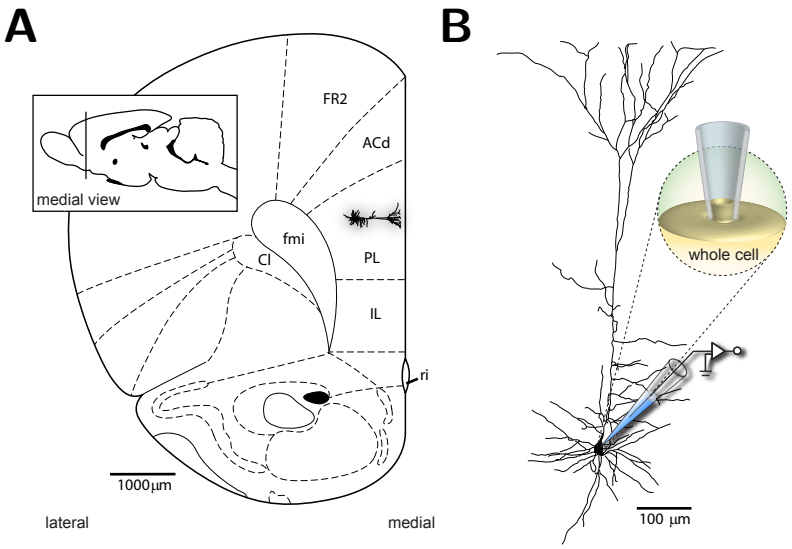

Figure 4.1: WHOLE-CELL PATCH-CLAMP OF PYRAMIDAL NEURONS IN RAT MPFC. (A) Coronal slice of the rat brain containing the mPFC. An example layer V pyramidal neuron is depicted at the approximate location from which cells were recorded, i.e., ACd and PL. In addition to mPFC areas, some anatomical landmarks are given. See also Fig. 1.2C. Abbreviations: ACd, dorsal anterior cingulate area; Cl, claustrum; fmi, forceps minor of the corpus callosum; FR2, frontal cortex area 2; IL, infralimbic area; PL, prelimbic area; ri, rhinal incisura. *Inset:* Approximate position of the slice in the rat brain in a medial view. Adapted from Paxinos & Watson (1998). (B) Layer V pyramidal neuron with a patch pipette at its soma. *Inset:* Illustration of the whole-cell patch-clamp mode.

synaptic currents that are statistically independent and summed linearly, one can consider the total synaptic current as Gauss distributed with mean m, variance s^2 and exponentially auto-correlated with a length τ. The input current $I(t)$ can be generated as an Ornstein-Uhlenbeck stochastic process by temporal iteration of the following expression (Cox & Miller, 1965):

$$I(t+\Delta t) = I(t) - \frac{I(t)-m}{\tau}\Delta t + s\,\xi(t)\sqrt{\frac{2\Delta t}{\tau}}\,. \tag{4.1}$$

The quantity $\xi(t)$ is a random variable drawn from a Gauss distribution with zero mean and unitary variance at every time step Δt. Typically, the process is generated and injected at a rate of 10 kHz ($\Delta t = 0.1$ ms) for neurophysiological purposes. The parameter τ is called correlation length and is a measure of the time interval up to which two values of the current are correlated, i.e., the current values at two time points t_1 and t_2 depend on each other, if their distance $|t_2 - t_1| < \tau$. Since the value of the correlation length τ somehow represents the decay

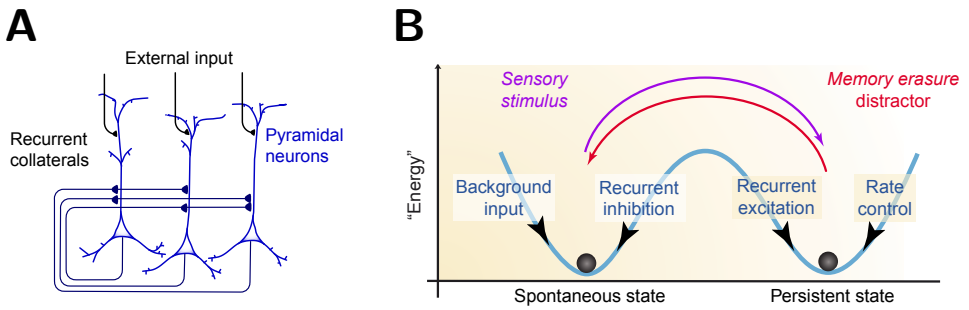

Figure 4.2: DESIGN OF OUR ATTRACTOR NETWORK MODEL (A) Architecture of our model network. Pyramidal neurons are connected by recurrent collaterals via excitatory synapses. External excitatory input is delivered when a stimulus is present or inhibitory input is injected to signal a distracting stimulus. (B) Illustration of bistability as an energy landscape, in which stable states correspond to minima. Reduced version of Figure 3.3B and adapted from Wang (2001) and Durstewitz & Seamans (2008).

time constant of individual synaptic currents, it was set to 3 ms to represent fast (AMPA/$GABA_A$) as well as slow (NMDA/$GABA_B$) currents. The resulting membrane potential evolves as a random walk, which resembles the fluctuations of the membrane potential *in vivo* (Destexhe et al., 2003).

Pharmacology. Pharmacological tools offer a straightforward way to investigate the specific influences of neuromodulatory substances like DA. The experimenter is able to divide different types of receptors according to their pharmacological properties. Since DA in principle can act onto two different classes of receptors – D1 and D2 –, we used different specific agonists and antagonists (reviewed in Missale et al., 1998) to investigate differential contributions of DA receptor subtypes in our experiments.

Furthermore, pharmacological substances are used in *in vitro* experiments to isolate single neurons from the network of neurons they are embedded in. We pharmacologically blocked fast/ionotropic excitatory and inhibitory synaptic transmission throughout our experiments; metabotropic synaptic transmission (e.g., $GABA_B$) was not blocked specifically.

All pharmacological substances were bath-applied via the artificial cerebrospinal fluid (aCSF). In case of DA and its agonists/antagonsists this corresponds to a tonic rather than a phasic signal and is supposed to mimic the slow time course of DA in the PFC *in vivo* (see also Sec. 2.2.4).

4.4 Computational modeling

The $f-I$ curve provides a straightforward way to incorporate experimental findings into computational models of single neurons. Integrate-and-fire neurons were chosen as neuron models to proof that the results are applicable to spiking neural networks and are not due to firing rate models. The input-output function of the integrate-and-fire neuron was fitted to the experimental $f-I$ curve extracting the parameters of the model neurons directly from the data.

We connected the model neurons in an attractor neural network and simulated the impact of gain-increase in PFC networks. The network was specifically designed to understand the impact of single cell gain-increase on recurrent activity. A lot of features of attractor neural networks, which were elaborated extensively by modeling studies have been left aside, when they were not necessary. Let us try to understand the design by means of the illustration in Figure 4.2B:

- *Background input:* Since it is known that persistent activity can be evoked in a subgroup of cells from a recurrently connected network, we simplified the approach by restricting our simulations to the coding subgroup, i.e., the cell assembly. The larger network to which the subgroup belongs was modeled as direct noisy background input. Moreover, the background input was held constant for both the network without and with DA influence. Therefore we had to assume – in line with the approaches by Daniel Durstewitz and colleagues (Durstewitz et al., 2000a; Durstewitz & Seamans, 2002) – that DA decreases the level of spontaneous activity.

- *Recurrent inhibition:* Inhibition was not modeled explicitly, since we did not perform experiments on inhibitory neurons. The non-linear sigmoidal shape of the neuronal input-output function makes bistability possible in a purely excitatory network (Fusi & Mattia, 1999; Brunel, 2000). Recurrent inhibition would simply widen the range of synaptic strengths that allows for bistability (Amit & Brunel, 1997). Of course this would act similarly in both the networks without and with DA.

- *Recurrent excitation:* The excitatory synapses were modeled with long time constants, i.e., they are N-methyl-D-aspartic acid (NMDA) receptor-driven (Wang, 1999).

- *Rate control:* No feedback inhibition or other mechanisms are introduced to restrict the firing rates in the network. The saturation of the $f-I$ curve serves as rate control (Fusi & Mattia, 1999; Brunel, 2000).

Sensory stimuli were introduced as changes in the mean of the noisy background current. Working memory cues were positive currents. Distracting stimuli were negative currents. Negative currents can be interpreted as lateral inhibition

activated by a population of cells being selective for another stimulus. We also skipped the explicit modeling of several subpopulations with different stimulus selectivity and their interaction. For mathematical details see also the Appendix (Sec. 4.5).

J Neurophysiol 99: 2985–2997, 2008.
First published April 9, 2008; doi:10.1152/jn.01098.2007.

Dopamine Increases the Gain of the Input-Output Response of Rat Prefrontal Pyramidal Neurons

Kay Thurley, Walter Senn, and Hans-Rudolf Lüscher
Department of Physiology, University of Bern, Switzerland

Submitted 3 October 2007; accepted in final form 1 April 2008

Thurley K, Senn W, Lüscher H-R. Dopamine increases the gain of the input-output response of rat prefrontal pyramidal neurons. *J Neurophysiol* 99: 2985–2997, 2008. First published April 9, 2008; doi:10.1152/jn.01098.2007. Dopaminergic modulation of prefrontal cortical activity is known to affect cognitive functions like working memory. Little consensus on the role of dopamine modulation has been achieved, however, in part because quantities directly relating to the neuronal substrate of working memory are difficult to measure. Here we show that dopamine increases the gain of the frequency-current relationship of layer 5 pyramidal neurons in vitro in response to noisy input currents. The gain increase could be attributed to a reduction of the slow afterhyperpolarization by dopamine. Dopamine also increases neuronal excitability by shifting the input-output functions to lower inputs. The modulation of these response properties is mainly mediated by D1 receptors. Integrate-and-fire neurons were fitted to the experimentally recorded input-output functions and recurrently connected in a model network. The gain increase induced by dopamine application facilitated and stabilized persistent activity in this network. The results support the hypothesis that catecholamines increase the neuronal gain and suggest that dopamine improves working memory via gain modulation.

INTRODUCTION

Prefrontal cortical function subserves higher-order cognitive processes, including working memory, i.e., the mental ability to transiently store and manipulate information which guides forthcoming actions. The cellular correlate of working memory is thought to consist of sustained reverberating activity in prefrontal neurons after stimulus removal (Goldman-Rakic 1995). Dopamine (DA) is an important neuromodulator that supports working memory. In fact, antagonists of the DA D1 receptor dramatically reduce the performance of monkeys in various working-memory tasks (Sawaguchi and Goldman-Rakic 1991). DA is released by dense projections from the ventral tegmental area to the prefrontal cortex (PFC) (Seamans and Yang 2004).

Incited by the importance of the prefrontal cortex and DA for working memory, a huge number of studies, dealing with DA actions in prefrontal cortical areas, has emerged during the last decades (for review, see Seamans and Yang 2004). In general, DA has been found to enhance the excitability of prefrontal pyramidal neurons mediated by D1 receptor stimulation (e.g., Henze et al. 2000; Lavin and Grace 2001; Shi et al. 1997; Tseng and O'Donnell 2004; Yang and Seamans 1996; but see Gulledge and Jaffe 1998). This was assumed to stabilize working memory activity and gave rise to numerous modeling studies (for review, see e.g., Cohen et al. 2002; Durstewitz et al. 2000b; Wang 2001).

The present study gives insight into DA modulation of the intrinsic response properties of individual PFC pyramidal neurons, which are relevant for understanding persistent activity. Neuronal response properties can best be characterized by means of the input-output response function, i.e., the *f-I* curve, giving the rate of action potential discharge as a function of the injected current strength. An important computational feature of the neuronal transfer function is the modulation of its gain (i.e., the maximal slope of the *f-I* curve), which may either stabilize or switch working memory (Salinas and Sejnowski 2001). Gain modulation of neocortical layer 5 pyramidal neurons has been shown to arise from distal dendritic input (Larkum et al. 2004) and noisy input (Arsiero et al. 2007; Higgs et al. 2006) and has been described as a result of serotonin or noradrenaline application (Higgs et al. 2006; Zhang and Arsenault 2005). Gain increase by DA was reported by Lavin and Grace (2001) for short stimuli that evoke only a few spikes. Here we extend their findings by showing an even larger increase of neuronal gain for long-lasting quasi-stationary responses that are relevant for self-sustained network activity. Moreover, the synaptic input a neuron experiences in vivo is characterized by random fluctuations rather than a DC current. Because noisy inputs have been shown to reduce the gain of the neuronal response function (Chance et al. 2002; Rauch et al. 2003; Shu et al. 2003), this might counteract DA-mediated gain increase found with square pulses. We provide evidence that, nevertheless, DA increases the gain of the input-output function of prefrontal pyramidal neurons for noisy inputs. In addition, DA shifts the *f-I* curve to the left, i.e., to lower input currents. Together with previous results on neuronal gain modulation by serotonin or noradrenaline (Zhang and Arsenault 2005), our data support the idea put forward by Servan-Schreiber et al. (1990) that catecholamines modulate the gain of PFC neurons and, at the network level, increase the signal-to-noise ratio of the information transmission. Incorporating our findings into a recurrently connected model network shows that the DA modulation stabilizes the sustained activity underlying working-memory functions. A DA-induced gain increase therefore synergistically supports the previously described stabilization of persistent activity by dopaminergic modulation of synaptic transmission (Compte et al. 2000; Durstewitz et al. 2000a).

Address for reprint requests and other correspondence: K. Thurley, Dept. of Physiology, University of Bern, Buehlplatz 5, CH-3012 Bern, Switzerland (E-mail: thurley@pyl.unibe.ch).

The costs of publication of this article were defrayed in part by the payment of page charges. The article must therefore be hereby marked "*advertisement*" in accordance with 18 U.S.C. Section 1734 solely to indicate this fact.

METHODS

Experimental preparation and electrophysiological recordings

All experimental procedures were performed according to the *Ethical Principles and Guidelines for Experiments on Animals* of the Swiss Academy of Medical Sciences. Coronal slices (300 μm) containing the medial PFC (see, e.g., Yang et al. 1996) were prepared from 17- to 44-day-old Wistar rats (with 80% of the data from rats >30 days). The preparation procedure is described in detail in Rauch et al. (2003). Whole cell patch-clamp recordings were taken from the soma of layer 5 PFC pyramidal neurons. Series resistance and capacitance were compensated using the bridge balance and capacitance neutralization of the amplifier (BVC-700A, Dagan, Minneapolis, MN). Layer 5 medial PFC pyramidal neurons with their thick apical dendrite were identified under visual guidance using infrared differential video microscopy. Selection was electrophysiologically confirmed by means of the regular-spiking behavior and passive membrane properties, after whole cell patch-clamp mode was established (Zhang 2004). Patch pipettes were filled with (in mM) 130 K-gluconate, 5 KCl, 10 HEPES, 4 ATP-Mg, 0.3 Na_2-GTP, and 10 Na_2-phosphocreatine, pH adjusted to 7.3 with KOH. Pipette solution additionally contained 0.2% biocytin to reconstruct cell morphology after recording. Experiments were conducted at 34–35°C.

Stimulation protocol

Stimulation currents were designed according to an Ornstein-Uhlenbeck stochastic process to mimic in vivo synaptic barrage (for a detailed description, see Rauch et al. 2003). Such a process yields a good approximation for the spike distribution observed in higher cortical areas during stimulus evoked activity (e.g., Aggelopoulos et al. 2005) or during working memory (e.g., Compte et al. 2003). There is also some direct indication that the synaptic barrage in vivo matches an Ornstein-Uhlenbeck process (Destexhe and Paré 1999). The statistics of such currents are characterized by a Gaussian distribution with mean m, a SD s and by a correlation time τ. We fixed the correlation time $\tau = 3$ ms to resemble fast excitatory and inhibitory synaptic inputs. Current-clamp protocols of the present kind have been shown to result in negligible distortions of neuronal response functions compared with conductance-clamp experiments (LaCamera et al. 2004; Rauch et al. 2003). Thus a recorded neuron responds in a similar way to either current injection or conductance drive and using technically less demanding current-clamp methods, turns out to be reasonable.

The principal experimental protocol was as follows: stimulus trains with constant mean current m and SD s were injected, and the neuronal response frequency f was calculated as the total spike number divided by the stimulus duration. Recordings were not included in the analysis in case of considerable changes of spike amplitude and shape in the response (Rauch et al. 2003). Different trains were separated by several tens of seconds, depending on the concrete protocol (see following text), to let the cell recover after stimulation. First, the mean input current m was increased stepwise from a subthreshold value until the emission of a single or a few spikes. That gave the current threshold for spiking, i.e., the rheobase current (Rauch et al. 2003). Then in the current interval between threshold and *f-I* curve saturation (Arsiero et al. 2007), stimuli with different means m were chosen and injected in random order to prevent temporal correlations. About 30% of the values of m were repeated once or twice.

Two different protocols were used for the recordings. First, we recorded data for a SD $s = 100$ pA. The value 100 pA was arbitrarily chosen. It is, however, in a range comparable with other studies (Arsiero et al. 2007; Rauch et al. 2003). Single stimulus trains lasted 10 s. The break between pulses was 50–60 s. Recording one *f-I* curve took roughly 30 min.

In a second series of experiments, we recorded data for three different values of the SD s using a modified version of the previous protocol. At first, the response curve for $s = 50$ pA was determined. Then two other values of s were chosen as the values that gave responses of 5 and 10 Hz at rheobase current for $s = 50$ pA, respectively. Stimulus trains were shortened to 6 s. Shorter stimulation times necessitated shorter times for recovering, i.e., 30–40 s instead of 50–60 s. With that protocol, recording *f-I* curves for three different SDs s took ~30 min as well.

In addition, membrane resting potential and access resistance were monitored by injection of a hyperpolarizing square pulse (100 ms, −50 to −150 pA) preceding each noisy stimulus train. Recordings have been discontinued in case of large drifts, i.e., membrane potential changes more than ±3 mV, despite unmodified experimental conditions, or the series resistance exceeding 20 MΩ. The membrane time constant was determined by an exponential fit to the recovering voltage response after the square pulse.

Pharmacology

To exclude transient responses, recordings started 5–10 min after drug application (regarding the dependence of DA influence on application time, see also RESULTS). Application continued during data acquisition to ensure stable drug levels, mimicking the in vivo situation of tonic rather than phasic DA presence. Recording the *f-I* curve under drug treatment took ~30 min. By the end of the data acquisition under drug treatment, each cell was already held for almost 1.5 h. A washout of ≤30 min followed the period of drug application in case the recording remained stable (evaluated by means of membrane potential and series resistance). No consistent washout results were obtained for any of the substances (data not shown). Concentrations were as follows (in μM): 25, 50, or 100 DA always including 0.2% sodium bisulfite to prevent oxidation, 5 SKF 38393, 10 SCH 23390, 10 quinpirole, and 10 or 50 sulpiride.

In most experiments, synaptic currents were systematically blocked. Bicuculline (10 μM) was applied to block $GABA_A$ receptor-mediated currents. To suppress glutamatergic inputs, 6-cyano-7-nitroquinoxalene-2,3-dione (CNQX, 10 μM; to block AMPA receptors) and 2-amino-5-phosphonovaleric acid (APV, 50 μM, to block NMDA receptors) were used in all experiments with DA concentrations at 25 or 50 μM. For DA application (100 μM), experiments without synaptic blockers gave similar results and were therefore pooled with experiments under synaptic blockade—no significant differences were found in the changes of *f-I* curve parameters with ($n = 5$) and without ($n = 8$) synaptic blockers, i.e., in the transient and steady state phase $P \gg 0.05$ for rheobase shift, gain change, and change of maximum firing rate, one-way ANOVA, see also *Data analysis and statistics*). In experiments with DA anta-/agonists, glutamatergic currents were blocked with the unspecific glutamate receptor antagonist kynurenate (1 mM). DA modulation of the slow afterhyperpolarization (sAHP) was investigated without synaptic blockers in all cases.

Data analysis and statistics

The analysis of the experimentally measured input-output functions makes use of the constant leakage integrate-and-fire neuron with a floor (CLIFF) (see Fusi and Mattia 1999). The CLIFF neuron was shown to describe the firing pattern of pyramidal neurons in rat somatosensory cortex (Rauch et al. 2003). It also accounts well for our PFC data, obtained with a single SD s of the input current (but see Arsiero et al. 2007). The temporal development of the membrane voltage V is described by

$$C\frac{dV}{dt} = -\lambda + I(t) \qquad (1)$$

with the effective membrane capacitance C, the leakage λ and the input current $I(t)$. The spike threshold of the model neuron was set to $\theta = -45$ mV. Additionally, the model requires a reset value V_r after

spiking and a refractory period τ_r. To complete the neuron model, one needs to define a lower bound, the floor, which we set to −65 mV. For an input current according to an Ornstein-Uhlenbeck process, the firing rate f of the CLIFF neuron is given by (Fusi and Mattia 1999)

$$f(m) = \left[\tau_r + \frac{\theta - V_r}{m - \lambda} C + \frac{\tau s^2}{(m-\lambda)^2} \left(e^{-\frac{m-\lambda}{\tau s^2} C\theta} - e^{-\frac{m-\lambda}{\tau s^2} C V_r} \right) \right]^{-1} \quad (2)$$

Numerical values for the set of free parameters $\{\lambda, V_r, C, \tau_r\}$, i.e., CLIFF *f-I* curves, were determined by fitting *Eq. 2* to the experimental *f-I* curves. By means of the fitted CLIFF *f-I* curves, we numerically determined: the rheobase current, which was defined as the largest mean input current m with firing rate $f(m) = 0$, the gain of the *f-I* curve, i.e., of the $f(m)$ function, which was given by the maximum of the first derivative (slope) of $f(m)$, and the maximum firing rate, which we defined to be in physiological range at $f(m_{max})$ with m_{max} = 700 pA + rheobase current according to the first parameter. Differences in the three parameters were evaluated between the *f-I* curves before and during drug application. Then, the significance level was determined using Student's *t*-test, one- or two-way ANOVA. To evaluate statistical correlations, Pearson's linear correlation coefficient r was used.

Experiments on the sAHP: stimulation protocol and analysis

For the experiments on the sAHP, we followed the protocol used by Higgs et al. (2006). The resting potential of a cell was held at −65 mV, and exactly 30 spikes were triggered with 2-ms square pulses at 50 Hz. The amplitude of the sAHP was estimated by averaging the voltage trace of the membrane potential between 450 and 550 ms after the last action potential (see also Fig. 4*A*).

Steady-state analysis of recurrently connected neurons

The analysis of the network of recurrently connected integrate-and-fire neurons follows the approach of Brunel (2000). It offers a simplified mean field theory, based on the *f-I* curve of the single cells of a network, and provides a tool to study the impact of the modulation of the single-cell *f-I* curve on network behavior. We investigate a recurrently connected network of N CLIFF neurons with parameters given by the average of the n = 13 recorded cells in the DA (100 μM) application experiments. Neurons are connected with a probability c. A single neuron receives input from as well as provides output to the network it is embedded in. The basic assumption in mean field theory is that in a homogeneous group of neurons in a network, a single cell reflects the average behavior of all cells in that homogeneous group. Therefore one can look at the response dynamics of a single cell exemplarily for the whole group. Like in the simulations (see following text), our network consists of one group of neurons, only. The activity state of each neuron is characterized by its firing rate $f = f(m)$ as a function of the mean input m (*Eq. 2*) and satisfies the self-consistent equation

$$m = cN\tau_c J(f - f_{sp}) + m_{sp} \quad (3)$$

where c is the average fraction of presynaptic neurons targeting a postsynaptic neuron, N the total number of neurons, τ_c the current decay time constant, J the average connection strength, and f_{sp} the spontaneous firing rate in response to the spontaneous background current m_{sp}. As a simplification, the SD of all currents is expected to be constant and unaffected by the state of the network and any input. The mean input m_{sp} contains a contribution from the recurrent excitatory network, which fires with frequency f_{sp}, and an additional external current that reflects summed excitatory and inhibitory input. Note that we keep the level of spontaneous activity f_{sp} the same for dopaminergic and nondopaminergic cases, i.e., we adjust the corresponding spontaneous background current m_{sp}. Otherwise, an excitability increase would obviously enhance the response to background input, which would counteract if not abolish bistability and thus storing working-memory items. Therefore we use the assumption of stable spontaneous activity independent of the responsiveness in our model, without explicitly modeling its emergence. Such adjustment of spontaneous activity levels can be interpreted as balancing activity from inhibitory interneurons. It is known that D1 agonists also enhance the amplitude and the frequency of GABAergic inputs to PFC pyramidal neurons (Seamans and Yang 2004; Seamans et al. 2001b). Other modeling studies showed that this might not only keep spontaneous activity constant but rather may lead to the reduction of the latter (Durstewitz and Seamans 2002; Durstewitz et al. 2000a)—an assumption recently confirmed experimentally (Lavin et al. 2005). Thus assuming the level of spontaneous activity to be independent of DA influence is justified. A decrease of spontaneous activity levels would even pronounce our results because it widens the basins of attraction for persistent activity, which further enhances stability (Durstewitz and Seamans 2002).

A stable state in the network is reached when the output frequency f of each neuron together with external inputs provides enough current to the network to evoke the same output again. In terms of our exemplary single cell, this condition is fulfilled at the intersection of the *f-I* curve (*Eq. 2*) with a line obtained by rewriting *Eq. 3* to the form

$$f = (m - m_{sp})/(cNt_c J) + f_{sp} \quad (4)$$

The intersections are fixed points of the system. Looking for the points of intersection provides the possibility to investigate the appearance and modulation of bistability, i.e., the coexistence of states of spontaneous and persistent activity, in dependence on parameters that characterize the network.

Simulations of recurrently connected integrate-and-fire neurons

We constructed a network of n = 260 CLIFF neurons with parameters given by the n = 13 recorded cells in the DA application experiments. The sets of parameters were in equal numbers assigned to the model neurons. For each neuron i, the input current $I(t)$ in *Eq. 1* consists of contributions from inside (recurrent) and outside the network. The recurrent contribution is chosen as $I(t) = \Sigma_j J_{ij} \Sigma_k \exp((t - t_j^{(k)} - d)/\tau_c)\Theta(t - t_j^{(k)} - d)$, with $\Theta(t)$ denoting the Heaviside step function, $\Theta(t) = 1$ for $t \geq 0$, and $\Theta(t) = 0$ otherwise. The value of $t_j^{(k)}$ gives the time when the presynaptic neuron j emitted the kth spike, which is received by neuron i after a delay d = 1 ms. For each connection from a neuron j to a neuron i, the connection strength J_{ij} was chosen to be $J_{ij} = J > 0$ with probability c = 0.1, and $J_{ij} = 0$ otherwise. Hence we have a purely excitatory network. Note that J_{ij} is measured in pA. The current time constant τ_c = 25 ms was set to overcome the long refractory period obtained by the fit and reflects the importance of NMDA receptors in stabilizing persistent activity (Wang 1999). External inputs reflecting items to be stored in working memory or distracting inputs are provided by DC injections. Additionally background activity, composed of contributions from inside and outside the network, results in an input current of a mean m_{sp} in each neuron that evokes a spontaneous firing rate f_{sp}. We keep the level of spontaneous activity f_{sp} the same for dopaminergic and nondopaminergic cases, i.e., we adjust the corresponding spontaneous background current m_{sp}. The SD of the background current was set to 100 pA.

RESULTS

DA-mediated increase of excitability

Prefrontal cortical layer 5 pyramidal neurons (Fig. 1*A*) were injected with noisy currents, which resemble synaptic barrage in vivo (see METHODS). We determined the input-output rela-

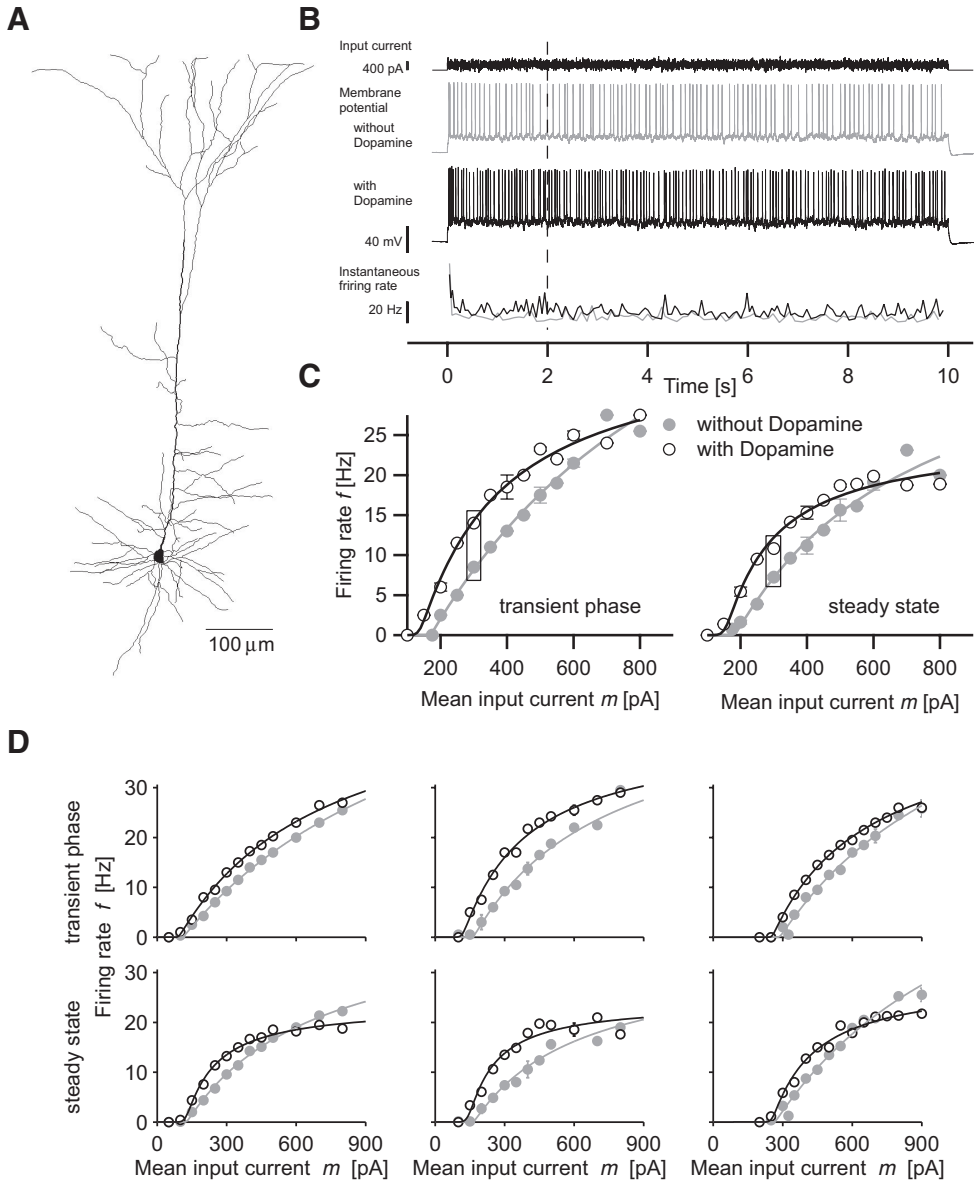

FIG. 1. Dopamine differentially affects layer 5 pyramidal neurons in the prefrontal cortex (PFC). *A*: reconstruction of a layer 5 PFC pyramidal neuron. *B*: example of the noisy current stimulus with a mean of 250 pA (*top*) and corresponding voltage traces before (*2nd panel*) and during (*3rd panel*) dopamine application. *Bottom*: the instantaneous firing rate. - - -, division of response phases that were defined as transient and steady-state response. *C*: example of the influence of dopamine on the response curve of a layer 5 PFC pyramidal neuron. Curves are given for the transient phase at the beginning of the stimulation (*left*) and for the steady-state response (*right*). ●, data before dopamine application; ○, values during application. The SD (error bars) is given in case the stimulus was repeated at the particular value of m (30% of the values). —, fits of the data with the CLIFF model neuron. □, values belonging to the traces in the *top panels*. *D*: 3 further examples of modulation of PFC pyramidal cell response by dopamine (DA). A DA concentration of 100 μM was used in the experiments shown in the figure.

tionship (*f-I* curve) of the cells before and during DA application, measuring the frequency of action potential discharge in response to different mean input currents (Fig. 1*B* gives an example). The first 1–2 s of the response of neocortical pyramidal neurons to long-lasting stimulation have been shown to comprehend temporally variable components due to processes on short time scales like spike frequency adaption and facilitation (LaCamera et al. 2006; Rauch et al. 2003). After the first few seconds the response stays quasi-stationary until the end of stimulation, i.e., the response frequency changes negligible subsequently, apart from possible slow spike frequency adaption. However, pyramidal cells are not able to sustain high output rates for very large depolarizing inputs, limiting the range of suitable values for the mean input current m (Rauch et al. 2003). The appropriate range of mean input currents depends on properties of the particular cell such as its input resistance and was adapted for each experiment (see also METHODS).

For the analysis, we divided the neural response into two parts: a transient phase consisting of the first 2 s of the response and the subsequent part, which we refer to as "steady" state (Fig. 1*B*). We discuss the principle findings by means of the example shown in Fig. 1*C*: the results were similar between transient phase and steady state—except for absolute firing frequencies, which were higher in the transient phase because of incomplete spike frequency adaptation. At low current values, i.e., lower than ~600 pA in Fig. 1*C*, DA increased excitability through a shift of the *f-I* curve to lower current values and a gain increase, i.e., increase of the maximum slope of the *f-I* curve. For high mean input, i.e., greater than ~600 pA in Fig. 1*C*, the output frequency was decreased in the steady state, indicating lower responsiveness but not in the transient phase. Similar results were obtained in other neurons (Fig. 1*D*).

To ensure that the preceding results are not due to fluctuations in the dopaminergic modulation of neural responses, noisy current pulses of 1-s duration were injected at a rate of 0.1 Hz, and the output spikes were monitored. The mean current m was adjusted to evoke an average of roughly seven

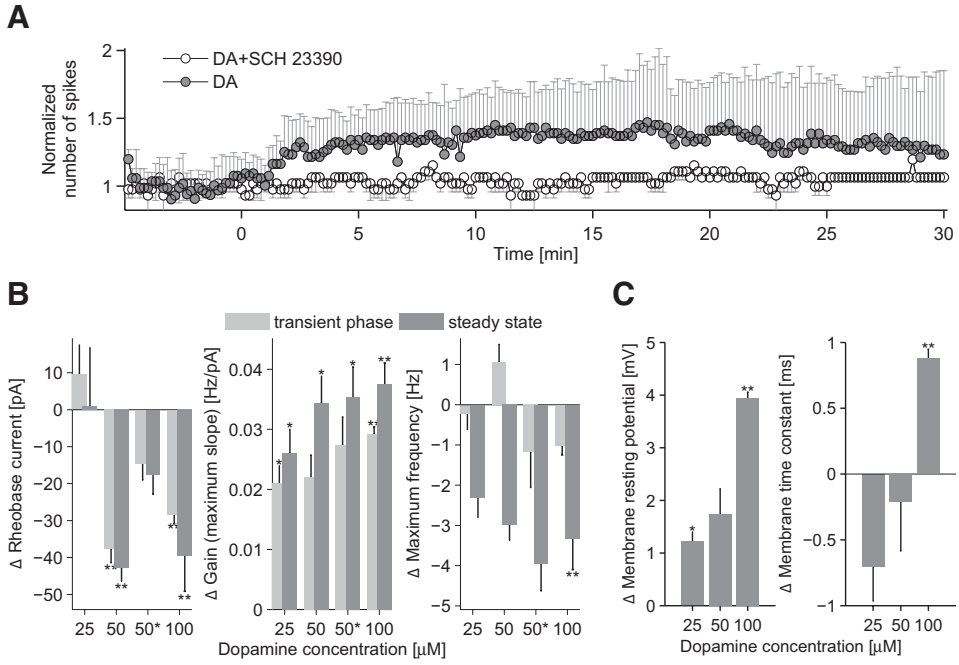

FIG. 2. Characterization of the modulation of PFC pyramidal cell response by DA. *A*: time development of pyramidal cell response to a stimulus that was fixed to trigger spikes at 7 Hz before drug application. Normalized average number of spikes ± SD of $n = 7$ cells for DA and $n = 3$ cells for DA+SCH 23390. Time point 0 is the start of application. *B* and *C*: dose-dependent changes of the parameters for the *f-I* curve, i.e., rheobase current, gain, maximum firing frequency (*B*), and for the passive membrane properties, i.e., membrane resting potential, membrane time constant (*C*). Mean values ± SE for differences between parameter pairs before and during DA application are given for the transient phase (▤) and the steady state (▨). At position 50* in *B*, values are reported for experiments with fixed resting membrane potential. *, significant differences before and during DA application: *, $P \leq 0.05$; **, $P \leq 0.01$, paired *t*-test.

spikes in response to the 1-s current pulses during the 5-min control phase prior to DA application. The SD *s* of the input current was fixed to 100 pA. Then for ~30 min, the response was recorded under DA presence (50 μM). About 2 min after the start of DA application the response increased and stabilized at higher level after ~5 min of application (Fig. 2*A*). The response remained stable for almost 25 min, although at the end of the recording it started to decrease slightly. Blocking DA D1 receptors with SCH 23390 (10 μM), occluded an excitability increase with DA (50 μM), Fig. 2*A*.

Quantification of dopaminergic f-I curve modulation

To quantify the results, we fitted the *f-I* curves with an integrate-and-fire model neuron (CLIFF) and extracted three parameters, i.e., rheobase current, as a measure of the shift of the *f-I* curve, gain (maximum slope), and maximum frequency (see METHODS). Figure 2*B* reports the DA mediated changes of *f-I* curve parameters and Table 1*A* lists the corresponding mean values and SD; see also supplemental material.[1] Experiments were conducted at three different DA concentrations, i.e., 25, 50, and 100 μM. Data for 100 μM was acquired with the "first" stimulation protocol and for 25 and 50 μM with the "second" (see *Stimulation protocol* in METHODS and *Dopamine effects remain for different amount of input fluctuations* in the following text). Therefore we analyzed *f-I* curves, which correspond to values of the SD *s* between 100 and 225 pA, in case of 25 and 50 μM DA, and to $s = 100$ pA for 100 μM DA.

The general outcome is similar for all DA concentrations, although nonsignificant (one-way ANOVA) variations between different DA concentrations are apparent. Under DA, the mean rheobase current was decreased for DA at 100 μM ($n = 13$) and 50 μM ($n = 7$) but not for 25 μM ($n = 6$). We found indications for a dose-dependent increase of the gain of the *f-I* relationship; the gain increase was larger with higher DA concentration. Both smaller rheobase current and larger gain indicate an increase of excitability evoked by DA in PFC pyramidal neurons at small input currents. Furthermore, Fig. 2*B* corroborates similar DA mediated changes of the *f-I* curves for the transient phase and the steady state. Note, however, that the gain change under DA is larger in the steady state than in the transient phase. After DA administration, the absolute values of the gain are even significantly different between transient and steady-state response (see supplemental material). The maximum firing rate decreased with increasing DA concentration during the steady-state phase; although significant only for 100 μM DA.

DA modulates passive membrane properties

To monitor the stability of the recoding, we injected hyperpolarizing square pulses, preceding each noisy current stimulus (see METHODS). That way we additionally estimated effects of drug application onto passive membrane properties (Fig. 2*C*). The membrane resting potential was increasingly depolarized for higher DA levels. The input resistance, as reflected by the membrane time constant, was increased for 100 μM and showed a tendency to decrease at lower concentrations.

Gain increase is independent of membrane potential increase

In a next set of experiments, we aimed to test if the effect of DA on *f-I* curves was independent of the accompanying membrane depolarization. Therefore we kept the cellular resting potential at −65 mV by compensating DC-current injection and recorded *f-I* curves with and without 50 μM DA (50* in Fig. 2*B* and Table 1*A*). The gain increase was in a range comparable to the experiments without fixed resting potential. The rheobase current was still reduced somewhat and the maximum firing frequency was strongly reduced although not significantly (see also DISCUSSION).

[1] The online version of this article contains supplemental data.

TABLE 1. *Characterization of the f-I curve (A) and passive membrane properties (B) without and with application of DA or its agonists and antagonists*

	Rheobase Current [pA]		Gain (maximum slope) [Hz/pA]		Maximum Frequency [Hz]		
	Before	During	Before	During	Before	During	*n*
			A. Characterization of the f-I curve				
DA							
25 μM							
t	224 ± 104	234 ± 91	0.078 ± 0.022	0.099 ± 0.035*	26.1 ± 2.4	25.9 ± 3.4	6
s	217 ± 103	218 ± 115	0.077 ± 0.024	0.103 ± 0.032*	23.2 ± 2.8	20.9 ± 4.5	
50 μM							
t	137 ± 105	99 ± 102**	0.107 ± 0.037	0.129 ± 0.021	30.5 ± 4.3	31.6 ± 6.1	7
s	140 ± 94	97 ± 97**	0.101 ± 0.01	0.136 ± 0.024*	29.4 ± 5.9	26.5 ± 4.8	
50 μM*							
t	175 ± 120	160 ± 133	0.130 ± 0.035	0.157 ± 0.047	52.1 ± 6.4	51.0 ± 8.7	4
s	165 ± 118	147 ± 137	0.124 ± 0.029	0.159 ± 0.038*	49.0 ± 6.5	45.0 ± 7.7	
100 μM							
t	151 ± 45	123 ± 45**	0.074 ± 0.016	0.104 ± 0.018**	31.0 ± 4.1	29.9 ± 4.1	13
s	155 ± 40	115 ± 48**	0.085 ± 0.022	0.122 ± 0.019**	28.6 ± 4.5	25.2 ± 4.6**	
SKF 38393	179 ± 65	147 ± 56*	0.092 ± 0.033	0.115 ± 0.025**	26.3 ± 4.7	21.6 ± 4.6**	9
Quinpirole	153 ± 56	110 ± 39**	0.086 ± 0.027	0.099 ± 0.024	24.5 ± 5.5	24.5 ± 6.8	7
DA+SCH 23390	9 ± 105	166 ± 101	0.11 ± 0.038	0.087 ± 0.023	27.9 ± 10.2	24.6 ± 8.9	4
SCH 23390	191 ± 105	186 ± 94	0.11 ± 0.038	0.112 ± 0.04	27.9 ± 10.2	23.0 ± 8.1	4
DA+Sulpiride	119 ± 64	84 ± 43*	0.102 ± 0.024	0.116 ± 0.017*	29.0 ± 8.5	25.8 ± 7.2**	6
Sulpiride	193 ± 66	207 ± 95	0.085 ± 0.030	0.085 ± 0.034	21.1 ± 2.6	21.1 ± 3.0	3

	Membrane Resting Potential [mV]		Membrane Time Constant [ms]		
	Before	During	Before	During	*n*
		B. Passive membrane properties			
DA					
25 μM	−65.4 ± 2.3	−64.2 ± 2.9*	16.2 ± 3.1	15.5 ± 2.1	6
50 μM	−67.7 ± 2.3	−66.0 ± 3.9	17.4 ± 6.5	17.2 ± 5.9	7
100 μM	−69.1 ± 3.3	−65.2 ± 3.0**	13.6 ± 3.3	14.5 ± 3.4**	13
SKF 38393	−69.3 ± 0.5	−68.9 ± 0.5	17.5 ± 0.9	18.7 ± 0.6*	8
Quinpirole	−68.0 ± 0.6	−67.2 ± 0.5	15.6 ± 0.7	16.6 ± 0.6**	7
DA+SCH 23390	−66.4 ± 4.2	−67.0 ± 4.8	12.5 ± 4.2	12.7 ± 6.1	4
SCH 23390	−66.4 ± 4.2	−66.4 ± 4.5	12.5 ± 4.2	14.4 ± 7.6	4
DA+Sulpiride	−65.7 ± 0.5	−62.9 ± 0.6**	22.4 ± 1.2	22.2 ± 1.2	6
Sulpiride	−66.0 ± 0.5	−66.9 ± 0.4	20.0 ± 1.1	19.0 ± 0.7	3

Values are means ± SD. For dopamine (DA) values for transient (t) as well as steady state (s) phases are given. Data for experiments with fixed resting membrane potential is given under the entry 50 μM*. For the DA anta-/agonists only values for the steady state are listed. In case of SCH 23390 first control data was acquired, then data in presence of SCH and finally data for DA and SCH together. A visual aid is given to quickly detect significant differences between control conditions and drug application, i.e., * for $P \leq 0.05$ and ** for $P \leq 0.01$, paired *t*-test. See supplemental material for plots of the listed values and for the parameters of the CLIFF model neuron after fitting to the experimental data.

No temporal effects underlie the excitability increase by DA

To exclude that the reported DA effects are an artifact of the experimental procedure, we recorded four cells using the same temporal protocol as in the preceding text but did not apply any drug. We found no significant change in any of the parameters, i.e., the rheobase current (from 158 ± 84 to 175 ± 72 pA, $P = 0.163$, paired *t*-test), the gain of the *f-I* curve (from 0.094 ± 0.051 to 0.086 ± 0.044 Hz/pA, $P = 0.166$, paired *t*-test), and the maximum firing rate (form 26.5 ± 8.3 to 24.8 ± 7.7 Hz, $P = 0.104$, paired *t*-test). Moreover, the minor changes, i.e., increase of the rheobase, gain decrease, and reduction of the maximum firing rate are in line with a time-dependent rundown of cellular responsiveness rather than with increased excitability as found after DA application. The time-dependent decrease of the maximum firing rate might—at least in part—account for the reduction of the maximum firing rate we found with DA application. Slow inactivation of voltage-gated sodium channels appears for strong stimuli and limits the maximum firing frequency (Fleidervish et al. 1996). Possibly sodium channel inactivation was augmented time dependently in our experiments.

D1 receptors account for most reported DA effects

To test whether DA D1 or D2 receptors are involved in the DA-mediated modulation of the *f-I* curve, we separately applied the D1 receptor agonist SKF 38393 and the D2 receptor agonist quinpirole (Table 1 and supplemental material). SKF 38393 (5 μM) modulated the *f-I* curve similar to DA and increased the membrane time constant. The membrane potential, however, was not affected. The D2 receptor agonist quinpirole (10 μM) evoked a reduction of the rheobase current and increased the membrane time constant; the other *f-I* curve parameters remained unaffected.

In a second series of experiments, we did recordings in presence of D1 (SCH 23390) or D2 (sulpiride) receptor antagonists. We applied DA (50 μM) together with SCH 23390 (10 μM). SCH 23390 blocked the effects of DA onto the *f-I* curve and passive membrane properties (Table 1 and supplemental

material). SCH 23390 applied alone did not show significant influences. Applying DA (100 μM) together with sulpiride resulted in effects on the *f-I* curve comparable with the application of DA or the D1 receptor agonist (Table 1 and supplemental material). We tested with a sulpiride level of 10 μM ($n = 4$) and 50 μM ($n = 2$) to have a DA-sulpiride ratio comparable with values from the literature (e.g., Seamans and Yang 2004). Both sulpiride levels gave similar results and were pooled for analysis. Furthermore the membrane resting potential was significantly increased, but not the membrane time constant as this was the case for the application of the D1 receptor agonist. Sulpiride (50 μM) itself showed no significant influences on the parameters of interest.

A cross-activation of nondopaminergic receptors, e.g., β-adrenergic receptors, becomes possible with the high concentrations of DA used in our experiments, i.e., 25–100 μM. Testing this possibility by blocking β-adrenergic receptors with propanolol (10 μM) reduced the effects of DA (50 μM) on the *f-I* curve and passive membrane properties (see supplemental Fig. S8 in the supplemental material). The rheobase current was still significantly reduced by DA application in presence of propanolol as well as the maximum firing rate. Under propanolol, the gain of the *f-I* curve was reduced similar to experiments without drug application, indicating temporal rundown of cellular responsiveness (see preceding text). Subsequent addition of DA increased the gain back to control levels in the steady-state phase—gain changes were, however, not significant in none of the cases: $P > 0.05$, two-way ANOVA. Note, that the experiments had been done as a single recording session, i.e., first the control *f-I* curve was measured, then the *f-I* curve with propanolol, and finally the *f-I* curve with propanolol and DA together. Passive membrane properties, i.e., membrane potential and membrane time constant, were unaffected.

Dopamine effects remain for different amount of input fluctuations

In the previous experiments, we investigated the response of layer 5 PFC pyramidal neurons to noisy input currents with only one amplitude of the input fluctuation, i.e., SD *s*. We therefore injected currents of three different amplitudes of input fluctuation into $n = 7$ cells with 50 μM DA and $n = 6$ cells with 25 μM DA, yielding qualitatively similar results as the example in Fig. 3. The features of DA modulation remain for different values of the amplitude of input fluctuations (Fig. 3, DA at 50 μM); i.e., increase of the rheobase current, gain increase, and reduced maximum firing rate is present in the transient as well as the steady-state phase.

The *f-I* curves in PFC pyramidal neurons are sensitive to the amount of input fluctuations over the whole range of input currents (Arsiero et al. 2007) and show a gain increase with increasing noise (Higgs et al. 2006). Figure 3 confirms that both features are preserved under DA presence.

Because the gain increase has been indicated to correlate with a decrease of slow spike frequency adaptation and sAHP (Higgs et al. 2006; see also following text), it might be that combination of DA with noise does not lead to an *additional* gain increase. We therefore had a closer look at the gain increase by DA at different amount of input fluctuation. The gain increase by noise was somewhat smaller after application of DA than before. It was, however, not significant (-0.0340 ± 0.0210 before and -0.0213 ± 0.0229 during DA, $P = 0.299$, one-way ANOVA).

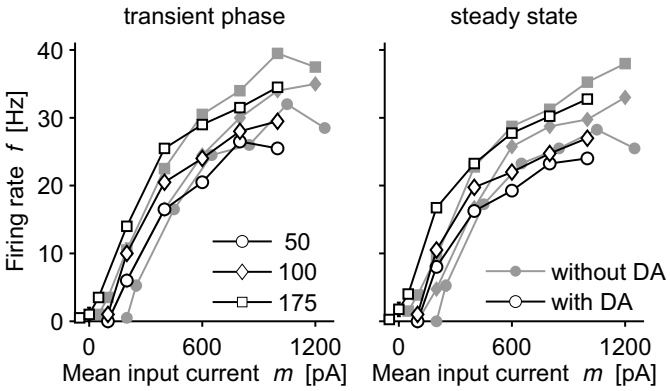

FIG. 3. Dopamine effects remain for different SD of the injected current. Three different values of the SD *s* were injected, i.e., 50 pA (circles), 100 pA (diamonds), and 175 pA (squares). Left: the response of the cell during the transient phase at the beginning of stimulation; right: the corresponding steady-state responses. Data before DA application are drawn in gray and during DA application in black.

Dopamine decreases the sAHP

The response of neocortical pyramidal neurons comprehends adaption—and facilitation—processes on several time scales from a few milliseconds up to the order of seconds (e.g., LaCamera et al. 2006; Rauch et al. 2003). The attenuating effects of noise onto slow adaptation (Tang et al. 1997) and slow afterhyperpolarization have been shown to be related to gain increase in neurons of the somatosensory cortex (Higgs et al. 2006). To test if the modulation of slow adaption might underlie the gain increase mediated by DA, we chose two different approaches.

First, we investigated DA modulation of the sAHP, using the same protocol as Higgs et al. (2006) (see also METHODS). The evoked sAHPs were reduced by application of 50 μM DA ($n = 6$, Fig. 4*A*). Estimating the amplitude of the sAHP between 450 and 550 ms after the last pulse confirmed a DA-induced reduction of the sAHP (Fig. 4*C*). The reduction was partially reversible during wash out. It decayed back to control values over time in five of seven neurons (data not shown), and after 30 min of wash out, the mean sAHP was larger than under DA treatment but still smaller than in control conditions (Fig. 4*C*). We refer to the most hyperpolarized part of the AHP as the medium AHP (mAHP, i.e., tens of to a few hundreds of milliseconds after the last action potential). DA also reduced the mAHP (see Fig. 4*A*, data not quantified). Blocking D1 receptors with 10 μM SCH 23390 only partially blocked the reduction of the sAHP by 50 μM DA (see supplemental Fig. S9). The dopaminergic reduction of the AHP has been suggested to be due to cross-activation of β-adrenergic receptors in hippocampal pyramidal neurons (Malenka and Nicoll 1986; but see Pedarzani and Storm 1995. To investigate whether such cross-activation might underlie our findings in prefrontal pyramidal cells, we blocked β-adrenergic receptors using propanolol (10 μM). The presence of propanolol occluded the reduction of the mAHP by DA (Fig. 4*B*, data not quantified). However, the sAHP was still substantially reduced by DA (50 μM) despite propanolol presence (Fig. 4, *B* and *D*).

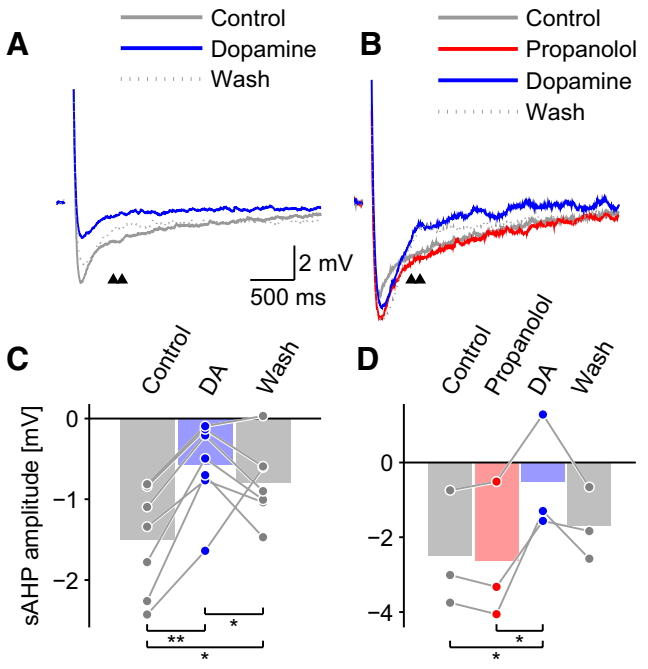

FIG. 4. Dopamine induced decrease of the slow afterhyperpolarization (sAHP). *A*: The sAHP (average of 5 responses) after 30 spikes at 50 Hz in control solution (gray solid line), during DA application at 50 μM (blue solid line), and after washout (gray dashed line). DA reduced the amplitude of the sAHP, which was partially reversible after 30-min wash out. Arrow heads demarcate the part of the voltage trace that was used to estimate the sAHP. We refer to the most hyperpolarized part of the voltage trace as the medium AHP (mAHP). *B*: same protocol as in *A* but under presence of propanolol at 10 μM (red solid line). Propanolol itself augmented the mAHP but did not affect the sAHP. DA still reduced the sAHP but not the mAHP. *C*: the sAHP amplitude for all cells (dots) with related values connected by lines. The data correspond to the example in *A*. The sAHP was quantified between 450 and 550 ms after the last pulse (arrow heads in *A*). Underlying bars are the mean values. Asterisks mark significant differences between indicated pairs: *, $P \leq 0.05$; **, $P \leq 0.01$, paired *t*-test. *D*: same as *C* but under presence of propanolol.

As a second approach, we analyzed the instantaneous firing frequency of PFC pyramidal neurons. LaCamera et al. (2006) showed that slow adaptation in the order of seconds is present in the time course of the instantaneous firing frequency in somatosensory cortex neurons when driven sufficiently strong. Additionally, they observed facilitation in the order of few tens of milliseconds. In contrast, we did not observe facilitation and slow adaption in PFC layer 5 pyramidal neurons (see Fig. 1*B* as an example). The time course of the instantaneous firing frequency comprised solely two decaying components: a very fast initial one in the order of a few milliseconds and a slower component lasting tens of milliseconds. Afterward the response remained stable. We fitted the instantaneous firing rate with two exponential functions to evaluate DA-mediated changes of the time constants of the instantaneous firing rate. DA-mediated influences were, however, not apparent (data not shown).

DA enables and stabilizes persistent activity—mean field analysis

Persistent activity, which is thought to underlie PFC function, is, for example, observed during working-memory tasks (Goldman-Rakic 1995). It is a network phenomenon in that it is assumed to be sustained by reverberating excitatory synaptic activity between recurrently connected cells (see, e.g., Wang 2001). To investigate what the effects of DA on the input-output relationship of PFC pyramidal neurons imply for persistent activity, we subsequently analyze a network of recurrently connected excitatory neurons via a mean field description (Brunel 2000) (see also METHODS).

The excitatory neurons, i.e., pyramidal cells, are described by CLIFF model neurons using average parameters identified from our experimental data for the steady-state response at 100 μM DA. Firing rate adaptation and dopaminergic influences on sAHP are assumed to be at stable values and are not modeled. The cells of the network are assumed to be randomly connected. We also incorporate a spontaneous background activity $f_{sp} = 0.5$ Hz, which is assumed to be unaffected by DA (see METHODS).

Without synaptic input, the activity of our network may be self-sustained inside the neural population by synaptic reverberation, i.e., the network assumes a *stable state*. The stable activity states of the network are identified by the intersection points of the *f-I* curve (*Eq. 2*) with a straight line of slope $1/(cNJ\tau_c)$ and appropriate offset (see Fig. 5*A*, *Eq. 4* and METHODS). Here, c denotes the connectivity, N the number of neurons, and τ_c the decay time constant of single EPSCs. The product cNJ characterizes to the total synaptic current to a cell of the network that comes from recurrent connections. By focusing at the synaptic feedback cNJ rather than just the synaptic coupling strength J, we can discuss the behavior of the network independently of the network size.

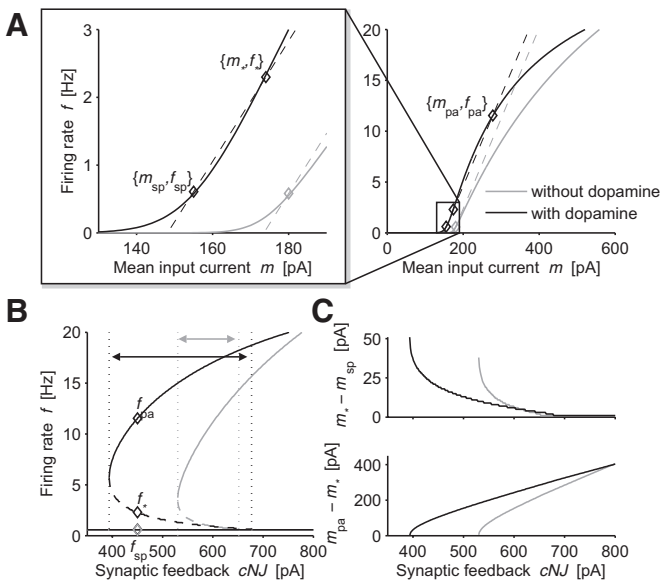

FIG. 5. Mean field description of DA influence on the behavior of a network of excitatory cells. *A*: stable states of the firing rate are intersections between *f-I* curves (solid lines) and a corresponding straight line (dashed, same color, here the synaptic feedback $cNJ = 450$ pA). Diamonds mark stable state values. Cases without DA are shown in gray and with DA in black throughout the figure. *Left*: an extension of the marked area in the *right panel*. *B*: bifurcation diagram showing stable state firing rates as a function of cNJ. Solid lines depict the stable lower and upper fixed points and the dashed line indicates the unstable intermediate fixed point. Diamonds mark stable-state values for a synaptic feedback $cNJ = 450$ pA as in *A*. Dotted lines demarcate the range of values of cNJ with bistability without (gray arrow) and with DA (black arrow). *C, top*: minimum input current above spontaneous input m_{sp} necessary to evoke elevated self-sustained persistent activity as a function of cNJ. *Bottom*: input current necessary to break down persistent activity as a function of cNJ. Parameters are $f_{sp} = 0.5$ Hz, $s = 100$ pA, and $\tau_c = 25$ ms.

Networks of recurrently connected neurons show bistability, i.e., coexistence of spontaneous background activity and elevated persistent activity. Coexistence of a low and a high activity state is a prerequisite to encode information via distinct network states. In networks composed of excitatory units only, bistability is found over a limited range of synaptic feedback *cNJ* (Fusi and Mattia 1999). The emergence of bistability can be understood by means of the graphical approach provided in Fig. 5*A*: for low synaptic feedback *cNJ* the slope of the straight line (*Eq. 4*) is high, only one point of intersection (fixed point) at $\{m_{sp}, f_{sp}\}$ exists, and the network is spontaneously active; as an illustration see the gray *f-I* curve in the case without DA in Fig. 5*A*. Increasing the synaptic feedback *cNJ*—either by increasing the effective number of connections *cN* or the synaptic strength *J*—decreases the slope of the line, and above a certain value of *cNJ*, one finds three points of intersection; as an illustration see the black *f-I* curve in Fig. 5*A,* which shows the case with DA. The lower point still corresponds to stable spontaneous activity, the intermediate one $\{m_*, f_*\}$ belongs to an unstable state and the upper intersection to stable persistent activity $\{m_{pa}, f_{pa}\}$. Due to the two stable fixed points, we have bistability between spontaneous and persistent activity at these values of *cNJ*, i.e., the network can reside self-sustained in one of the two states. Further increase of synaptic feedback *cNJ* results in the lower and middle fixed points merging together and becoming unstable. Only the upper intersection remains stable and reflects nontriggered high-frequency persistent network activity.

How does the dopaminergic modulation of the *f-I* curve, i.e., the rheobase reduction, the gain increase and the stronger saturation, influence the state space description? Due to our assumption that the spontaneous firing rate f_{sp} remains the same for dopaminergic and nondopaminergic cases, a shift of the *f-I* curve to lower current values by DA does not change the stable states, i.e., the points of intersection. Thus a simple excitability increase through rheobase reduction does not affect persistent activity at all. However, a DA-induced gain increase allows for persistent activity at lower synaptic strengths (Fig. 5*B*). Because a gain increase acts as a factor in front of the synaptic feedback *cNJ*, the result is a left shift of the *f-cNJ* curve to lower values of synaptic feedback *cNJ*. Persistent activity becomes more stable because the basin of attraction of the upper fixed point widens.

To quantify the above-mentioned effects, we extracted the minimal current needed to push the network from low spontaneous activity to high persistent activity. Figure 5*C, top,* shows for each value of the synaptic feedback *cNJ* the current $m_* - m_{sp}$ above spontaneous levels required to reach the basin of attraction for the persistent activity state. This is reached as soon as the total synaptic current crosses the value m_* corresponding to the unstable fixed point. As reflected by the graph, DA enables persistent activity at much lower values of *cNJ*, and less input current is required to reach this state. DA also widens the basin of attraction for the persistent activity state, represented by the current difference between persistent and unstable fixed point, $m_{pa} - m_*$ (Fig. 5*C, bottom*). This current difference is also the minimal negative, i.e., inhibitory, current required to move the network out of the attraction domain for persistent activity. In the presence of DA, stronger distractor currents are needed to irrecoverably perturb persistent activity. Note that aside from the external contribution, the currents m_{sp}, m_*, m_{pa} and their differences (Fig. 5*C*) contain a contribution from the recurrent network and do not directly correspond to the external currents necessary to evoke or interrupt persistent activity.

Interestingly, DA acts in a nonlinear way on the *f-I* curve which goes beyond pure gain modulation. If DA would only act as a constant gain factor, the range of *cNJ* that allows for bistability would only marginally increase; because a pure gain increase moves also, the point where spontaneous activity state and unstable fixed point merge to lower values of *cNJ*. However, in our experiments, DA increased the input resistance of PFC pyramidal neurons. Larger input resistance results in larger fluctuations of the membrane potential for the same fluctuations of the input current. Therefore the initial part of the *f-I* curve at low-frequency values, i.e., close to f_{sp}, extends over a larger range of mean input currents *m* (Fig. 5A). At the network level the point where spontaneous activity state and unstable fixed point merge becomes shifted to larger values of *cNJ*. Thus the range of synaptic feedback *cNJ* with bistability widens (dotted lines and arrows in Fig. 5*B*), i.e., bistability becomes more robust against fluctuations in the network parameters.

We conclude that DA application increases the range of synaptic strengths *J* that allow for network bistability. At the same time, DA makes the high activity state more stable against distractors.

DA enables and stabilizes persistent activity—simulations

As an example of the implications of dopaminergic modulation of the input-output relationship of PFC pyramidal neurons, we provide simulations of a recurrently connected network of excitatory integrate-and-fire neurons. The pyramidal cells are described by CLIFF neurons using parameters identified from the 13 cells in our experimental data for a DA concentration of 100 μM. The number of neurons was increased 20 times to $n = 260$ with a connection probability $c = 0.1$ (see METHODS). To be more biologically plausible, we incorporate a spontaneous activity of 0.5 Hz.

First, synaptic weights *J* are set in such a way that the neurons of the network start firing due to an external trigger, i.e., stimulus current in form of a square pulse underlying noisy background current delivered to each neuron. After stimulus removal, activity ceases without DA (Fig. 6*A*) but not in presence of DA (Fig. 6*B*). Hence DA enabled, but did not evoke, persistent activity in the example. Note that firing stabilizes at lower rate after stimulus removal than during stimulus presentation (Fig. 6*B*). The lower firing rate corresponds to a stable state between input and output within the network in absence of external input (Amit and Brunel 1997).

Second, we increase synaptic weights *J* so that persistent activity is provoked without and with DA (Fig. 6, *C* and *D*). However, distracting input disrupts persistent activity without DA (Fig. 6*C*), whereas with DA (Fig. 6*D*), persistent activity remains and the working-memory item is not erased. DA therefore stabilizes persistent activity in the example. Distracting input is modeled as a negative current injection into every neuron. Note that the only way to silence, i.e., *distract* in our case, the activity of an attractor neuronal network that resides in its "high activity" fixed point, is via negative current injection (cf. *DA enables and stabilizes persistent activity—mean*

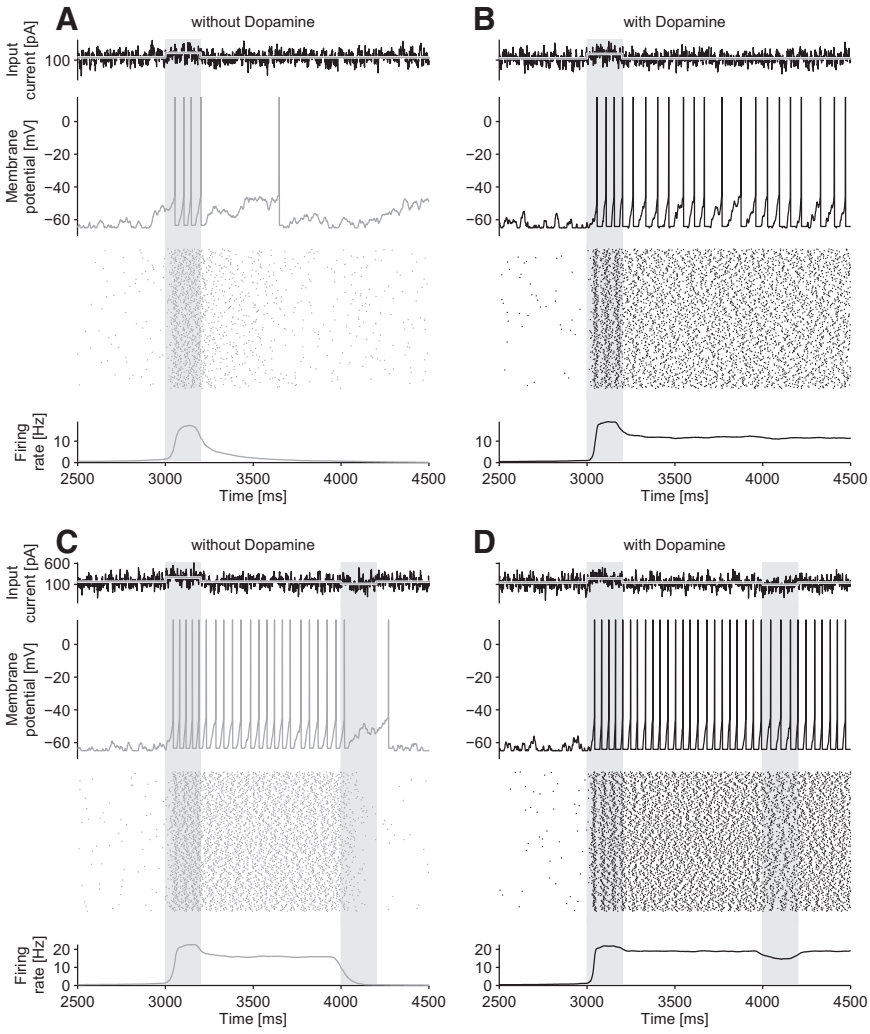

FIG. 6. Dopamine enables and stabilizes persistent activity. *A–D, top*: the injected current, i.e., noisy background and the mean input current (overlayed in gray) with square pulses for working memory item and distractor, respectively. *Second panel*: voltage trace of one example neuron; *third panel*: output spikes (dots) of the whole network (1 row corresponds to 1 of the 260 cells); *bottom*: the mean firing rate of the whole network. *A* and *B*: with synaptic weights $J = 17$ pA, injection of a 100-pA current pulse for 200 ms (gray shaded area) does not provoke persistent activity without (*A*) but in presence of dopamine (*B*). *C* and *D*: with synaptic weights $J = 25$ pA, persistent activity is found in both cases but breaks down by injection of distracting input (−50 pA, 200 ms) without dopamine. Parameters are $f_{sp} = 0.5$ Hz, $s = 100$ pA.

field analysis and Fig. 5*C*). In the present model, negative current might represent input from inhibitory neurons. These inhibitory cells may themselves be activated by a competing population of pyramidal neurons that respond to another stimulus (to keep things simple not explicitly modeled here).

DISCUSSION

We investigated the DA-mediated modulation of the input-output function of layer 5 pyramidal neurons in rat prefrontal cortex. Bath application of DA increased the excitability of pyramidal cells by reducing the rheobase current and increasing the gain of the input-output function. The DA-induced effects were found to be largely mediated by D1 receptor activation. We, however, cannot completely rule out a contribution of nondopaminergic receptors, e.g., β-adrenergic receptors, activated by the high DA concentrations (25–100 μM). For strong and long stimulation exceeding 2 s, the maximum firing rate was decreased. Incorporating these findings into a recurrently connected network of model pyramidal neurons, we could show that the experimentally observed dopaminergic modulation of the input-output function facilitates and stabilizes persistent activity. Our results confirm the original hypothesis of Servan-Schreiber et al. (1990) that catecholamines modulate the gain of the neuronal input-output function.

DA-mediated increase of excitability

Dopaminergic enhancement of pyramidal cell excitability via D1 receptor stimulation in the PFC has previously been reported. A considerable amount of in vitro studies revealed increased excitability after bath application of DA, a D1 receptor agonist (Henze et al. 2000; Lavin and Grace 2001; Shi et al. 1997; Tseng and O'Donnell 2004; Wang and O'Donnell 2001; Yang and Seamans 1996) or synaptically evoked DA release from VTA projections (Chen et al. 2007; Lavin et al. 2005; Lewis and O'Donnell 2000). Most studies, including our own, made use of (pre-)pubertal animals. However, DA modulation of PFC function has been shown to be age-dependent in that some DA effects change after puberty (Tseng and O'Donnell 2005). We can therefore not rule out that our results may change for adult animals.

DA modulation of PFC neurons has further been reported to comprise "transient" (on a scale of seconds) and longer-lasting components (Geijo-Barrientos and Pastore 1995; Gulledge and Jaffe 1998; Rotaru et al. 2007; Seamans and Yang 2004; Seamans et al. 2001b), suggesting that excitability may initially decrease but then reverse and stabilize at a higher level. We performed similar experiments, using a fixed amount of input current as in previous studies, to investigate the time course of the excitability modulation by

DA. Application of DA under blockade of synaptic inputs led to an excitability increase in our experiments but without a preceding transient reduction. Similar findings were made by others (Gulledge and Jaffe 2001). The excitability increase was stable after 5 min of DA application up to 25 minutes. Afterward, a slow excitability decrease appeared, suggesting receptor desensitization.

Indications for a DA-induced gain modulation in PFC layer 5 pyramidal neurons were already reported by Lavin and Grace (2001). Using square pulses of few hundred milliseconds, they compared responses of cells intermediately clamped at de- or hyperpolarized membrane potentials that were supposed to mimic cortical up and down states. They found a gain increase after DA administration for both membrane potential states. However, Lavin and Grace (2001) showed their gain increase only for a range of input of several tens of picoampere. We could confirm these findings and extend them over a broad range of input currents of several hundred picoampere.

The barrage of synaptic input a neuron experiences in vivo is characterized by large random fluctuations rather than a DC input. But noisy inputs have been shown to reduce the gain of the neuronal response function (Chance et al. 2002; Rauch et al. 2003; Shu et al. 2003), potentially counteracting DA-mediated gain increase. Using fluctuating input currents, we could show that, nevertheless a DA-induced gain increase is preserved for different amounts of input fluctuations.

Working-memory activity is believed to be formed by self-sustained network activity in prefrontal cortex. Insight into the ability of a neuronal network to sustain activity over prolonged periods of time requires responses to long-lasting neuronal stimuli. With long-lasting stimulation extending across seconds, we showed that the gain of the neural response function depends on the duration of the stimulation, a finding recently reported also in somatosensory cortex neurons (Higgs et al. 2006). The amount of gain change induced by DA, however, was not different between early (transient) and subsequent response phases.

DA effects on the input-output response function were associated with a depolarization of the membrane potential of PFC pyramidal neurons in agreement with previous reports (Gulledge and Jaffe 1998; Shi et al. 1997; but see Henze et al. 2000; Yang and Seamans 1996). However, in our experiments, membrane potential depolarization was not required for gain increase by DA. Holding the membrane potential constant before and during DA application did not occlude DA-mediated gain increase in control experiments.

Dopaminergic modulation of PFC pyramidal cell excitability has largely been reported to be due to changes of synaptic input (Gulledge and Jaffe 2001; Tseng and O'Donnell 2004; Wang and O'Donnell 2001) or intrinsic currents, e.g., persistent sodium current, persistent potassium current and calcium currents (Yang et al. 1996; Gorelova and Yang 2000; Chen et al. 2007). By systematically blocking all synaptic inputs, we intended to focus solely on single cell properties amenable to DA modulation. Our results suggest the involvement of currents that contribute to slow sAHP and slow spike frequency adaptation.

Involvement of D1, D2, and nondopaminergic receptors

D1 receptors are the predominant receptors at prefrontal pyramidal neurons (Goldman-Rakic et al. 2000) and excitability increases were shown in vitro to be mediated by D1 receptor activation (e.g., Chen et al. 2007; Tseng and O'Donnell 2004; Wang and O'Donnell 2001;). Excitability decreases are mostly due to increased inhibition mediated by D2 receptor activation located on interneurons (e.g., Gulledge and Jaffe 2001). In the present study, the specific D1 receptor agonist, SKF 38393, modulated the input-output relationship of pyramidal neurons similar to the action of DA itself, but the agonist did not increase the membrane resting potential. A reduction of the rheobase current was also present under application of the specific D2 receptor agonist, quinpirole, but was not accompanied by the other features found with DA application and in particular a gain increase was not present. The D1 receptor antagonist SCH 23390 occluded the influences of DA on the *f-I* curve. Blocking β-adrenergic receptors with propanolol, however, reduced the effects of DA somewhat but not completely. These findings indicate that the modulation of the *f-I* curve by DA is mainly mediated by D1 receptors.

Both D1 and D2 agonists increased the input resistance, accounting for the rheobase reduction under DA application. The additional depolarization observed under DA application might not be due to D1 or D2 receptor activation but another mechanism (Shi et al. 1997). This was confirmed by co-application of DA and a D2 receptor antagonist: the cell depolarized, in addition to a rheobase-reduction, a gain increase, and a decrease of the maximum frequency.

We conclude that it is mainly the D1 receptor that mediates the tonic effects of DA on the input-output relationship of layer 5 pyramidal neurons in the PFC. A cross-activation of nondopaminergic receptors can, however, not be entirely excluded.

DA effects onto slow spike frequency adaptation and the relationship to gain increase

The AHP following repetitive firing is composed of a fast (fAHP, up to few milliseconds), medium (mAHP, up to several hundred milliseconds), and slow component (sAHP, up to several seconds) with the peak of the hyperpolarization a few milliseconds after the peak of the action potential (Sah and Faber 2002). The slow AHP component reflects Ca^{2+}- and Na^{+}-dependent K^{+} conductances that are involved in spike frequency adaptation (see e.g., Higgs et al. 2006; Sah and Faber 2002; Viana et al. 1993) and therefore possibly take part in the modulation of neuronal output rates. DA has been reported to modulate the AHP in the striatum (Nicola et al. 2000) and induce a slow afterdepolarization in the amygdala (Yamamoto et al. 2007). At the time, however, there is no evidence that DA modulates Ca^{2+}- and Na^{+}-dependent K^{+} conductances in the PFC (Seamans and Yang 2004). In contrast to our results, the absence of DA effects on the (slow) AHP has been reported (Lavin and Grace 2001). A sAHP, however, is reliably found only after repetitive firing at high firing rate (Higgs et al. 2006; Zhang and Arsenault 2005). Using a protocol with strong drive of the PFC layer 5 pyramidal neurons (Higgs et al. 2006), we could show that DA nevertheless reduces the sAHP. Reduction of the sAHP was shown to be related to gain increase in prefrontal pyramidal

neurons (Zhang and Arsenault 2005), in somatosensory pyramidal neurons (Higgs et al. 2006), and also in hypoglossal motoneurons (Viana et al. 1993). We therefore presume that a reduction of the sAHP amplitude might underlie gain increase in layer 5 pyramidal neurons of the PFC.

Dopaminergic reduction of the AHP has been suggested to arise from a cross-activation of β-adrenergic receptors in hippocampal pyramidal neurons (Malenka and Nicoll 1986). No cross-activation was, however, reported by Pedarzani and Storm (1995). We tested whether cross-activation might underlie AHP reduction by DA in our experiments with PFC pyramidal neurons. Blocking β-adrenergic receptors with propanolol, in fact largely abolished DA effects on the medium part of the AHP. However, the sAHP was still substantially reduced by DA. The sAHP reduction by DA could, however, not be completely blocked by co-application of the D1 receptor antagonist SCH 23390. Thus the relevance of the sAHP for gain increase and the importance of D1 and/or other receptors in the relationship between both features is not entirely clear and needs further clarification.

DA-mediated facilitation and stabilization of persistent activity

The fit of the *f-I* curve with an integrate-and-fire model neuron allowed us to study the DA effects in a recurrently connected network model. Previous modeling studies provide detailed insight into the concept of stabilizing delay-type activity by DA in the PFC (e.g., Braver et al. 1999; Brunel and Wang 2001; Compte et al. 2000; Dreher and Burnod 2002; Durstewitz et al. 2000a). These studies, however, mainly focused on the dopaminergic modulation of synaptic inputs found in previous experimental studies (e.g., Gao and Goldman-Rakic 2003; Gao et al. 2001, 2003; Seamans et al. 2001a,b). Our findings support and extend the insights offered by these studies: DA stabilizes persistent network activity against distracting input by a gain increase of the neuronal input-output function. This is achieved by enlarging the basins of attraction of the persistent activity state.

We conclude that the effects of DA on the neuronal input-output function reported here functionally match the previously described effects of DA on synaptic transmission in the PFC. In view of the diversity of results on DA modulation of PFC function (e.g., Seamans and Yang 2004), this reveals a remarkable convergence between the DA modulation of single neurons and synapses on the level of the network.

ACKNOWLEDGMENTS

We thank T. Berger, M. Giugliano, D. Ledergerber, and R. Urbanczik for valuable discussion and comments on the manuscript.

GRANTS

This work was supported by Swiss National Science Foundation Grant 31-61335.00 to H.-R. Lüscher.

REFERENCES

Aggelopoulos NC, Franco L, Rolls ET. Object perception in natural scenes: encoding by inferior temporal cortex simultaneously recorded neurons. *J Neurophysiol* 93: 1342–1357, 2005.

Amit DJ, Brunel N. Model of global spontaneous activity and local structured activity during delay periods in the cerebral cortex. *Cereb Cortex* 7: 237–252, 1997.

Arsiero M, Lüscher HR, Lundstrom BN, Giugliano M. The impact of input fluctuations on the frequency-current relationships of layer 5 pyramidal neurons in the rat medial prefrontal cortex. *J Neurosci* 27: 3274–3284, 2007.

Braver TS, Barch DM, Cohen JD. Cognition and control in schizophrenia: a computational model of dopamine and prefrontal function. *Biol Psychiatry* 46: 312–328, 1999.

Brunel N. Persistent activity and the single-cell frequency-current curve in a cortical network model. *Network* 11: 261–280, 2000.

Brunel N, Wang XJ. Effects of neuromodulation in a cortical network model of object working memory dominated by recurrent inhibition. *J Comput Neurosci* 11: 63–85, 2001.

Chance FS, Abbott LF, Reyes AD. Gain modulation from background synaptic input. *Neuron* 35: 773–782, 2002.

Chen L, Bohanick JD, Nishihara M, Seamans JK, Yang CR. Dopamine D1/5 receptor-mediated long-term potentiation of intrinsic excitability in rat prefrontal cortical neurons: Ca^{2+}-dependent intracellular signaling. *J Neurophysiol* 97: 2448–2464, 2007.

Cohen JD, Braver TS, Brown JW. Computational perspectives on dopamine function in prefrontal cortex. *Curr Opin Neurobiol* 12: 223–229, 2002.

Compte A, Brunel N, Goldman-Rakic PS, Wang XJ. Synaptic mechanisms and network dynamics underlying spatial working memory in a cortical network model. *Cereb Cortex* 10: 910–923, 2000.

Compte A, Constantinidis C, Tegner J, Raghavachari S, Chafee MV, Goldman-Rakic PS, Wang XJ. Temporally irregular mnemonic persistent activity in prefrontal neurons of monkeys during a delayed response task. *J Neurophysiol* 90: 3441–3454, 2003.

Destexhe A, Paré D. Impact of network activity on the integrative properties of neocortical pyramidal neurons in vivo. *J Neurophysiol* 81: 1531–1547, 1999.

Dreher JC, Burnod Y. An integrative theory of the phasic and tonic modes of dopamine modulation in the prefrontal cortex. *Neural Netw* 15: 583–602, 2002.

Durstewitz D, Seamans JK. The computational role of dopamine D1 receptors in working memory. *Neural Netw* 15: 561–572, 2002.

Durstewitz D, Seamans JK, Sejnowski TJ. Dopamine-mediated stabilization of delay-period activity in a network model of prefrontal cortex. *J Neurophysiol* 83: 1733–1750, 2000a.

Durstewitz D, Seamans JK, Sejnowski TJ. Neurocomputational models of working memory. *Nat Neurosci* 3, *Suppl*: 1184–1191, 2000b.

Fleidervish IA, Friedman A, Gutnick MJ. Slow inactivation of Na^+ current and slow cumulative spike adaptation in mouse and guinea-pig neocortical neurones in slices. *J Physiol* 493: 83–97, 1996.

Fusi S, Mattia M. Collective behavior of networks with linear (VLSI) integrate-and-fire neurons. *Neural Comput* 11: 633–652, 1999.

Gao WJ, Goldman-Rakic PS. Selective modulation of excitatory and inhibitory microcircuits by dopamine. *Proc Natl Acad Sci USA* 100: 2836–2841, 2003.

Gao WJ, Krimer LS, Goldman-Rakic PS. Presynaptic regulation of recurrent excitation by D1 receptors in prefrontal circuits. *Proc Natl Acad Sci USA* 98: 295–300, 2001.

Gao WJ, Wang Y, Goldman-Rakic PS. Dopamine modulation of perisomatic and peridendritic inhibition in prefrontal cortex. *J Neurosci* 23: 1622–1630, 2003.

Geijo-Barrientos E, Pastore C. The effects of dopamine on the subthreshold electrophysiological responses of rat prefrontal cortex neurons in vitro. *Eur J Neurosci* 7: 358–366, 1995.

Goldman-Rakic PS. Cellular basis of working memory. *Neuron* 14: 477–485, 1995.

Goldman-Rakic PS, Muly EC, Williams GV. D1 receptors in prefrontal cells and circuits. *Brain Res Brain Res Rev* 31: 295–301, 2000.

Gorelova NA, Yang CR. Dopamine D1/D5 receptor activation modulates a persistent sodium current in rat prefrontal cortical neurons in vitro. *J Neurophysiol* 84: 75–87, 2000.

Gulledge AT, Jaffe DB. Dopamine decreases the excitability of layer V pyramidal cells in the rat prefrontal cortex. *J Neurosci* 18: 9139–9151, 1998.

Gulledge AT, Jaffe DB. Multiple effects of dopamine on layer V pyramidal cell excitability in rat prefrontal cortex. *J Neurophysiol* 86: 586–595, 2001.

Henze DA, González-Burgos GR, Urban NN, Lewis DA, Barrionuevo G. Dopamine increases excitability of pyramidal neurons in primate prefrontal cortex. *J Neurophysiol* 84: 2799–2809, 2000.

Higgs MH, Slee SJ, Spain WJ. Diversity of gain modulation by noise in neocortical neurons: regulation by the slow afterhyperpolarization conductance. *J Neurosci* 26: 8787–8799, 2006.

LaCamera G, Rauch A, Thurbon D, Lüscher HR, Senn W, Fusi S. Multiple time scales of temporal response in pyramidal and fast spiking cortical neurons. *J Neurophysiol* 96: 3448–3464, 2006.

LaCamera G, Senn W, Fusi S. Comparison between networks of conductance- and current-driven neurons: stationary spike rates and subthreshold depolarization. *Neurocomputing* 58–60: 253–258, 2004.

Larkum ME, Senn W, Lüscher HR. Top-down dendritic input increases the gain of layer 5 pyramidal neurons. *Cereb Cortex* 14: 1059–1070, 2004.

Lavin A, Grace AA. Stimulation of D1-type dopamine receptors enhances excitability in prefrontal cortical pyramidal neurons in a state-dependent manner. *Neuroscience* 104: 335–346, 2001.

Lavin A, Nogueira L, Lapish CC, Wightman RM, Phillips PEM, Seamans JK. Mesocortical dopamine neurons operate in distinct temporal domains using multimodal signaling. *J Neurosci* 25: 5013–5023, 2005.

Lewis BL, O'Donnell P. Ventral tegmental area afferents to the prefrontal cortex maintain membrane potential "up" states in pyramidal neurons via D1 dopamine receptors. *Cereb Cortex* 10: 1168–1175, 2000.

Malenka RC, Nicoll RA. Dopamine decreases the calcium-activated afterhyperpolarization in hippocampal CA1 pyramidal cells. *Brain Res* 379: 210–215, 1986.

Nicola SM, Surmeier J, Malenka RC. Dopaminergic modulation of neuronal excitability in the striatum and nucleus accumbens. *Annu Rev Neurosci* 23: 185–215, 2000.

Pedarzani P, Storm JF. Dopamine modulates the slow Ca(2+)-activated K^+ current I_{AHP} via cyclic AMP-dependent protein kinase in hippocampal neurons. *J Neurophysiol* 74: 2749–2753, 1995.

Rauch A, LaCamera G, Lüscher HR, Senn W, Fusi S. Neocortical pyramidal cells respond as integrate-and-fire neurons to in-vivo-like input currents. *J Neurophysiol* 90: 1598–1612, 2003.

Rotaru DC, Lewis DA, Gonzalez-Burgos G. Dopamine D1 receptor activation regulates sodium channel-dependent EPSP amplification in rat prefrontal cortex pyramidal neurons. *J Physiol* 581: 981–1000, 2007.

Sah P, Faber ESL. Channels underlying neuronal calcium-activated potassium currents. *Prog Neurobiol* 66: 345–353, 2002.

Salinas E, Sejnowski TJ. Gain modulation in the central nervous system: where behavior, neurophysiology, and computation meet. *Neuroscientist* 7: 430–440, 2001.

Sawaguchi T, Goldman-Rakic PS. D1 dopamine receptors in prefrontal cortex: involvement in working memory. *Science* 251: 947–950, 1991.

Seamans JK, Durstewitz D, Christie BR, Stevens CF, Sejnowski TJ. Dopamine D1/D5 receptor modulation of excitatory synaptic inputs to layer V prefrontal cortex neurons. *Proc Natl Acad Sci USA* 98: 301–306, 2001a.

Seamans JK, Gorelova NA, Durstewitz D, Yang CR. Bidirectional dopamine modulation of GABAergic inhibition in prefrontal cortical pyramidal neurons. *J Neurosci* 21: 3628–3638, 2001b.

Seamans JK, Yang CR. The principal features and mechanisms of dopamine modulation in the prefrontal cortex. *Prog Neurobiol* 74: 1–58, 2004.

Servan-Schreiber D, Printz H, Cohen JD. A network model of catecholamine effects: gain, signal-to-noise ratio, and behavior. *Science* 249: 892–895, 1990.

Shi WX, Zheng P, Liang XF, Bunney BS. Characterization of dopamine-induced depolarization of prefrontal cortical neurons. *Synapse* 26: 415–422, 1997.

Shu Y, Hasenstaub A, Badoual M, Bal T, McCormick DA. Barrages of synaptic activity control the gain and sensitivity of cortical neurons. *J Neurosci* 23: 10388–10401, 2003.

Tang AC, Bartels AM, Sejnowski TJ. Effects of cholinergic modulation on responses of neocortical neurons to fluctuating input. *Cereb Cortex* 7: 502–509, 1997.

Tseng KY, O'Donnell P. Dopamine-glutamate interactions controlling prefrontal cortical pyramidal cell excitability involve multiple signaling mechanisms. *J Neurosci* 24: 5131–5139, 2004.

Tseng KY, O'Donnell P. Post-pubertal emergence of prefrontal cortical up states induced by D1-NMDA co-activation. *Cereb Cortex* 15: 49–57, 2005.

Viana F, Bayliss DA, Berger AJ. Multiple potassium conductances and their role in action potential repolarization and repetitive firing behavior of neonatal rat hypoglossal motoneurons. *J Neurophysiol* 69: 2150–2163, 1993.

Wang J, O'Donnell P. D1 dopamine receptors potentiate NMDA-mediated excitability increase in layer V prefrontal cortical pyramidal neurons. *Cereb Cortex* 11: 452–462, 2001.

Wang XJ. Synaptic basis of cortical persistent activity: the importance of NMDA receptors to working memory. *J Neurosci* 19: 9587–9603, 1999.

Wang XJ. Synaptic reverberation underlying mnemonic persistent activity. *Trends Neurosci* 24: 455–463, 2001.

Yamamoto R, Ueta Y, Kato N. Dopamine induces a slow afterdepolarization in lateral amygdala neurons. *J Neurophysiol* 98: 984–992, 2007.

Yang CR, Seamans JK. Dopamine D1 receptor actions in layers V-VI rat prefrontal cortex neurons in vitro: modulation of dendritic-somatic signal integration. *J Neurosci* 16: 1922–1935, 1996.

Yang CR, Seamans JK, Gorelova NA. Electrophysiological and morphological properties of layers V-VI principal pyramidal cells in rat prefrontal cortex in vitro. *J Neurosci* 16: 1904–1921, 1996.

Zhang Z. Maturation of layer V pyramidal neurons in the rat prefrontal cortex: intrinsic properties and synaptic function. *J Neurophysiol* 91: 1171–1182, 2004.

Zhang Z, Arsenault D. Gain modulation by serotonin in pyramidal neurons of the rat prefrontal cortex. *J Physiol* 566: 379–394, 2005.

Supplemental Material

The present section provides figures that characterize the parameters of the $f - I$ curve, i.e. rheobase current, gain (maximum slope), maximum firing frequency, and passive membrane properties, i.e. membrane resting potential, membrane time constant, for experiments without and with application of dopamine (DA) and its agonists and antagonists. For DA (100 μM), for the D1 antagonist SCH 23390, and for the blocker of β-adrenergic receptors, propanolol, values are given for the transient and the steady state phase. For the remaining DA agonists and antagonists values are given for the steady state phase, only.

Dopamine

For the experiments with DA only data, which was acquired at a concentration of 100 μM is given. A two-way ANOVA was used rather than a paired t-Test like otherwise, to detect significant differences exceeding general variability especially when comparing transient phase and steady state.

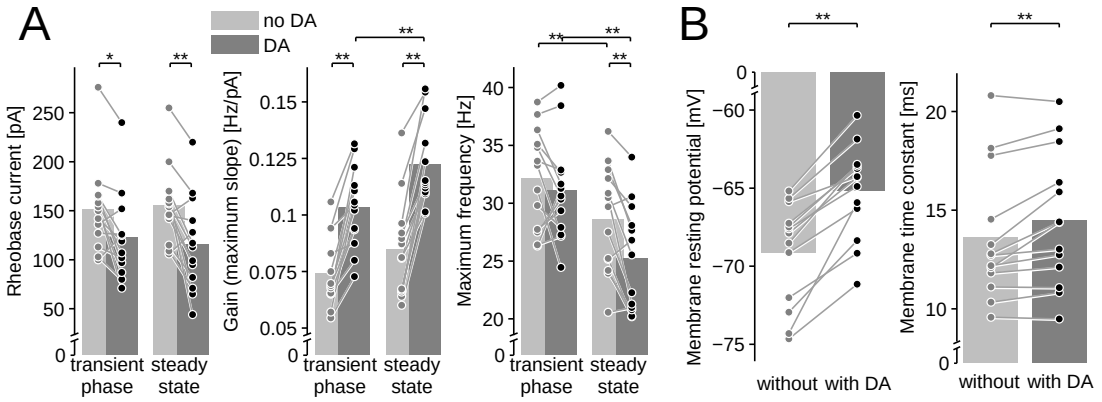

Figure S1: Characterization of the $f - I$ curve and passive membrane properties without and with application of DA (100 μM). (A) The $f - I$ curves (rheobase current, gain, maximum firing frequency) are compared for the transient phase and steady state before (light gray bars) and during DA application (dark gray bars). The values for all 13 cells are given as dots, corresponding values are connected by lines. Underlying bars depict the mean values. Asterisks mark significant differences between indicated pairs: $*$ for $P \leq 0.05$ and $**$ for $P \leq 0.01$, two-way ANOVA. (B) Comparison of the passive membrane properties (membrane resting potential, membrane time constant) without and with DA. Asterisks encode the significance levels as in (A). Here a paired t-Test was used.

The table below lists the parameters of the constant leakage integrate-and-fire neuron model with a floor (CLIFF) after fitting to the experimentally acquired data

for 100 μM dopamine. The response function of the CLIFF neuron for input current according to an Ornstein-Uhlenbeck process is given by

$$f(m) = \left[\tau_r + \frac{\theta - V_r}{m - \lambda} C + \frac{\tau s^2}{(m-\lambda)^2}\left(e^{-\frac{m-\lambda}{\tau s^2} C\theta} - e^{-\frac{m-\lambda}{\tau s^2} C V_r}\right)\right]^{-1},$$

as described in Methods (Eq. 2). For fitting, the threshold θ was fixed to 20 mV above resting potential at zero given by the floor of the CLIFF neuron. In the simulations, however, the floor of the CLIFF neuron was set to -65 mV and all other parameters are used with respect to -65 mV, i.e., the threshold $\theta = -45$ mV and the reset potential V_r. The standard deviation $s = 100$ pA and the correlation time length $\tau = 3$ ms were fixed as well during fitting. The refractory period τ_r, the reset potential V_r, the membrane capacitance C and the leakage λ are free parameters of the fit. The table below list these values for all 13 recorded cells.

Table S1: The parameters for the CLIFF neuron without (control) and with application of dopamine (100 μM). A number was assigned to each cell, listed in the first column.

	Control				Dopamine			
#	τ_r [ms]	V_r [mV]	C [pF]	λ [pA]	τ_r [ms]	V_r [mV]	C [pF]	λ [pA]
1	23.8	1.0	708.7	130.3	42.6	1.9	295.4	129.9
2	23.3	1.0	695.2	186.1	40.2	1.6	318.2	160.6
3	29.7	0.6	713.2	169.4	41.5	2.4	263.9	150.0
4	20.8	1.6	375.1	178.1	30.4	0.8	197.2	178.9
5	19.4	1.5	438.6	191.9	32.6	1.8	141.9	185.0
6	16.3	0.9	572.6	220.0	28.2	1.7	417.5	197.9
7	18.6	1.1	507.9	132.6	27.1	2.1	286.2	120.6
8	19.9	1.5	290.9	206.2	23.9	1.9	220.3	182.8
9	25.3	1.5	565.7	167.0	39.6	8.2	595.5	181.4
10	13.9	0.8	803.8	118.6	20.7	9.3	848.8	138.8
11	20.2	1.0	486.1	170.8	39.0	2.0	317.2	183.0
12	25.2	9.8	1045.4	166.2	28.6	0.0	356.7	81.0
13	14.0	0.0	707.2	270.2	35.0	1.5	345.3	259.2

The D1 receptor agonist SKF 38393

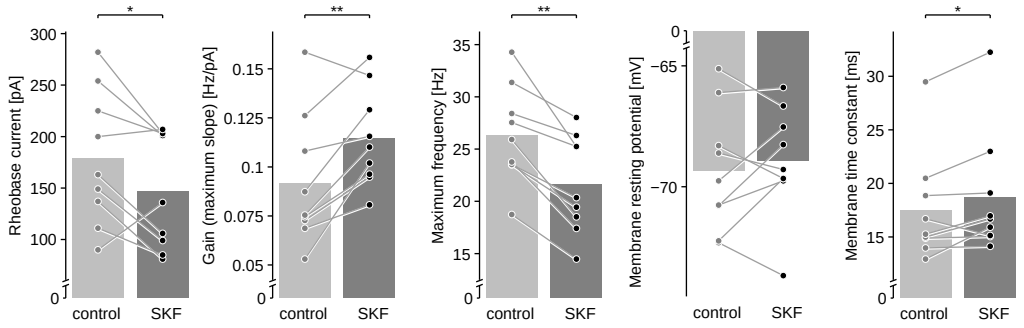

Figure S2: Characterization of the $f - I$ curve (rheobase current, gain (maximum slope), maximum firing frequency) and passive membrane properties (membrane resting potential, membrane time constant) without and with application of the D1 receptor agonist SKF 38393 (5 μM). The values for all 9 cells are given. Underlying bars depict corresponding mean values. Asterisks mark significant differences to the control situation: $*$ for $P \leq 0.05$ and $**$ for $P \leq 0.01$, paired t-Test.

The D2 receptor agonist quinpirole

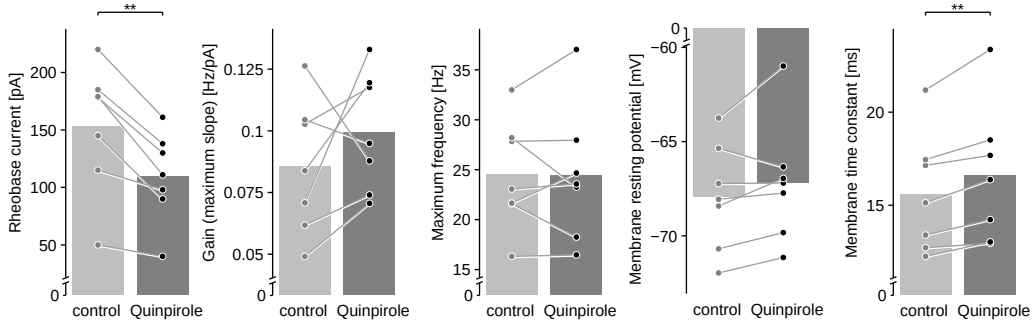

Figure S3: Characterization of the $f - I$ curve (rheobase current, gain (maximum slope), maximum firing frequency) and passive membrane properties (membrane resting potential, membrane time constant) without and with application of quinpirole (10 μM). The values for all 7 recorded cells are given. Underlying bars depict corresponding mean values. Asterisks mark significant differences to the control situation: $*$ for $P \leq 0.05$ and $**$ for $P \leq 0.01$, paired t-Test.

Dopamine and the D1 receptor antagonist SCH 23390

Recordings with the D1 receptor antagonist SCH 23390 had been done as a single recording session, i.e. first the control $f - I$ curve was measured, then the $f - I$ curve with SCH 23390 and finally the $f - I$ curve with SCH 23390 and DA together. Similar to the second, shorter protocol stimulus trains of 6 s and single standard deviation $s = 100$ pA were used for stimulation (see *Stimulation protocol* in Methods). We took a two-way ANOVA, to detect significant differences exceeding general variability especially when comparing control experiments, mere SCH 23390 application and combined DA and SCH 23390 application. Dopamine was applied at 50 μM and SCH 23390 at 10 μM.

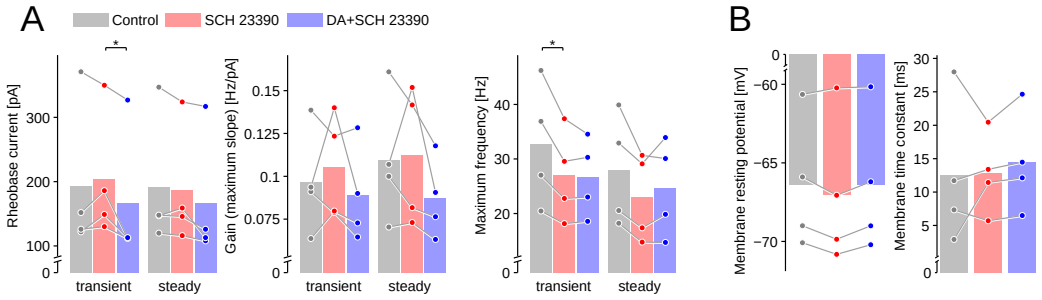

Figure S4: Characterization of the $f - I$ curve and passive membrane properties without and with application of dopamine (50 μM) and the D1 receptor antagonist SCH 23390 (10 μM). (A) The $f - I$ curves (i.e. rheobase current, gain, maximum firing frequency) are compared for the transient phase and steady state before drug application (gray bars), in presence of alone SCH 23390 (red bars) and of DA and SCH 23390 (blue bars). The values for the 4 recorded cells are given as dots, corresponding values are connected by lines. Underlying bars depict the mean values. Asterisks mark significant differences between indicated pairs: $*$ for $P \leq 0.05$ and $**$ for $P \leq 0.01$, two-way ANOVA. (B) Comparison of the passive membrane properties (membrane resting potential, membrane time constant) without and with DA. Asterisks encode the same significance levels as in (A).

Dopamine and the D2 receptor antagonist sulpiride

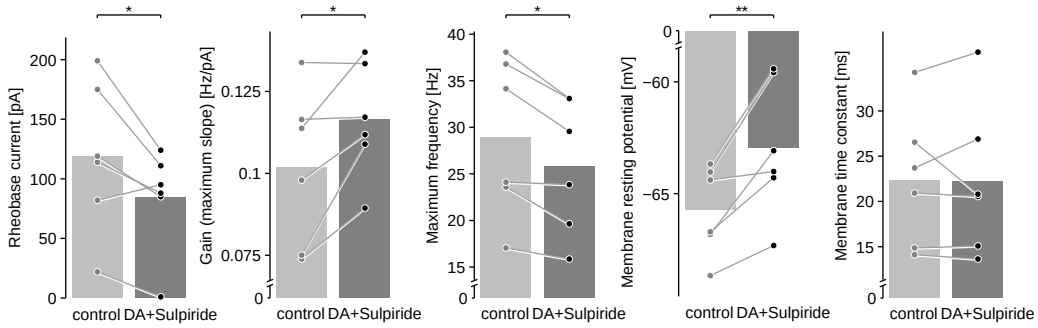

Figure S5: Characterization of the $f - I$ curve (rheobase current, gain (maximum slope), maximum firing frequency) and passive membrane properties (membrane resting potential, membrane time constant) without and with co-application of Dopamine (100 μM) and the D2 receptor antagonist Sulpiride (10 or 50 μM). The values for all 6 recorded cells are given. Underlying bars depict corresponding mean values. Asterisks mark significant differences to the control situation: $*$ for $P \leq 0.05$ and $**$ for $P \leq 0.01$, paired t-Test.

The D2 receptor antagonist sulpiride

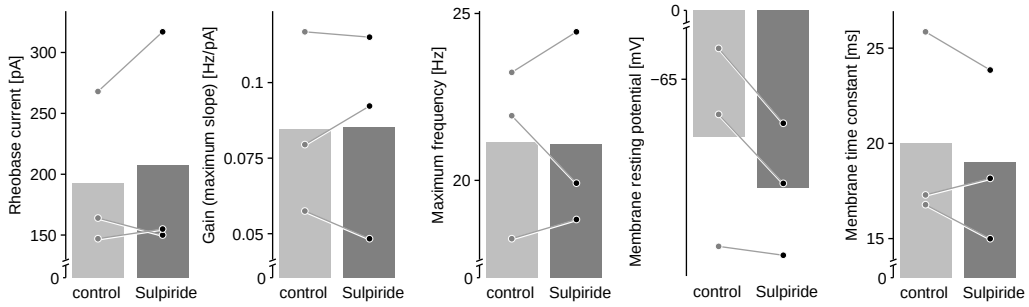

Figure S6: Characterization of the $f - I$ curve (rheobase current, gain (maximum slope), maximum firing frequency) and passive membrane properties (membrane resting potential, membrane time constant) without and with application of the D2 receptor antagonist sulpiride (50 μM). The values for all 3 recorded cells are given. Underlying bars depict corresponding mean values. Asterisks mark significant differences to the control situation: $*$ for $P \leq 0.05$ and $**$ for $P \leq 0.01$.

No drug application

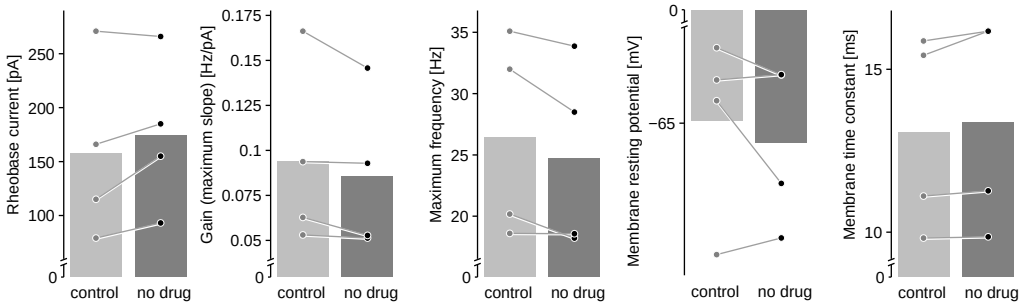

Figure S7: Characterization of the $f - I$ curve (rheobase current, gain (maximum slope), maximum firing frequency) and passive membrane properties (membrane resting potential, membrane time constant) without application of any drugs but using the same temporal protocol. The values for all 4 recorded cells are given. Underlying bars depict corresponding mean values. Asterisks mark significant differences to the control situation: $*$ for $P \leq 0.05$ and $**$ for $P \leq 0.01$, paired t-Test.

Dopamine and the β-adrenergic receptor antagonist propanolol

In contrast to the other experiments, recordings with the antagonist of β-adrenergic receptors, propanolol, had been done as a single recording session, i.e. first the control $f - I$ curve was measured, then the $f - I$ curve with propanolol and finally the $f - I$ curve with propanolol and DA together. Similar to the second, shorter protocol stimulus trains of 6 s and single standard deviation $s = 100$ pA were used for stimulation (see *Stimulation protocol* in Methods). We took a two-way ANOVA, to detect significant differences exceeding general variability especially when comparing control experiments, mere propanolol application and combined DA and propanolol application. Dopamine was applied at 50 μM and propanolol at 10 μM.

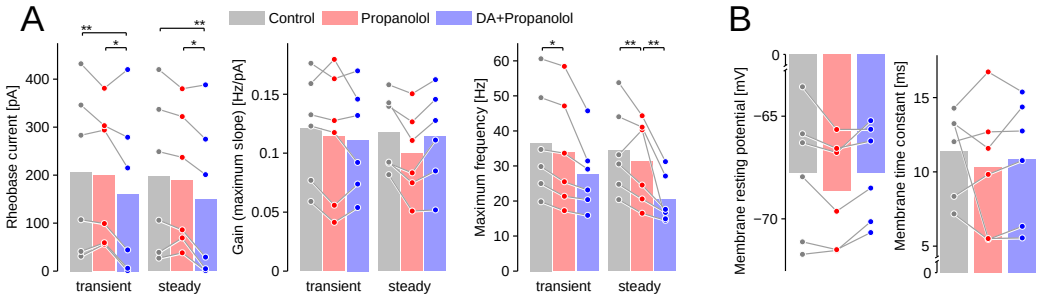

Figure S8: Characterization of the $f - I$ curve and passive membrane properties without and with application of DA (50 μM) and propanolol a antagonist of β-adrenergic receptors (10 μM). (A) The $f - I$ curves (i.e. rheobase current, gain, maximum firing frequency) are compared for the transient phase and steady state before drug application (gray bars), in presence of propanolol alone (red bars) and of DA and propanolol (blue bars). The values for the 6 recorded cells are given as dots, corresponding values are connected by lines. Underlying bars depict the mean values. Asterisks mark significant differences between indicated pairs: $*$ for $P \leq 0.05$ and $**$ for $P \leq 0.01$, two-way ANOVA. (B) Comparison of the passive membrane properties (membrane resting potential, membrane time constant) without and with DA. Asterisks encode the same significance levels as in (A).

The slow after-hyperpolarization in presence of dopamine and the D1 receptor antagonist SCH 23390

See also *Experiments on the after-hyperpolarization: stimulation protocol and analysis* in Methods for stimulation protocol and *Dopamine decreases the slow after-hyperpolarization* in Results.

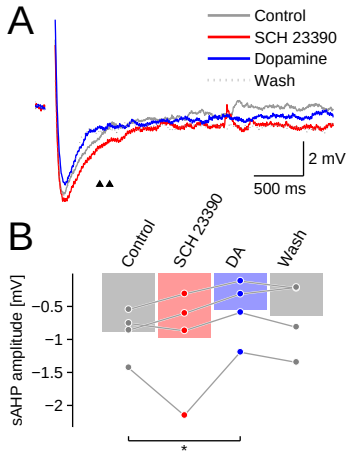

Figure S9: Modulation of the slow after-hyperpolarization (sAHP) by dopamine in presence of the D1 receptor antagonist SCH 23390. (A) The sAHP (average of 5 responses) after 30 spikes at 50 Hz in control solution (gray solid line), in presence of SCH 23390 at 10 μM (red solid line), during additional DA application at 50 μM (blue solid line) and after washout (gray dashed line). Arrow heads demarcate the part of the voltage trace that was used to estimate the sAHP. (B) The sAHP amplitude for $n = 4$ cells (dots) with related values connected by lines. Underlying bars are the mean values. Asterisks mark significant differences between indicated pairs: $*$ for $P \leq 0.05$ and $**$ for $P \leq 0.01$, paired t-Test.

4.5 Appendix

4.5.1 Mathematical details for the CLIFF model neuron

Model neuron. The computational modeling makes use of the constant leakage integrate-and-fire neuron with a floor (CLIFF). The temporal development of the CLIFF membrane voltage V is described by

$$C\frac{dV}{dt} = -\lambda + I(t) \;, \tag{4.2}$$

with the effective membrane capacitance C, the leakage λ and the input current $I(t)$. Additionally, the model requires a spike threshold θ, a reset value V_r after spiking and a refractory period τ_r. To complete the neuron model one needs to define a lower bound, the floor, which we set to -65 mV.

Here I provide a few analytical solutions to Eq. (4.2), which might help the reader to understand the behavior of the model neuron – although we numerically solved Eq. (4.2) in the network simulations for the publication. For arbitrary input current $I(t)$, the membrane potential V of the CLIFF neuron is obtained by integrating Eq. (4.2) between time points t_0 and t_1

$$V(t_1) = V_0 - \frac{\lambda}{C}(t_1 - t_0) + \frac{1}{C}\int_{t_0}^{t_1} I(t)\; dt \;. \tag{4.3}$$

We see that each arbitrary input $I(t)$ to the CLIFF neuron is counteracted or decays away, respectively, with constant rate λ/C. The parameter V_0 denotes the membrane potential at time point t_0, i.e., $V_0 = V(t_0)$.

To describe an arbitrary synaptic input current one can use $I(t) = \sum_j J_{ij} \sum_k \delta(t - t_j^{(k)} - d)$, with the synaptic strength J_{ij}, the time $t_j^{(k)}$ of the kth spike of presynaptic neuron j, the synaptic delay d, and the Dirac function $\delta(t)$, $\delta(0) = \infty$ and $\delta(t) = 0$, otherwise. Injecting such a current into the CLIFF model neuron we obtain

$$\begin{aligned} V(t_1) &= V_0 - \frac{\lambda}{C}(t_1 - t_0) + \frac{1}{C}\sum_j J_{ij} \sum_k \int_{t_0}^{t_1} dt\; \delta(t - t_j^{(k)} - d) \\ &= V_0 - \frac{\lambda}{C}(t_1 - t_0) \\ &\quad + \frac{1}{C}\sum_j J_{ij} \sum_k \Big[\Theta(t_1 - t_j^{(k)} - d) - \Theta(t_0 - t_j^{(k)} - d)\Big] \;, \end{aligned}$$

$\Theta(t)$ denotes the Heaviside step function, $\Theta(t) = 1$ for $t \geq 0$ and $\Theta(t) = 0$, otherwise. For simplification let us set time point t_1 after the last spike, i.e., $t_1 = t > t_j^{(k)} + d$ and t_0 before the first spike $t_0 < t_j^{(k)} + d$, getting

$$V(t) = V_0 - \frac{\lambda}{C}t + \frac{1}{C}\sum_j J_{ij} \sum_k \Theta(t - t_j^{(k)} - d) \;. \tag{4.4}$$

In the last expression we see that single synaptic currents result in a step of size J_{ij}, add up with previous inputs and decay away with a rate λ/C. With less artificial input in form of an exponentially decaying current resembling an EPSC, $I(t) = \sum_j J_{ij} \sum_k \exp((t - t_j^{(k)} - d)/\tau_c)\ \delta(t - t_j^{(k)} - d)$, and setting $t_1 = t,\ t_0 = 0$, we obtain

$$\begin{aligned} V &= V_0 - \frac{\lambda}{C} t \\ &+ \frac{\tau_c}{C} \sum_j J_{ij} \sum_k \left[e^{-\left(-t_j^{(k)} - d\right)/\tau_c} - e^{-\left(t - t_j^{(k)} - d\right)/\tau_c} \right] \Theta\left(t - t_j^{(k)} - d\right) \end{aligned}$$

To gain a more illustrative description, let us focus at only one input spike from one presynaptic neuron at $t^{(k)} = 0$. We further simplify, by setting the synaptic strength $J_{ij} \Rightarrow J$, neglecting the synaptic delay $d = 0$, starting at membrane potential $V_0 = 0$. We get

$$V = -\frac{\lambda}{C} t + \frac{J\tau_c}{C} \left[1 - \exp\left(-t/\tau_c\right)\right] \ . \tag{4.5}$$

We can solve Eq. (4.5) to determine the time of the maximum $t_{\max}$ and the value of the postsynaptic potential $V\left(t_{\max}\right)$

$$t_{\max} = \tau_c \ln \frac{J}{\lambda} \ , \tag{4.6}$$

$$V\left(t_{\max}\right) = \frac{\tau_c}{C} \left[\lambda \ln \frac{\lambda}{J} + J - \lambda \right] \ . \tag{4.7}$$

For an exitatory postsynaptic potential (EPSP), the righthand side of Eq. (4.7) has to be larger than zero

$$\begin{aligned} 0 &< \lambda \ln \frac{\lambda}{J} + J - \lambda \\ \frac{J}{\lambda} &> \ln \frac{\lambda}{J} + 1 \ . \end{aligned} \tag{4.8}$$

The last expression is true for every positive value of J/λ. But from Eq. (4.6), we see that an EPSP is only evoked when the synaptic strength $J > \lambda$.

An inhibitory postsynaptic potential (IPSP) can not be described directly in the above way, since λ evokes a constant decay to the resting potential (the floor). Values below the floor are not allowed. A typical IPSP shape, with a minimum deflection below resting potential and a decay back to the latter, is thus not possible with the CLIFF. However, a solution can be found, if we counteract the constant decay by additionally injecting a positive direct current $I_{\rm DC}$. Mathematically, this is equivalent to substituting $\lambda \Rightarrow \lambda - I_{\rm DC}$ in Eqs. (4.5-4.8). For an IPSP the righthand side of the corresponding variant of Eq. (4.7) has to be smaller then zero. Then we see from the corresponding variant of Eq. (4.6) two further requirements for an IPSP, $I_{\rm DC} > \lambda$ and $J < \lambda - I_{\rm DC}$.

Noisy input current. For an input current according to an Ornstein-Uhlenbeck process, the firing rate f of the CLIFF neuron is given by:

$$f(m) = \left[\tau_r + \frac{\theta - V_r}{m-\lambda}C + \frac{\tau s^2}{(m-\lambda)^2}\left(e^{-\frac{m-\lambda}{\tau s^2}C\theta} - e^{-\frac{m-\lambda}{\tau s^2}CV_r}\right)\right]^{-1} , \qquad (4.9)$$

with τ_r the refractory period, θ the firing threshold, V_r the reset potential, m the mean value of the noisy current, s the standard deviation of the noisy current, τ the auto-correlation time of the noisy current, λ the constant decay of the CLIFF, and C its capacitance. The derivation of Eq. 4.2 can be found in Fusi & Mattia (1999).

Numerical integration. For numerically integrating the differential equation underlying the CLIFF model neuron (Eq. 4.2), we used (Dayan & Abbott, 2001)

$$V(t+\Delta t) = V(t) - \frac{\lambda + I(t)}{C}\Delta t \ . \qquad (4.10)$$

The expression is based on the assumption that $I(t)$ is constant for a "fairly" small time step Δt.

4.5.2 Mean-field description of the attractor neural network

The mean-field analysis of our model network follows the approach of Brunel (2000); see the paper for details. The approach offers a simplified mean field theory, based on the $f-I$ curve of the single cells of a network. In the approach the fixed-points of the attractor neural network are intersections of the $f-I$ curve (Eq. 4.9) with a line given by

$$f \ = \ (m - m_{\mathrm{sp}}) \,/\, (cN\tau_c J) + f_{\mathrm{sp}} \ . \qquad (4.11)$$

where N is the number of neurons, c the connection probability, τ_c the decay time constant of the exitatory postsynaptic currents (EPSCs), J the average connection strength, and f_{sp} the spontaneous firing rate in response to the spontaneous background current m_{sp}. Note that I keep the level of spontaneous activity f_{sp} the same in the following, i.e., I adjust the spontaneous background current m_{sp} appropriately.

What is the feature of dopaminergic modulation of the single cell $f-I$ curve, which explains the impact on network behavior, the rheobase reduction, i.e., a shift of the $f-I$ curve to lower input values, or the gain-increase of the $f-I$ curve? Here I provide a description for the dependencies on the shape of $f-I$ curve of the behavior of our neural network model (Fig. 4.3). Since an exhaustive analytical derivation turned out to be hard due to the transcendental functions involved in Eq. (4.9), I present numerical solutions to the mean-field description of the model network. I always alter the case without DA subsequently:

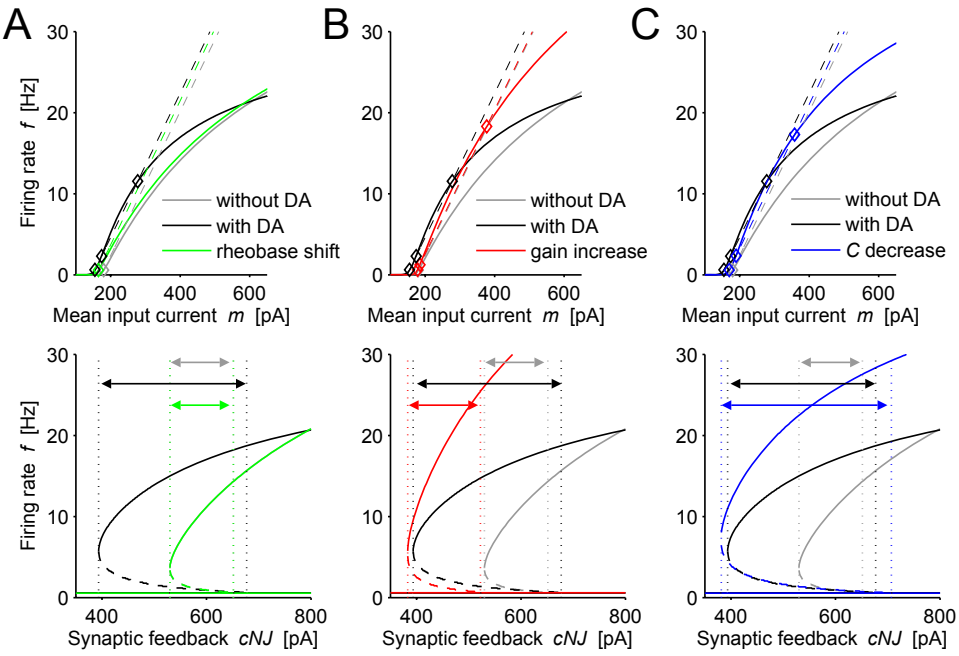

Figure 4.3: Comparison of different $f-I$ curve properties in the mean-field description of the attractor network. Each column gives the cases without DA (gray) and with DA (black) and a special case, i.e., a pure shift, m_s, of the $f-I$ curve to lower input values (A), a gain-increase, γ (B), and a decrease of the membrane capacitance C (C set to the mean value with DA) (C). *Top panels:* Steady state values of the firing rate are intersections between $f-I$ curves (solid lines) and corresponding straight line (dashed, same color, here with the synaptic feedback $cNJ = 450$ pA). Diamonds mark the steady state values. *Bottom panels:* Bifurcation diagram showing the steady state firing rates as a function of cNJ. Solid lines depict the stable lower and upper fixed-points and the dashed line indicates the unstable intermediate fixed-point. Dotted lines and arrows demarcate the range of values of cNJ with bistability (colors like in the upper panel). Parameters are $f_{\mathrm{sp}} = 0.5$ Hz, $s = 100$ pA, $m_s = -40$ pA, $\gamma = 1.4$, and $\tau_c = 25$ ms.

(A) Rheobase reduction. A reduction of the rheobase current means a shift of the whole $f-I$ curve to lower input values by an amount m_s, i.e., $f = f(m - m_s)$. The shift m_s also has to be incorporated into the input current m_{sp} that evokes spontaneous activity, which also shifts the line that determines the fixed-points. The slope of the line, however, is not affected. Wee see that a simple left shift does not influence the level of synaptic strength necessary for bistability at all. Note, however, that the minimum input current is reduced that is necessary to drive the network from spontaneous to persistent activity.

(B) Gain increase. A pure gain-increase only acts as a constant factor γ added to the $f - I$ curve. The gain-increase moves the range of bistability to lower values of synaptic feedback cNJ. It is therefore possible to evoke persistent activity at lower synaptic strength. Furthermore, persistent activity is more stable, as can be seen from the increased basin of attraction of the upper fixed-point. In fact again one only observes a simple shift to lower values of cNJ. The total range for bistability is only slightly increased. The slight increase is due to a small enhancement of the curvature of the $f - I$ curve at small input currents m or firing rates f, respectively.

(C) Decrease of the membrane capacitance. A gain modulation of the CLIFF $f - I$ can be due to either an increase of the reset potential V_r or a decrease of the effective capacitance C (Eq. 4.9). Increasing V_r leaves the shape of the $f - I$ curve unaffected close to rheobase. In contrast, a decrease of the capacitance C increases not only the gain but also the curvature of the $f - I$ curve close to rheobase. Decreasing the capacitance C shifts the range for bistability to lower synaptic feedback cNJ and also the range of values of cNJ with bistability widens, i.e., bistability becomes more robust against fluctuations in the network parameters. This is due to a shift to larger values of cNJ of the point where spontaneous activity state and unstable fixed-point merge.

To conclude let us look at the case with DA. Dopamine increased the input resistance in the experiments. Larger input resistance results in larger fluctuations of the membrane potential for noisy input current. Therefore the initial part of the $f - I$ curve at low frequency values, i.e. close to f_{sp}, extends over a larger range of mean input currents m. In the fits this results in a decrease of the CLIFF capacitance C. Combined C-decrease and increase of the reset potential V_r explains the gain-increase under DA, The gain-increase results in a shift of the range of bistability to lower values of the synaptic feedback cNJ – facilitation of persistent activity – and a larger bassin of attraction for persistent activity – stabilization of persistent activity. Decreased effective membrane capacitance C and increased curvature close to threshold extend the range of synaptic feedback cNJ that allows for bistability – robustness against chances in synaptic strength.

4.5.3 List of symbols

c connection probability

C membrane capacitance of the CLIFF

f firing rate

$f_{\mathbf{sp}}$ spontaneous firing rate

d synaptic delay

$I(t)$ input current

J synaptic strength

λ constant leakage of the CLIFF

m mean input current

$m_{\mathbf{sp}}$ background input current

N the number of neurons

s standard deviation of the input current

τ auto-correlation length of the input current, i.e., of the Ornstein-Uhlenbeck process

τ_c decay time constant of an EPSC

τ_r refractory period of the CLIFF

θ spike threshold of the CLIFF

V membrane voltage

V_r reset value after spiking of the CLIFF

Part III

Discussion

The prefrontal cortex (PFC) has an outstanding role in higher order cognitive functions, including working memory, i.e., the ability to keep events "in mind" for immediate need (Chapter 3). The PFC is particularly developed in primates; however, other mammalian species have analogous neocortical regions (Chapter 1). In rats the medial PFC (mPFC) is the region, which is most comparable to the primate PFC and therefore received most attention in experimental studies. Our experimental work also focused on the rat mPFC.

Dopamine is one of the prevalent neuromodulators of PFC function in general and working memory in particular. We learned from Chapter 2 that dopamine (DA) has a variety of different influences on neurons and networks of neurons in the PFC. *In vitro*, DA differentially modulates various voltage-gated and synaptic conductances in the PFC. Therefore, it is hard to draw conclusions on the collective influence of DA, which is relevant for PFC network function *in vivo*. In general, without staying close to an – at least expected – function and keeping in mind that particular relevance, it is hard to tell whether the phenomena under investigation are not only artifacts. Focusing at the DA modulation of the input-output function of single layer V PFC pyramidal neurons, we tried to circumvent this issue. Our experimental results are in line with the general notion that DA via D1 receptors increases the excitability of PFC pyramidal neurons. Moreover, we confirmed that an important computational feature is modulated by DA via D1 receptors, namely the gain of the input-output function. Dopamine increased the gain of the input-output function of PFC pyramidal neurons in our experiments. Servan-Schreiber et al. (1990) proposed from theoretical considerations more than 15 years ago that catecholamines modulate the gain of the neuronal input-output function, and that a gain-increase would increase the signal-to-noise ratio and thus the information transfer in a network of interconnected cells.

Excitatory synaptic reverberation within a network of recurrently connected cortical neurons is currently the most widely accepted hypothesis for the mechanism of persistent activity underlying working memory (Chapter 3). Supporting this hypothesis, prefrontal areas show some specific histological, morphological and cellular features like extensive horizontal excitatory connections and reciprocal inhibition, highly branched dendritic trees with a lot of spines and synaptic facilitation (Chapter 1). Dopamine has been suggested from neural network models to stabilize persistent activity and increase the signal-to-noise ratio. Most studies, however, focused on the dopaminergic modulation of synaptic inputs and particular membrane conductances. The $f - I$ curves that we measured in our experiments offered a direct way to incorporate our single cell data into a model neuron and relate the findings to model network behavior possibly underlying working memory. Our findings support and extend the insights offered by other studies: DA stabilizes persistent network activity against distracting input by a gain increase of the neuronal input-output function. The effects of DA on the neuronal input-output function thus functionally match the previously described effects of DA on synaptic transmission in the PFC (Chapter 3). In view of the diversity of DA effects on the physiological properties of the PFC (Chapter 2) this reveals a remarkable convergence between the DA modulation of single neurons and of synapses in networks of neurons.

Focusing on the DA modulation of experimentally measured input-output functions, we were able to directly mediate between *in vitro* experiments on DA modulation (Chapter 2), the stabilization of persistent activity in attractor neural networks and the enhancement of the signal-to-noise ratio via gain-increase (Chapter 3). Our model complements both the biophysical and the connectionist approaches, since a DA-induced change in the gain of the single neuron input/output function as in connectionist models directly translates into stable persistent activity like in biophysical models.

Beside all the different aspects of the PFC and DA reported in the literature and our somewhat more collective view via the input-output properties of single neurons, the final confirmation, i.e., the direct investigation of DA modulation of persistent network activity similar to prefrontal *in vivo* activity during working memory tasks is lacking. Experimental work would have to focus more specifically on the underpinnings of persistent activity on the network level and it modulation by DA.

The present thesis was devoted to the role of the PFC in working memory. I tried to argue for the peculiar importance of the PFC's working memory function in non-human and human cognition. Let me therefore conclude with a quotation borrowed from still one of the most influential personalities in the field, Patricia S. Goldman-Rakic:

> [..] the brain's working memory function, i.e., the ability to bring to mind events in the absence of direct stimulation, may be its inherently most flexible mechanism and its evolutionarily most significant achievement. At the most elementary level, our basic conceptual ability to appreciate that an object exists when out of view depends on the capacity to keep events in mind beyond the direct experience of those events. [.. *working memory provides*] the temporal and spatial continuity between our past experience and present actions.
>
> — Goldman-Rakic (1995)

Since Patricia S. Goldman-Rakic in the same breath scratches the issues of causality, let me answer with the words of David Hume:

> Nature has not left this [*the existence of objects*] to [*one's*] choice, and has doubtless, esteem'd it an affair of too great importance to be trusted to our uncertain reasonings and speculations.
>
> — Hume (1739-1740) A treatise of human nature.

Part IV

Appendix

List of Abbreviations

AC	adenylate cyclase
AMPA	α-amino-3-hydroxy-5-methyl-4-isoxazolepropionic acid
cAMP	cyclic adenosine monophosphate
AHP	after-hyperpolarization
sAHP	slow after-hyperpolarization (AHP)
CLIFF	constant leakage integrate-and-fire neuron with a floor
CNS	central nervous system
CREB	cAMP response element-binding protein
aCSF	artificial cerebrospinal fluid
DA	dopamine
DAG	diacylglycerol
DARPP-32	dopamine- and cyclic AMP-regulated phosphoprotein with molecular weight 32 kDa
EPSC	exitatory postsynaptic current
EPSP	exitatory postsynaptic potential
GABA	γ-aminobutyric acid
G protein	guanine nucleotide-binding protein

IPSC	inhibitory postsynaptic current
IPSP	inhibitory postsynaptic potential
IRKC	inwardly rectifying potassium channel
LTD	long-term depression
LTP	long-term potentiation
fMRI	functional magnetic resonance imaging
NMDA	N-methyl-D-aspartic acid
PET	positron emission tomography
PFC	prefrontal cortex
mPFC	medial PFC
PKA	protein kinase A
PKC	protein kinase C
PLC	phospholipase C
PP-1	protein phosphatase 1
VTA	ventral tegmental area

List of Figures

Bibliography

Abeles M (1991) Corticonics: Neural Circuits of the Cerebral Cortex. Cambridge Univ. Press, Cambridge. [cited at p. 40]

Amit DJ, Brunel N (1997) Model of global spontaneous activity and local structured activity during delay periods in the cerebral cortex. Cereb Cortex 7:237–252. [cited at p. 34, 37, 38, and 56]

Arsiero M, Lüscher HR, Lundstrom BN, Giugliano M (2007) The impact of input fluctuations on the frequency-current relationships of layer 5 pyramidal neurons in the rat medial prefrontal cortex. J Neurosci 27:3274–3284. [cited at p. 45]

Asaad WF, Rainer G, Miller EK (2000) Task-specific neural activity in the primate prefrontal cortex. J Neurophysiol 84:451–459. [cited at p. 28]

Ashby FG, Casale MB (2003) A model of dopamine modulated cortical activation. Neural Netw 16:973–984. [cited at p. 41]

Baddeley A (1992) Working memory. Science 255:556–559. [cited at p. 27]

Baddeley A (2003) Working memory: looking back and looking forward. Nat Rev Neurosci 4:829–839. [cited at p. 27]

Baeg EH, Kim YB, Huh K, Mook-Jung I, Kim HT, Jung MW (2003) Dynamics of population code for working memory in the prefrontal cortex. Neuron 40:177–188. [cited at p. 30]

Bandyopadhyay S, Gonzalez-Islas C, Hablitz JJ (2005) Dopamine enhances spatiotemporal spread of activity in rat prefrontal cortex. J Neurophysiol 93:864–872. [cited at p. 22 and 33]

Bandyopadhyay S, Hablitz JJ (2007) Dopaminergic modulation of local network activity in rat prefrontal cortex. J Neurophysiol 97:4120–4128. [cited at p. 22 and 33]

Bear MF, Conners BW, Paradiso MA (2007) Neuroscience: exploring the brain. Lippincott Williams & Wilkins, 3rd edition. [cited at p. 11, 12, and 31]

Beggs JM, Plenz D (2003) Neuronal avalanches in neocortical circuits. J Neurosci 23:11167–11177. [cited at p. 33]

Braver TS, Barch DM, Cohen JD (1999) Cognition and control in schizophrenia: a computational model of dopamine and prefrontal function. Biol Psychiatry 46:312–328. [cited at p. 25 and 44]

Brody CD, Romo R, Kepecs A (2003) Basic mechanisms for graded persistent activity: discrete attractors, continuous attractors, and dynamic representations. Curr Opin Neurobiol 13:204–211. [cited at p. 39]

Brozoski TJ, Brown RM, Rosvold HE, Goldman PS (1979) Cognitive deficit caused by regional depletion of dopamine in prefrontal cortex of rhesus monkey. Science 205:929–932. [cited at p. 23 and 31]

Brunel N (2000) Persistent activity and the single-cell frequency-current curve in a cortical network model. Network 11:261–280. [cited at p. 38, 56, and 83]

Brunel N, Wang XJ (2001) Effects of neuromodulation in a cortical network model of object working memory dominated by recurrent inhibition. J Comput Neurosci 11:63–85. [cited at p. 25, 38, 42, and 43]

Camperi M, Wang XJ (1998) A model of visuospatial working memory in prefrontal cortex: recurrent network and cellular bistability. J Comput Neurosci 5:383–405. [cited at p. 33, 39, and 40]

Carlsson A, Lindqvist M, Magnusson T, Waldeck B (1958) On the presence of 3-hydroxytyramine in brain. Science 127:471. [cited at p. 15]

Castner SA, Goldman-Rakic PS, Williams GV (2004) Animal models of working memory: insights for targeting cognitive dysfunction in schizophrenia. Psychopharmacology (Berl) 174:111–125. [cited at p. 30 and 31]

Chance FS, Abbott LF, Reyes AD (2002) Gain modulation from background synaptic input. Neuron 35:773–782. [cited at p. 45 and 46]

Charney DS, Nestler EJ, editors (2004) Neurobiology of mental illness. Oxford University Press, 2nd edition. [cited at p. 16]

Chen L, Bohanick JD, Nishihara M, Seamans JK, Yang CR (2007) Dopamine D1/5 receptor-mediated long-term potentiation of intrinsic excitability in rat prefrontal cortical neurons: Ca2+-dependent intracellular signaling. J Neurophysiol 97:2448–2464. [cited at p. 18 and 22]

Compte A (2006) Computational and in vitro studies of persistent activity: edging towards cellular and synaptic mechanisms of working memory. Neuroscience 139:135–151. [cited at p. 32 and 33]

Compte A, Brunel N, Goldman-Rakic PS, Wang XJ (2000) Synaptic mechanisms and network dynamics underlying spatial working memory in a cortical network model. Cereb Cortex 10:910–923. [cited at p. 38 and 39]

Compte A, Constantinidis C, Tegner J, Raghavachari S, Chafee MV, Goldman-Rakic PS, Wang XJ (2003) Temporally irregular mnemonic persistent activity in prefrontal neurons of monkeys during a delayed response task. J Neurophysiol 90:3441–3454. [cited at p. 39]

Connors BW (2002) Single-neuron mnemonics. Nature 420:133–134. [cited at p. 32]

Constantinidis C, Williams GV, Goldman-Rakic PS (2002) A role for inhibition in shaping the temporal flow of information in prefrontal cortex. Nat Neurosci 5:175–180. [cited at p. 8, 14, 28, 33, and 39]

Cowen SL, McNaughton BL (2007) Selective delay activity in the medial prefrontal cortex of the rat: contribution of sensorimotor information and contingency. J Neurophysiol 98:303–316. [cited at p. 30 and 31]

Cox DR, Miller HD (1965) The theory of stochastic processes. New York: Chapman & Hall. [cited at p. 54]

Daw ND, Courville AC, Tourtezky DS, Touretzky DS (2006) Representation and timing in theories of the dopamine system. Neural Comput 18:1637–1677. [cited at p. 25]

Dayan P, Abbott LF (2001) Theoretical neuroscience: computational and mathematical modeling of neural systems. MIT Press. [cited at p. 83]

Destexhe A, Rudolph M, Par D (2003) The high-conductance state of neocortical neurons in vivo. Nat Rev Neurosci 4:739–751. [cited at p. 55]

Diesmann M, Gewaltig MO, Aertsen A (1999) Stable propagation of synchronous spiking in cortical neural networks. Nature 402:529–533. [cited at p. 40]

Dong Y, Cooper D, Nasif F, Hu XT, White FJ (2004) Dopamine modulates inwardly rectifying potassium currents in medial prefrontal cortex pyramidal neurons. J Neurosci 24:3077–3085. [cited at p. 20]

Dong Y, White FJ (2003) Dopamine D1-class receptors selectively modulate a slowly inactivating potassium current in rat medial prefrontal cortex pyramidal neurons. J Neurosci 23:2686–2695. [cited at p. 20]

Dreher JC, Burnod Y (2002) An integrative theory of the phasic and tonic modes of dopamine modulation in the prefrontal cortex. Neural Netw 15:583–602. [cited at p. 25 and 44]

Durstewitz D, Kelc M, Gntrkn O (1999) A neurocomputational theory of the dopaminergic modulation of working memory functions. J Neurosci 19:2807–2822. [cited at p. 25, 42, and 43]

Durstewitz D, Seamans JK (2002) The computational role of dopamine D1 receptors in working memory. Neural Netw 15:561–572. [cited at p. 21, 42, 43, and 56]

Durstewitz D, Seamans JK (2006) Beyond bistability: biophysics and temporal dynamics of working memory. Neuroscience 139:119–133. [cited at p. 29, 38, and 39]

Durstewitz D, Seamans JK (2008) The dual-state theory of prefrontal cortex dopamine function with relevance to catechol-o-methyltransferase genotypes and schizophrenia. Biol Psychiatry . [cited at p. 35, 44, and 55]

Durstewitz D, Seamans JK, Sejnowski TJ (2000a) Dopamine-mediated stabilization of delay-period activity in a network model of prefrontal cortex. J Neurophysiol 83:1733–1750. [cited at p. 25, 38, 42, 43, and 56]

Durstewitz D, Seamans JK, Sejnowski TJ (2000b) Neurocomputational models of working memory. Nat Neurosci 3 Suppl:1184–1191. [cited at p. 32]

Egorov AV, Hamam BN, Fransn E, Hasselmo ME, Alonso AA (2002) Graded persistent activity in entorhinal cortex neurons. Nature 420:173–178. [cited at p. 33]

Egorov AV, Unsicker K, von Bohlen und Halbach O (2006) Muscarinic control of graded persistent activity in lateral amygdala neurons. Eur J Neurosci 24:3183–3194. [cited at p. 33]

Elston GN (2003) Cortex, cognition and the cell: new insights into the pyramidal neuron and prefrontal function. Cereb Cortex 13:1124–1138. [cited at p. 9 and 14]

Euston DR, McNaughton BL (2006) Apparent encoding of sequential context in rat medial prefrontal cortex is accounted for by behavioral variability. J Neurosci 26:13143–13155. [cited at p. 30]

Fellous JM, Rudolph M, Destexhe A, Sejnowski TJ (2003) Synaptic background noise controls the input/output characteristics of single cells in an in vitro model of in vivo activity. Neuroscience 122:811–829. [cited at p. 45]

Fellous JM, Sejnowski TJ (2003) Regulation of persistent activity by background inhibition in an in vitro model of a cortical microcircuit. Cereb Cortex 13:1232–1241. [cited at p. 33]

FitzGerald MJT, Gruener G, Mtui E (2007) Clinical Neuroanatomy and Neuroscience. Elsevier Saunders, 5th edition. [cited at p. 6]

Floresco SB, Magyar O (2006) Mesocortical dopamine modulation of executive functions: beyond working memory. Psychopharmacology (Berl) 188:567–585. [cited at p. 24]

Floresco SB, Magyar O, Ghods-Sharifi S, Vexelman C, Tse MTL (2006) Multiple dopamine receptor subtypes in the medial prefrontal cortex of the rat regulate set-shifting. Neuropsychopharmacology 31:297–309. [cited at p. 24]

Frank MJ, Loughry B, O'Reilly RC (2001) Interactions between frontal cortex and basal ganglia in working memory: a computational model. Cogn Affect Behav Neurosci 1:137–160. [cited at p. 25 and 44]

Fransén E, Tahvildari B, Egorov AV, Hasselmo ME, Alonso AA (2006) Mechanism of graded persistent cellular activity of entorhinal cortex layer v neurons. Neuron 49:735–746. [cited at p. 40]

Funahashi S, Bruce CJ, Goldman-Rakic PS (1989) Mnemonic coding of visual space in the monkey's dorsolateral prefrontal cortex. J Neurophysiol 61:331–349. [cited at p. 28, 29, 30, and 39]

Fusi S, Mattia M (1999) Collective behavior of networks with linear (VLSI) integrate-and-fire neurons. Neural Comput 11:633–652. [cited at p. 38, 56, and 83]

Fuster JM (1973) Unit activity in prefrontal cortex during delayed-response performance: neuronal correlates of transient memory. J Neurophysiol 36:61–78. [cited at p. 28]

Fuster JM (2001) The prefrontal cortex–an update: time is of the essence. Neuron 30:319–333. [cited at p. 6, 7, 9, 28, 30, and 32]

Fuster JM, Alexander GE (1971) Neuron activity related to short-term memory. Science 173:652–654. [cited at p. 28]

Fuster JM, Alexander GE (1973) Firing changes in cells of the nucleus medialis dorsalis associated with delayed response behavior. Brain Res 61:79–91. [cited at p. 32]

Fuster JM, Bodner M, Kroger JK (2000) Cross-modal and cross-temporal association in neurons of frontal cortex. Nature 405:347–351. [cited at p. 28]

Fuster JM, Jervey JP (1981) Inferotemporal neurons distinguish and retain behaviorally relevant features of visual stimuli. Science 212:952–955. [cited at p. 29 and 30]

Gao C, Wolf ME (2008) Dopamine receptors regulate NMDA receptor surface expression in prefrontal cortex neurons. J Neurochem . [cited at p. 21]

Gao M, Liu CL, Yang S, Jin GZ, Bunney BS, Shi WX (2007) Functional coupling between the prefrontal cortex and dopamine neurons in the ventral tegmental area. J Neurosci 27:5414–5421. [cited at p. 13]

Gao WJ, Goldman-Rakic PS (2003) Selective modulation of excitatory and inhibitory microcircuits by dopamine. Proc Natl Acad Sci U S A 100:2836–2841. [cited at p. 22]

Gao WJ, Krimer LS, Goldman-Rakic PS (2001) Presynaptic regulation of recurrent excitation by D1 receptors in prefrontal circuits. Proc Natl Acad Sci U S A 98:295–300. [cited at p. 21]

Gao WJ, Wang Y, Goldman-Rakic PS (2003) Dopamine modulation of perisomatic and peridendritic inhibition in prefrontal cortex. J Neurosci 23:1622–1630. [cited at p. 22]

Geijo-Barrientos E, Pastore C (1995) The effects of dopamine on the subthreshold electrophysiological responses of rat prefrontal cortex neurons in vitro. Eur J Neurosci 7:358–366. [cited at p. 23]

Giudice PD, Fusi S, Mattia M (2003) Modelling the formation of working memory with networks of integrate-and-fire neurons connected by plastic synapses. J Physiol Paris 97:659–681. [cited at p. 38]

Goldman-Rakic PS (1995) Cellular basis of working memory. Neuron 14:477–485. [cited at p. 28, 29, 30, 32, 33, and 91]

Goldman-Rakic PS, Muly EC, Williams GV (2000) D1 receptors in prefrontal cells and circuits. Brain Res Brain Res Rev 31:295–301. [cited at p. 13, 17, 23, 27, and 31]

Gonzalez-Islas C, Hablitz JJ (2001) Dopamine inhibition of evoked IPSCs in rat prefrontal cortex. J Neurophysiol 86:2911–2918. [cited at p. 22]

Gonzalez-Islas C, Hablitz JJ (2003) Dopamine enhances EPSCs in layer II-III pyramidal neurons in rat prefrontal cortex. J Neurosci 23:867–875. [cited at p. 21]

Gorelova N, Seamans JK, Yang CR (2002) Mechanisms of dopamine activation of fast-spiking interneurons that exert inhibition in rat prefrontal cortex. J Neurophysiol 88:3150–3166. [cited at p. 20]

Gorelova NA, Yang CR (2000) Dopamine D1/D5 receptor activation modulates a persistent sodium current in rat prefrontal cortical neurons in vitro. J Neurophysiol 84:75–87. [cited at p. 18]

Greengard P (2001) The neurobiology of slow synaptic transmission. Science 294:1024–1030. [cited at p. 17]

Gruber AJ, Dayan P, Gutkin BS, Solla SA (2006) Dopamine modulation in the basal ganglia locks the gate to working memory. J Comput Neurosci 20:153–166. [cited at p. 25, 39, and 44]

Gulledge AT, Jaffe DB (1998) Dopamine decreases the excitability of layer V pyramidal cells in the rat prefrontal cortex. J Neurosci 18:9139–9151. [cited at p. 23]

Gulledge AT, Jaffe DB (2001) Multiple effects of dopamine on layer V pyramidal cell excitability in rat prefrontal cortex. J Neurophysiol 86:586–595. [cited at p. 23]

Gulledge AT, Stuart GJ (2003) Action potential initiation and propagation in layer 5 pyramidal neurons of the rat prefrontal cortex: absence of dopamine modulation. J Neurosci 23:11363–11372. [cited at p. 18]

Gurden H, Takita M, Jay TM (2000) Essential role of D1 but not D2 receptors in the NMDA receptor-dependent long-term potentiation at hippocampal-prefrontal cortex synapses in vivo. J Neurosci 20:RC106. [cited at p. 23]

Gurney K, Prescott TJ, Wickens JR, Redgrave P (2004) Computational models of the basal ganglia: from robots to membranes. Trends Neurosci 27:453–459. [cited at p. 25]

Hebb DO (1949) The Organization of Behavior: A Neuropsychological Theory. Wiley. [cited at p. 27, 32, and 34]

Heidbreder CA, Groenewegen HJ (2003) The medial prefrontal cortex in the rat: evidence for a dorso-ventral distinction based upon functional and anatomical characteristics. Neurosci Biobehav Rev 27:555–579. [cited at p. 10, 11, and 12]

Hempel CM, Hartman KH, Wang XJ, Turrigiano GG, Nelson SB (2000) Multiple forms of short-term plasticity at excitatory synapses in rat medial prefrontal cortex. J Neurophysiol 83:3031–3041. [cited at p. 9, 14, 33, and 41]

Henze DA, Gonzlez-Burgos GR, Urban NN, Lewis DA, Barrionuevo G (2000) Dopamine increases excitability of pyramidal neurons in primate prefrontal cortex. J Neurophysiol 84:2799–2809. [cited at p. 22]

Higgs MH, Slee SJ, Spain WJ (2006) Diversity of gain modulation by noise in neocortical neurons: regulation by the slow afterhyperpolarization conductance. J Neurosci 26:8787–8799. [cited at p. 45, 46, and 53]

Hopfield JJ (1982) Neural networks and physical systems with emergent collective computational abilities. Proc Natl Acad Sci U S A 79:2554–2558. [cited at p. 34]

Hyman SE, Malenka RC, Nestler EJ (2006) Neural mechanisms of addiction: the role of reward-related learning and memory. Annu Rev Neurosci 29:565–598. [cited at p. 13 and 15]

Klinke R, Pape HC, Silbernagl S (2005) Physiologie. Georg Thieme Verlag, Stuttgart, 5. edition. [cited at p. 6]

Koulakov AA, Raghavachari S, Kepecs A, Lisman JE (2002) Model for a robust neural integrator. Nat Neurosci 5:775–782. [cited at p. 39]

Krettek JE, Price JL (1977) Projections from the amygdaloid complex to the cerebral cortex and thalamus in the rat and cat. J Comp Neurol 172:687–722. [cited at p. 10]

Kröner S, Krimer LS, Lewis DA, Barrionuevo G (2007) Dopamine increases inhibition in the monkey dorsolateral prefrontal cortex through cell type-specific modulation of interneurons. Cereb Cortex 17:1020–1032. [cited at p. 20]

Kubota K, Niki H (1971) Prefrontal cortical unit activity and delayed alternation performance in monkeys. J Neurophysiol 34:337–347. [cited at p. 28]

Lapish CC, Kroener S, Durstewitz D, Lavin A, Seamans JK (2007) The ability of the mesocortical dopamine system to operate in distinct temporal modes. Psychopharmacology (Berl) 191:609–625. [cited at p. 12, 13, 19, and 25]

Larkum ME, Kaiser KM, Sakmann B (1999a) Calcium electrogenesis in distal apical dendrites of layer 5 pyramidal cells at a critical frequency of back-propagating action potentials. Proc Natl Acad Sci U S A 96:14600–14604. [cited at p. 20 and 46]

Larkum ME, Senn W, Lüscher HR (2004) Top-down dendritic input increases the gain of layer 5 pyramidal neurons. Cereb Cortex 14:1059–1070. [cited at p. 46]

Larkum ME, Zhu JJ, Sakmann B (1999b) A new cellular mechanism for coupling inputs arriving at different cortical layers. Nature 398:338–341. [cited at p. 20]

Lau PM, Bi GQ (2005) Synaptic mechanisms of persistent reverberatory activity in neuronal networks. Proc Natl Acad Sci U S A 102:10333–10338. [cited at p. 33]

Lavin A, Grace AA (2001) Stimulation of D1-type dopamine receptors enhances excitability in prefrontal cortical pyramidal neurons in a state-dependent manner. Neuroscience 104:335–346. [cited at p. 22 and 46]

Lavin A, Nogueira L, Lapish CC, Wightman RM, Phillips PEM, Seamans JK (2005) Mesocortical dopamine neurons operate in distinct temporal domains using multimodal signaling. J Neurosci 25:5013–5023. [cited at p. 13 and 22]

Lewis BL, O'Donnell P (2000) Ventral tegmental area afferents to the prefrontal cortex maintain membrane potential 'up' states in pyramidal neurons via D1 dopamine receptors. Cereb Cortex 10:1168–1175. [cited at p. 22]

Lisman JE, Fellous JM, Wang XJ (1998) A role for NMDA-receptor channels in working memory. Nat Neurosci 1:273–275. [cited at p. 40]

Lorente De Nó R (1938) Analysis of the activity of the chains of internuncial neurons. J Neurophysiol 1:207–244. [cited at p. 32]

Machens CK, Brody CD (2008) Design of continuous attractor networks with monotonic tuning using a symmetry principle. Neural Comput 20:452–485. [cited at p. 39]

Machens CK, Romo R, Brody CD (2005) Flexible control of mutual inhibition: a neural model of two-interval discrimination. Science 307:1121–1124. [cited at p. 29 and 39]

Marder E, Abbott LF, Turrigiano GG, Liu Z, Golowasch J (1996) Memory from the dynamics of intrinsic membrane currents. Proc Natl Acad Sci U S A 93:13481–13486. [cited at p. 33]

Matsuda Y, Marzo A, Otani S (2006) The presence of background dopamine signal converts long-term synaptic depression to potentiation in rat prefrontal cortex. J Neurosci 26:4803–4810. [cited at p. 23]

Maurice N, Tkatch T, Meisler M, Sprunger LK, Surmeier DJ (2001) D1/d5 dopamine receptor activation differentially modulates rapidly inactivating and persistent sodium currents in prefrontal cortex pyramidal neurons. J Neurosci 21:2268–2277. [cited at p. 18]

McCormick DA, Shu Y, Hasenstaub A, Sanchez-Vives M, Badoual M, Bal T (2003) Persistent cortical activity: mechanisms of generation and effects on neuronal excitability. Cereb Cortex 13:1219–1231. [cited at p. 33]

McNab F, Klingberg T (2008) Prefrontal cortex and basal ganglia control access to working memory. Nat Neurosci 11:103–107. [cited at p. 44]

Miller EK, Cohen JD (2001) An integrative theory of prefrontal cortex function. Annu Rev Neurosci 24:167–202. [cited at p. 8, 9, 10, and 31]

Miller EK, Erickson CA, Desimone R (1996) Neural mechanisms of visual working memory in prefrontal cortex of the macaque. J Neurosci 16:5154–5167. [cited at p. 28, 30, and 33]

Miller P, Brody CD, Romo R, Wang XJ (2003) A recurrent network model of somatosensory parametric working memory in the prefrontal cortex. Cereb Cortex 13:1208–1218. [cited at p. 39]

Missale C, Nash SR, Robinson SW, Jaber M, Caron MG (1998) Dopamine receptors: from structure to function. Physiol Rev 78:189–225. [cited at p. 15, 17, 19, and 55]

Mitchell SJ, Silver RA (2003) Shunting inhibition modulates neuronal gain during synaptic excitation. Neuron 38:433–445. [cited at p. 46]

Mongillo G, Amit DJ (2001) Oscillations and irregular emission in networks of linear spiking neurons. J Comput Neurosci 11:249–261. [cited at p. 38]

Mongillo G, Barak O, Tsodyks M (2008) Synaptic theory of working memory. Science 319:1543–1546. [cited at p. 40 and 41]

Montague PR, Hyman SE, Cohen JD (2004) Computational roles for dopamine in behavioural control. Nature 431:760–767. [cited at p. 25]

Mountcastle VB (1997) The columnar organization of the neocortex. Brain 120 (Pt 4):701–722. [cited at p. 7]

Neve KA, Seamans JK, Trantham-Davidson H (2004) Dopamine receptor signaling. J Recept Signal Transduct Res 24:165–205. [cited at p. 17, 18, 19, and 20]

Nevian T, Larkum ME, Polsky A, Schiller J (2007) Properties of basal dendrites of layer 5 pyramidal neurons: a direct patch-clamp recording study. Nat Neurosci 10:206–214. [cited at p. 20]

Numberger M, Draguhn A (1996) Patch-Clamp-Technik. Heidelberg; Berlin; Oxford: Spekturm, Akad. Verl. [cited at p. 53]

O'Donnell P (2003) Dopamine gating of forebrain neural ensembles. Eur J Neurosci 17:429–435. [cited at p. 44]

Öngür D, Price JL (2000) The organization of networks within the orbital and medial prefrontal cortex of rats, monkeys and humans. Cereb Cortex 10:206–219. [cited at p. 8 and 11]

O'Reilly RC, Frank MJ (2006) Making working memory work: a computational model of learning in the prefrontal cortex and basal ganglia. Neural Comput 18:283–328. [cited at p. 25 and 44]

Otani S, Daniel H, Roisin MP, Crepel F (2003) Dopaminergic modulation of long-term synaptic plasticity in rat prefrontal neurons. Cereb Cortex 13:1251–1256. [cited at p. 23]

Paxinos G, Watson C (1998) The Rat Brain in Stereotaxic Coordinates. Academic Press. [cited at p. 54]

Pedarzani P, Storm JF (1995) Dopamine modulates the slow Ca(2+)-activated K+ current IAHP via cyclic AMP-dependent protein kinase in hippocampal neurons. J Neurophysiol 74:2749–2753. [cited at p. 20]

Rainer G, Asaad WF, Miller EK (1998) Memory fields of neurons in the primate prefrontal cortex. Proc Natl Acad Sci U S A 95:15008–15013. [cited at p. 28]

Rao SC, Rainer G, Miller EK (1997) Integration of what and where in the primate prefrontal cortex. Science 276:821–824. [cited at p. 28]

Rao SG, Williams GV, Goldman-Rakic PS (1999) Isodirectional tuning of adjacent interneurons and pyramidal cells during working memory: evidence for microcolumnar organization in PFC. J Neurophysiol 81:1903–1916. [cited at p. 8, 14, 28, 33, and 39]

Rauch A, LaCamera G, Lüscher HR, Senn W, Fusi S (2003) Neocortical pyramidal cells respond as integrate-and-fire neurons to in vivo-like input currents. J Neurophysiol 90:1598–1612. [cited at p. 45]

Redgrave P, Gurney K (2006) The short-latency dopamine signal: a role in discovering novel actions? Nat Rev Neurosci 7:967–975. [cited at p. 25]

Renart A, Moreno-Bote R, Wang XJ, Parga N (2007) Mean-driven and fluctuation-driven persistent activity in recurrent networks. Neural Comput 19:1–46. [cited at p. 40]

Rolls ET, Loh M, Deco G, Winterer G (2008) Computational models of schizophrenia and dopamine modulation in the prefrontal cortex. Nat Rev Neurosci 9:696–709. [cited at p. 9]

Romo R, Brody CD, Hernndez A, Lemus L (1999) Neuronal correlates of parametric working memory in the prefrontal cortex. Nature 399:470–473. [cited at p. 28, 30, and 39]

Romo R, Salinas E (2003) Flutter discrimination: neural codes, perception, memory and decision making. Nat Rev Neurosci 4:203–218. [cited at p. 29, 30, and 39]

Rotaru DC, Lewis DA, Gonzalez-Burgos G (2007) Dopamine D1 receptor activation regulates sodium channel-dependent EPSP amplification in rat prefrontal cortex pyramidal neurons. J Physiol 581:981–1000. [cited at p. 18 and 21]

Roudi Y, Latham PE (2007) A balanced memory network. PLoS Comput Biol 3:1679–1700. [cited at p. 40]

Sah P, Faber ESL (2002) Channels underlying neuronal calcium-activated potassium currents. Prog Neurobiol 66:345–353. [cited at p. 20]

Salinas E, Sejnowski TJ (2001) Gain modulation in the central nervous system: where behavior, neurophysiology, and computation meet. Neuroscientist 7:430–440. [cited at p. 45]

Salinas E, Thier P (2000) Gain modulation: a major computational principle of the central nervous system. Neuron 27:15–21. [cited at p. 45]

Sanfey AG (2007) Social decision-making: insights from game theory and neuroscience. Science 318:598–602. [cited at p. 10]

Sawaguchi T, Goldman-Rakic PS (1991) D1 dopamine receptors in prefrontal cortex: involvement in working memory. Science 251:947–950. [cited at p. 23 and 31]

Sawaguchi T, Goldman-Rakic PS (1994) The role of d1-dopamine receptor in working memory: local injections of dopamine antagonists into the prefrontal cortex of rhesus monkeys performing an oculomotor delayed-response task. J Neurophysiol 71:515–528. [cited at p. 23 and 31]

Schiller J, Major G, Koester HJ, Schiller Y (2000) NMDA spikes in basal dendrites of cortical pyramidal neurons. Nature 404:285–289. [cited at p. 20]

Schultz W (1998) Predictive reward signal of dopamine neurons. J Neurophysiol 80:1–27. [cited at p. 25]

Schultz W (2002) Getting formal with dopamine and reward. Neuron 36:241–263. [cited at p. 12 and 25]

Schultz W (2006) Behavioral theories and the neurophysiology of reward. Annu Rev Psychol 57:87–115. [cited at p. 24]

Schultz W (2007a) Behavioral dopamine signals. Trends Neurosci 30:203–210. [cited at p. 25]

Schultz W (2007b) Multiple dopamine functions at different time courses. Annu Rev Neurosci 30:259–288. [cited at p. 12 and 15]

Seamans JK, Durstewitz D, Christie BR, Stevens CF, Sejnowski TJ (2001a) Dopamine D1/D5 receptor modulation of excitatory synaptic inputs to layer V prefrontal cortex neurons. Proc Natl Acad Sci U S A 98:301–306. [cited at p. 21]

Seamans JK, Floresco SB, Phillips AG (1998) D1 receptor modulation of hippocampal-prefrontal cortical circuits integrating spatial memory with executive functions in the rat. J Neurosci 18:1613–1621. [cited at p. 23 and 31]

Seamans JK, Gorelova NA, Durstewitz D, Yang CR (2001b) Bidirectional dopamine modulation of GABAergic inhibition in prefrontal cortical pyramidal neurons. J Neurosci 21:3628–3638. [cited at p. 22]

Seamans JK, Nogueira L, Lavin A (2003) Synaptic basis of persistent activity in prefrontal cortex in vivo and in organotypic cultures. Cereb Cortex 13:1242–1250. [cited at p. 33]

Seamans JK, Yang CR (2004) The principal features and mechanisms of dopamine modulation in the prefrontal cortex. Prog Neurobiol 74:1–58. [cited at p. 12, 13, 16, 17, 18, 20, 21, 22, 23, 24, 25, and 45]

Servan-Schreiber D, Printz H, Cohen JD (1990) A network model of catecholamine effects: gain, signal-to-noise ratio, and behavior. Science 249:892–895. [cited at p. 26, 41, 43, and 89]

Seung HS, Lee DD, Reis BY, Tank DW (2000) Stability of the memory of eye position in a recurrent network of conductance-based model neurons. Neuron 26:259–271. [cited at p. 39]

Shi WX, Zheng P, Liang XF, Bunney BS (1997) Characterization of dopamine-induced depolarization of prefrontal cortical neurons. Synapse 26:415–422. [cited at p. 22]

Shu Y, Hasenstaub A, Badoual M, Bal T, McCormick DA (2003a) Barrages of synaptic activity control the gain and sensitivity of cortical neurons. J Neurosci 23:10388–10401. [cited at p. 45]

Shu Y, Hasenstaub A, McCormick DA (2003b) Turning on and off recurrent balanced cortical activity. Nature 423:288–293. [cited at p. 33]

Simon H, Scatton B, Moal ML (1980) Dopaminergic A10 neurones are involved in cognitive functions. Nature 286:150–151. [cited at p. 23 and 31]

Tanaka S (2002a) Dopamine controls fundamental cognitive operations of multi-target spatial working memory. Neural Netw 15:573–582. [cited at p. 25, 38, 43, and 44]

Tanaka S (2002b) Multi-directional representation of spatial working memory in a model prefrontal cortical circuit. Neurocomputing 44-46:1001–1008. [cited at p. 25, 43, and 44]

Thierry AM, Blanc G, Sobel A, Stinus L, Golwinski J (1973) Dopaminergic terminals in the rat cortex. Science 182:499–501. [cited at p. 18]

Thurley K, Leibold C, Gundlfinger A, Schmitz D, Kempter R (2008a) Phase precession through synaptic facilitation. Neural Comput 20:1285–1324. [cited at p. 41]

Thurley K, Senn W, Lüscher HR (2008b) Dopamine increases the gain of the input-output response of rat prefrontal pyramidal neurons. J Neurophysiol 99:2985–2997. [cited at p. 14, 20, 26, 43, 46, and 47]

Trantham-Davidson H, Neely LC, Lavin A, Seamans JK (2004) Mechanisms underlying differential D1 versus D2 dopamine receptor regulation of inhibition in prefrontal cortex. J Neurosci 24:10652–10659. [cited at p. 22]

Trepel M (2004) Neuroanatomie: Struktur und Funktion. Elsevier GmbH, Urban & Fischer Verlag, 3. edition. [cited at p. 6 and 13]

Tseng KY, O'Donnell P (2004) Dopamine-glutamate interactions controlling prefrontal cortical pyramidal cell excitability involve multiple signaling mechanisms. J Neurosci 24:5131–5139. [cited at p. 21 and 22]

Tseng KY, O'Donnell P (2005) Post-pubertal emergence of prefrontal cortical up states induced by D1-NMDA co-activation. Cereb Cortex 15:49–57. [cited at p. 23]

Tseng KY, O'Donnell P (2007) Dopamine modulation of prefrontal cortical interneurons changes during adolescence. Cereb Cortex 17:1235–1240. [cited at p. 20 and 23]

Tsodyks MV, Markram H (1997) The neural code between neocortical pyramidal neurons depends on neurotransmitter release probability. Proc Natl Acad Sci U S A 94:719–723. [cited at p. 38]

Tzschentke TM (2001) Pharmacology and behavioral pharmacology of the mesocortical dopamine system. Prog Neurobiol 63:241–320. [cited at p. 8, 12, 15, and 17]

Uylings HBM, Groenewegen HJ, Kolb B (2003) Do rats have a prefrontal cortex? Behav Brain Res 146:3–17. [cited at p. 8 and 11]

Viana F, Bayliss DA, Berger AJ (1993) Multiple potassium conductances and their role in action potential repolarization and repetitive firing behavior of neonatal rat hypoglossal motoneurons. J Neurophysiol 69:2150–2163. [cited at p. 46]

Vijayraghavan S, Wang M, Birnbaum SG, Williams GV, Arnsten AFT (2007) Inverted-U dopamine D1 receptor actions on prefrontal neurons engaged in working memory. Nat Neurosci 10:376–384. [cited at p. 23 and 24]

Walz W, Boulton AA, Baker GB, editors (2002) Patch-Clamp Analysis, Advanced Techniques. Humana Press, Totowa, New Jersey. [cited at p. 53]

Wang J, O'Donnell P (2001) D1 dopamine receptors potentiate NMDA-mediated excitability increase in layer V prefrontal cortical pyramidal neurons. Cereb Cortex 11:452–462. [cited at p. 21 and 22]

Wang M, Vijayraghavan S, Goldman-Rakic PS (2004) Selective D2 receptor actions on the functional circuitry of working memory. Science 303:853–856. [cited at p. 24]

Wang X, Zhong P, Gu Z, Yan Z (2003) Regulation of NMDA receptors by dopamine D4 signaling in prefrontal cortex. J Neurosci 23:9852–9861. [cited at p. 21]

Wang X, Zhong P, Yan Z (2002) Dopamine D4 receptors modulate GABAergic signaling in pyramidal neurons of prefrontal cortex. J Neurosci 22:9185–9193. [cited at p. 22]

Wang XJ (1999) Synaptic basis of cortical persistent activity: the importance of NMDA receptors to working memory. J Neurosci 19:9587–9603. [cited at p. 38 and 56]

Wang XJ (2001) Synaptic reverberation underlying mnemonic persistent activity. Trends Neurosci 24:455–463. [cited at p. 32, 34, 35, and 55]

Wang Y, Markram H, Goodman PH, Berger TK, Ma J, Goldman-Rakic PS (2006) Heterogeneity in the pyramidal network of the medial prefrontal cortex. Nat Neurosci 9:534–542. [cited at p. 9, 14, 33, and 41]

Watanabe M, Kodama T, Hikosaka K (1997) Increase of extracellular dopamine in primate prefrontal cortex during a working memory task. J Neurophysiol 78:2795–2798. [cited at p. 25]

Williams GV, Rao SG, Goldman-Rakic PS (2002) The physiological role of 5-HT2A receptors in working memory. J Neurosci 22:2843–2854. [cited at p. 11]

Winograd M, Destexhe A, Sanchez-Vives MV (2008) Hyperpolarization-activated graded persistent activity in the prefrontal cortex. Proc Natl Acad Sci U S A 105:7298–7303. [cited at p. 34 and 40]

Witkowski G, Szulczyk B, Rola R, Szulczyk P (2008) D(1) dopaminergic control of G protein-dependent inward rectifier K(+) (GIRK)-like channel current in pyramidal neurons of the medial prefrontal cortex. Neuroscience 155:53–63. [cited at p. 20 and 22]

Yang CR, Seamans JK (1996) Dopamine D1 receptor actions in layers V-VI rat prefrontal cortex neurons in vitro: modulation of dendritic-somatic signal integration. J Neurosci 16:1922–1935. [cited at p. 18, 20, 21, and 22]

Yang CR, Seamans JK, Gorelova NA (1996) Electrophysiological and morphological properties of layers V-VI principal pyramidal cells in rat prefrontal cortex in vitro. J Neurosci 16:1904–1921. [cited at p. 9]

Yao WD, Spealman RD, Zhang J (2008) Dopaminergic signaling in dendritic spines. Biochem Pharmacol 75:2055–2069. [cited at p. 13 and 17]

Yoshida M, Fransn E, Hasselmo ME (2008) mGluR-dependent persistent firing in entorhinal cortex layer III neurons. Eur J Neurosci . [cited at p. 34]

Young CE, Yang CR (2004) Dopamine D1/D5 receptor modulates state-dependent switching of soma-dendritic Ca2+ potentials via differential protein kinase A and C activation in rat prefrontal cortical neurons. J Neurosci 24:8–23. [cited at p. 20]

Zhang Z, Arsenault D (2005) Gain modulation by serotonin in pyramidal neurones of the rat prefrontal cortex. J Physiol 566:379–394. [cited at p. 11 and 46]

Zheng P, Zhang XX, Bunney BS, Shi WX (1999) Opposite modulation of cortical N-methyl-D-aspartate receptor-mediated responses by low and high concentrations of dopamine. Neuroscience 91:527–535. [cited at p. 21]

Danksagung

Am Ende meiner Arbeit möchte ich denjenigen herzlich danken, die massgeblich zum Gelingen derselben beigetragen haben:

Hans-Rudolf Lüscher ermöglichte mir am Institut für Physiologie zu doktorieren. Er gab mit vom ersten Tag an die Möglichkeit, hier die elektrophysiologischen Methoden zu erlernen und Experimente durchzuführen.

Walter Senn hat mir mit grundlegenden Ideen, Anregungen und kritischen Disskusionen vor allem in Bezug auf die mathematische Modellierung der experimentellen Daten geholfen.

Richard Kempter gab mir wichtiges Feedback zu meiner Arbeit und erklärte sich bereit als Koreferent zu fungieren und diese Dissertation zu begutachten.

Ernst Niggli danke ich als meinem Mentor für seine unkomplizierte Vermittlung und Kommunikation in Bezug auf die Belange der Graduate School for Cellular and Biomedical Sciences.

Den Praktikanten, Doktoranden und PostDocs am Institut für Physiologie, mit denen ich während meines Doktorats zusammenarbeiten durfte und welche mit fortwährender Unterstützung und intensiven Gesprächen ein lebhaftes wissenschaftliches Arbeitsumfeld geschaffen haben, danke ich von ganzem Herzen. Im besonderen möchte ich hier Debora Ledergerber erwähnen, die nicht zuletzt durch ihre kritischen und befruchtenden Kommentare zur vorliegenden Arbeit beigetragen hat. Desweiteren seien Maura Arsiero, Brice Bathellier, Olivier Gschwend, Michele Giugliano, Harold Köndgen, Rogier Min, Florian Neubauer, Enrique Pérez Garci, Roland Schäfer und Robert Urbanczik genannt.

Marc Thurley unterstützte mich in programmiertechnischen Dingen und gab viele Kommentare zu dieser Dissertation vor allem in sprachlicher Hinsicht.

Bewusst nenne ich an letzter Stelle, Maja; denn, wenn auch nicht jeder Gedanke mit ihr beginnt, so endet doch jeder bei ihr.

Curriculum vitæ

Personal/Contact Information

Name:	Kay Thurley
Date/Place of Birth:	03 Feb 1979 in Borna, Germany
Nationality:	German
Address (office):	Department of Physiology University of Bern Bühlplatz 5 CH-3012 Bern, Switzerland
Phone (office):	0041/31/631 8725
Fax (office):	0041/31/631 4611
Email:	thurley@pyl.unibe.ch

Professional Experience

January 2006 - 2008	Postgraduate research in the Group of Prof. Hans-Rudolf Lüscher at the Department of Physiology, University of Bern, Switzerland. Reasearch on the rat prefrontal cortex.

January - March 2005	Scientific coworker at the Theoretical Neuroscience Lab of Dr. Richard Kempter, Institute for Theoretical Biology (ITB), Humboldt-Universität zu Berlin (HU Berlin).
October 2003 - July 2004	Undergraduate research (diploma thesis in biology) at the Theoretical Neuroscience Lab of Dr. Richard Kempter, ITB, HU Berlin. *Title:* "Hippocampal Theta Phase Precession and Mossy Fibre Facilitation". In the thesis I developed a model of the generation of hippocampal phase precession in CA3 pyramidal neurons by means of mossy fibre facilitation.

Education

January 2006 - 2008	PhD Student in the Group of Prof. Hans-Rudolf Lüscher at the Department of Physiology, University of Bern, Switzerland.
19. July 2004	Diploma in biology
October 1999 - July 2004	Undergraduate studies of biology at the HU Berlin. Emphasis: Animal Physiology, Theoretical Biology, Computer Science
27. June 1998	University entrance diploma (Abitur) at the Lise-Meitner-Gymnasium Falkensee, Germany

Publications

Dopamine increases the gain of the input-output response of rat prefrontal pyramidal neurons
- **K. Thurley**, W. Senn, H.-R. Lüscher (2008) *J Neurophysiol* 99: 2985-2997

Temporal Compression Mediated by Short-Term Synaptic Plasticity
- C. Leibold, A. Gundlfinger, R. Schmidt, **K. Thurley**, D. Schmitz, R. Kempter (2008) *Proc. Natl. Acad. Sci. U.S.A.* 105(11): 4417-4422

Phase precession through synaptic facilitation
- **K. Thurley**, C. Leibold, A. Gundlfinger, D. Schmitz, R. Kempter (2008) *Neural Comput* 20(5): 1285-324

Conference Presentations

Computation in Cortical Circuits, Ascona 2008 (poster):
Dopaminergic modulation of the input-output response function of rat prefrontal pyramidal neurons in vitro
- **K. Thurley**, W. Senn, H.-R. Lüscher

Annual Meeting of the Swiss Physiological Society, Fribourg 2008 (talk):
Dopaminergic modulation of the input-output response function of rat prefrontal pyramidal neurons in vitro
- **K. Thurley**, W. Senn, H.-R. Lüscher

6th Forum of European Neuroscience, Geneva 2008 (poster):
Dopamine increases the gain of the input-output response of rat prefrontal pyramidal neurons.
- **K. Thurley**, W. Senn, H.-R. Lüscher

GABAB receptor-dependent tonic inhibition in L2/3 pyramidal neurons in the rat prefrontal cortex.
- Y. Wang, **K. Thurley**, F.B. Neubauer, H.-R. Lüscher

Giessbach Meeting 2008 (talk):
Dopaminergic modulation of the input-output response function of rat prefrontal pyramidal neurons in vitro
- **K. Thurley**, W. Senn, H.-R. Lüscher

7th Göttingen Meeting of the German Neuroscience Society 2007 (poster):
Dopamine differentially affects the input-output relationship of layer 5 pyramidal neurons in the prefrontal cortex
- **K. Thurley**, W. Senn, H.-R. Lüscher

Joint Meeting of SSN-NCCR Neuro-SSMS, Bern 2007 (poster):
Dopamine differentially affects the input-output relationship of layer 5 pyramidal neurons in the prefrontal cortex
- **K. Thurley**, W. Senn, H.-R. Lüscher

Second Meeting of Clinical Neuroscience Bern 2006 (talk/poster):
Dopamine differentially affects the input-output relationship of layer 5 pyramidal neurons in the prefrontal cortex
- **K. Thurley**, W. Senn, H.-R. Lüscher

5th Forum of European Neuroscience, Vienna 2006 (poster):
Hippocampal phase precession through mossy fiber facilitation
- **K. Thurley**, C. Leibold, D. Schmitz, R. Kempter

Schools and Courses

2006 - 2008	BENEFRI Program Neuroscience, Universities of Bern and Fribourg, Switzerland
2006 - 2008	PhD Programme in Cellular and Biomedical Sciences, Graduate School for Cellular and Biomedical Sciences, University of Bern, Switzerland
March 2007	"Spring School in Computational Neuroscience", CAS-MPG Partner Institute for Computational Biology (PICB), Shanghai Institutes for Biological Sciences (SIBS), Chinese Academy of Sciences (CAS), China

Declaration of Originality

Last name, first name: **Thurley, Kay**

Matriculation number: **05-119-474**

I hereby declare that this thesis represents my original work and that I have used no other sources except as noted by citations.
All data, tables, figures and text citations which have been reproduced from any other source, including the internet, have been explicitly acknowledged as such.
I am aware that in case of non-compliance, the Senate is entitled to divest me of the doctorate degree awarded to me on the basis of the present thesis, in accordance with the “Statut der Universität Bern (Universitätsstatut; UniSt)”, Art. 20, of 17 December 1997.

Place, date	Signature
Bern, 02.10.2008	
……	……